Electrophoretic Separation Strategies for Gentle Fractionation of Rapeseed

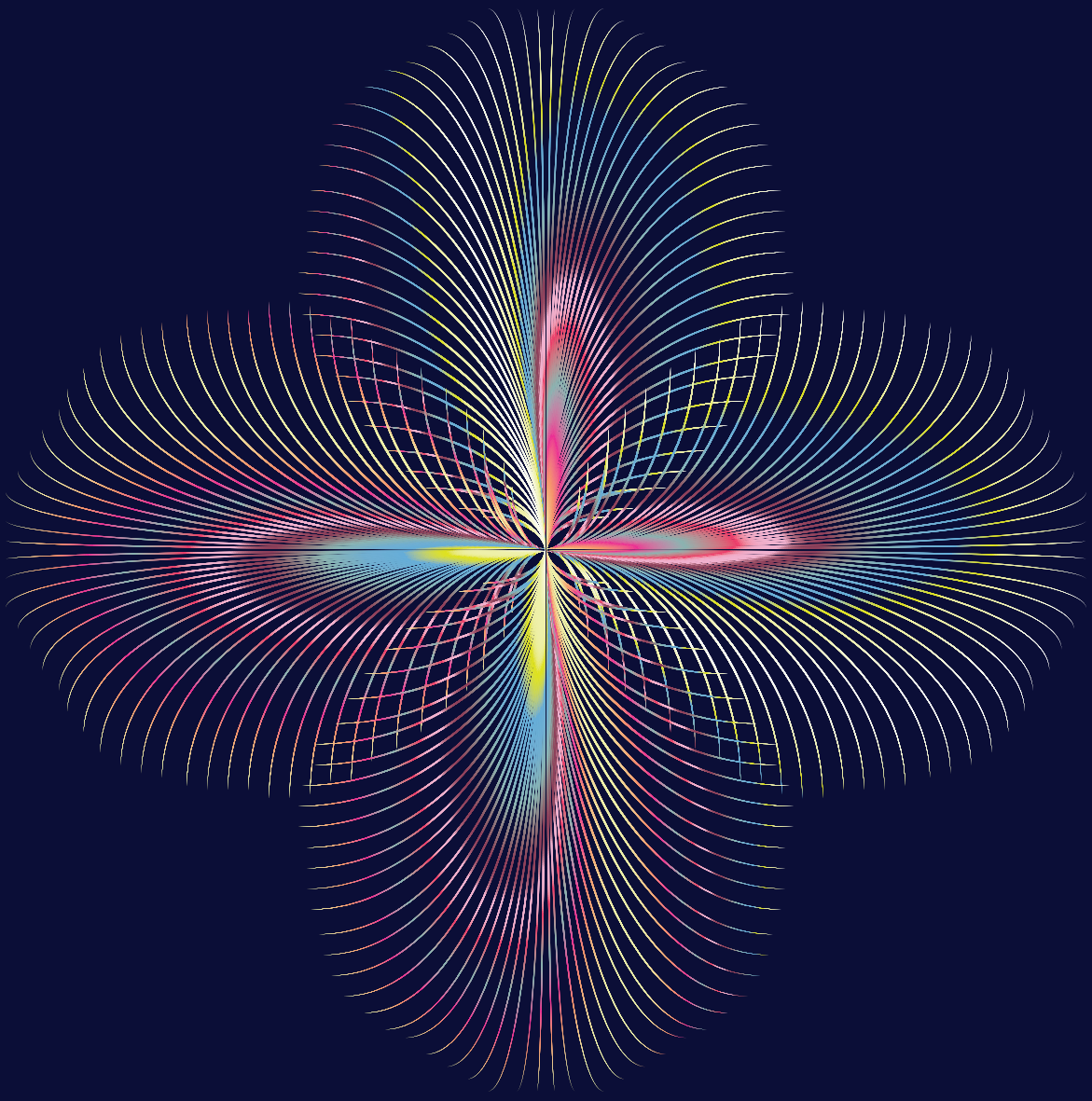

Kübra Ayan

Propositions

1. Counter-current electrophoresis enables multi-component separation.
   (this thesis)

2. Adsorption contributes significantly to the separation in electrodialysis.
   (this thesis)

3. Not sharing failed research negatively impacts the sustainability of doing research.

4. The power supply of a PhD candidate is self-motivation.

5. Over-optimism undermines one´s problem-solving ability.

6. Empathy is essential to appreciate the harmony inherent in diversity.

Propositions belonging to the thesis, entitled

Electrophoretic separation strategies
for gentle fractionation of rapeseed

Kübra Ayan

Wageningen, 11 November 2024

Electrophoretic separation strategies for gentle fractionation of rapeseed

Kübra Ayan

Thesis committee

Promotors

Prof. Dr Remko Marcel Boom
Professor of Food Process Engineering
Wageningen University & Research

Dr Constantinos V. Nikiforidis
Associate Professor, Biobased Chemistry & Technology Group
Wageningen University & Research

Other members

Prof. Dr Louis de Smet, Wageningen University & Research
Prof. Dr Marcel Ottens, Delft University of Technology
Dr H. Burak Eral, Delft University of Technology
Dr P. Maarten Biesheuvel, Wetsus, Leeuwarden

This research was conducted under the auspices of VLAG Graduate School (Biobased, Biomolecular, Chemical, Food, and Nutrition sciences)

Electrophoretic separation strategies for gentle fractionation of rapeseed

Kübra Ayan

Thesis
submitted in fulfilment of the requirements for the degree of doctor
at Wageningen University
by the authority of the Rector Magnificus,
Prof. Dr C. Kroeze,
in the presence of the
Thesis Committee appointed by the Academic Board
to be defended in public
on Monday 11 November 2024
at 3:30 p.m. in the Omnia Auditorium

Kübra Ayan

Electrophoretic separation strategies for gentle fractionation of rapeseed, 144 pages.

PhD thesis, Wageningen University, Wageningen, the Netherlands (2024)
With references, with summary in English

DOI: 10.18174/675375

Contents

Chapter 1	Introduction and thesis outline	8
Chapter 2	Continuous counter-current electrophoretic separation of oleosomes and proteins from oilseeds	18
Chapter 3	Scaling the electrophoretic separation of rapeseed proteins and oleosomes	42
Chapter 4	Electrophoretic removal of sinapic acid from rapeseed protein extract	62
Chapter 5	Electrophoretic dephenolization of rapeseed proteins: The influence of ionic strength on sinapic acid electromigration	82
Chapter 6	General discussion	108
	References	124
	Summary	134
	Appendices	138

CHAPTER 1

Introduction and thesis outline

1.1. CURRENT UTILIZATION OF OILSEEDS

Oilseeds are valuable agriproducts with their massive cultivation and oil-rich composition (Table 1.1). The industrial valorization of oleaginous seeds is currently centered on maximizing oil extraction yield. To achieve this, a combination of mechanical (pressing) and chemical extraction methods are used (Figure 1.1). Most of the oil is extracted with an expression step. However, the obtained oilseed press cake still contains 8 – 30% oil. Therefore, solvent extraction is used to recover most of the remaining oil. As a general practice, *n*-hexane is used for the solvent extraction and 90 – 98% of the remaining oil can be extracted. While this process gives very high oil extraction yield, the use of hexane raises environmental and health concerns, the desolventizing is energy intensive, and the recovered oil requires extensive refining to ensure high quality and avoid oxidation. Moreover, the process conditions (organic solvents, high temperature) also denature other constituents such as proteins, which reduces the value of the final press cake (Gharby, 2022; Nde & Foncha, 2020; Nehmeh et al., 2022).

Table 1.1: Proximate composition of the main oilseeds.

Oilseeds	**Soybean**	**Rapeseed**	**Sunflower Seeds**
Composition (%)			
Fat	20.5	44.3	40.6 – 41.3
Protein	38.3	20.9 – 25.7	17.2 - 23.0
Carbohydrate	29.7	20.0 – 31.4	33.5 – 51.7
Ash	4.4	3.8 – 4.8	2.7 – 3.6
Phenolics	4.7	3.8 – 5.9	3.9 – 5.0
References	Rosset et al., 2014; Sharma & Giri, 2022	Gagour et al., 2022; Szydlowska-Czerniak et al., 2010	Gagour et al., 2022

Within plant cells, oils are stored as triacylglycerols (TAGs) in organelles enclosed by a phospholipid and protein monolayer that protect TAGs against oxidation and environmental stress. These oleosomes or oil bodies can be extracted whole using an aqueous process, which yields a highly stable natural oil-in-water emulsion, eliminating the need of a homogenization process and surfactant addition for creating emulsion based products. During the conventional oil extraction process, the phospholipid and protein monolayer of oleosomes is degraded and separated from the oil (Nikiforidis, 2019; Weiss & Zhang, 2020). When used for creating emulsion based products, the extracted free oil then needs to be homogenized with surfactants or stabilizers to re-create oil droplets. This is not necessary when extracting whole oleosomes (Han et al., 2024).

As mentioned already, the conventional oil extraction process also denatures the oilseeds proteins. Proteins from plant sources are becoming ever more important in the food industry to limit the environmental impact of food production, providing plant-based functional food ingredients and meet the protein demand of a growing population (Balandrán-Quintana et al., 2019). Oilseeds contain a considerable amount of proteins (Table 1.1); however, it is not straight forward to extract oilseed meal proteins due to the harsh processing conditions during the de-oiling process and their complex composition including antinutrient compounds (phenolics).

The proteins tend to denature during oil extraction due to the high temperatures, especially in the desolventizing process, which impairs protein solubility and makes their extraction and utilization challenging. To increase the solubility of the proteins and ease their extraction, high alkaline pH (pH > 9.0) solutions are generally used; however, this then induces complexation of proteins with phenolics (Figure 1.1). Covalently bonded protein-phenolic complexes due to oxidation of phenolics to *o*-quinones give rise to even lower solubility, indigestibility, poor functionality and discoloration. All these effects hinder potential use of oilseed proteins in food products (Fetzer et al., 2020; Hadidi et al., 2024; Salazar-Villanea et al., 2016).

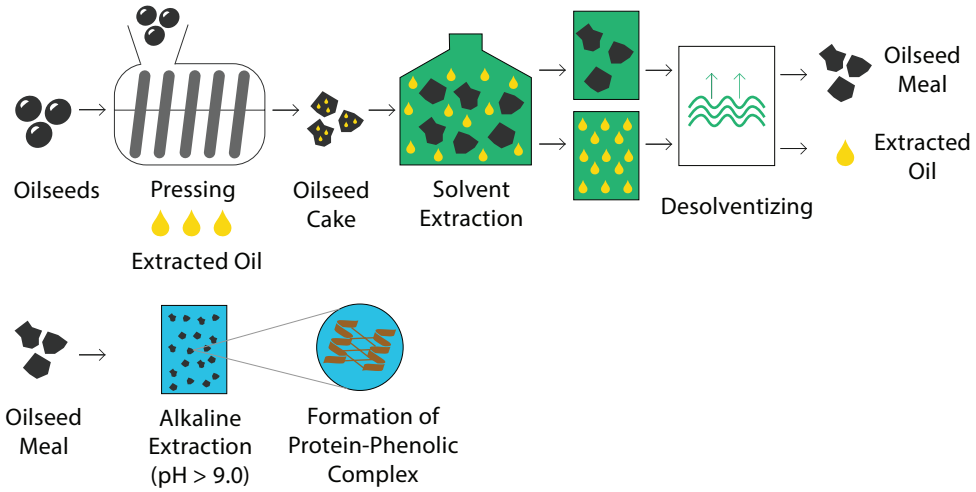

Figure 1.1: Schematic representation of the conventional utilization of oilseeds for oil extraction and further protein extraction.

To restrict the consequences of the protein – phenolic complexes and deliver oilseed proteins in a better quality, removal of the phenolics is necessary. This is often done by washing out phenolics using alcohol (ethanol) solutions. However, while simple, this method also brings some additional drawbacks. As in solvent extraction of oils, extraction of phenolic compounds using alcohol requires large amount of solvent which should be recovered from the final product. This renders the process slow and energy-intensive due to the high

temperatures needs to evaporate the solutions (Hadidi et al., 2024; Nandasiri et al., 2020). Besides, exposure of proteins to alcoholic solutions causes further protein denaturation (Peng et al., 2020; Shao et al., 2012).

Ultimately, the current de-oiling process prioritizing high oil extraction yield does not fully exploit the potential of oilseeds by degrading natural emulsion, oleosomes, and a potential alternative protein source. To enhance the valorization of oilseeds, the development of a gentler process omitting the need for organic solvents and elevated temperatures is necessary.

1.2. AQUEOUS OILSEED FRACTIONATION

To enable simultaneous oleosome and protein extraction from oilseeds without using solvents or high temperatures, aqueous extraction has been proposed. In this method, water instead of organic solvents is used as a dispersant. Therefore, both oleosomes due to hydrophilic nature of their outer membrane and proteins are extracted from plant cells into the water phase, and a mixture of whole oleosomes, proteins and other components such as phenolics is obtained. Separation of oleosomes from the co-extracted proteins is necessary to utilize them in different applications. Oleosomes and proteins can be separated making use of their different density. When centrifuged, the buoyant oleosomes cream up and can be separated from the heavier protein extract as a result of rotational forces (Figure 1.2) (Nikiforidis & Kiosseoglou, 2009; Rosenthal et al., 1996).

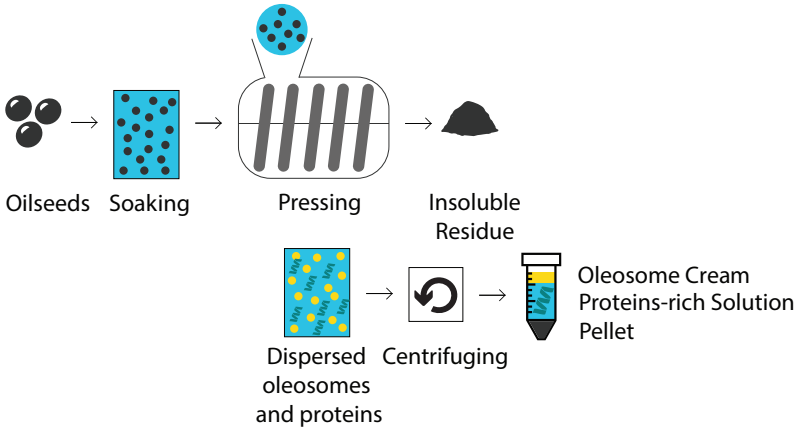

Figure 1.2: Schematic representation of the aqueous extraction of oleosomes and proteins from oilseeds.

Using the aqueous extraction omits the need of organic solvents, elevated temperatures, further reconstitution process to create emulsions and sequential oil and protein extraction process. Besides, it can be operated under mild alkaline pH (8 – 9) conditions and provides higher protein extraction yield with better solubility by eliminating the detrimental impact of defatting process on the proteins (Ntone et al., 2020). Nonetheless, this process is not optimal yet regarding oil extraction yield, water and energy consumption (Guzman, 2020; Lie-Piang et al., 2021; Lv & Wu, 2019). In addition, separation of proteins from phenolic compounds is still necessary. To render this process more resource-efficient and comprehensive, new approaches must be developed.

1.3. ELECTROPHORETIC SEPARATION

Electrophoretic separation is a technique to fractionate mixtures based on the electrophoresis rates of the individual components. Electrophoresis refers to the movement of a dispersed charged compound in a conductive liquid medium (electrolyte) when subjected to an external electric field. The electrophoretic velocity of a compound depends on its electrophoretic mobility (μ), defined as the migration rate under a unit electric field of 1 V/cm, and the applied electric field strength (E) (Equation 1.1). The electrophoretic mobility is a complex property influenced by both the intrinsic properties of a compound, such as its surface charge, its molecular weight and size, but also the extrinsic properties of the dispersion medium such as the pH, temperature, density, viscosity and ionic strength. However, the general rule is that a compound with greater charge density exhibits higher electrophoretic mobility (Buszewski et al., 2013).

$$\text{Electrophoretic velocity } (\mu\text{m/s}) = \mu\ (\mu\text{mcm/Vs}) \cdot \text{E}\ (\text{V/cm}) \qquad \text{Equation (1.1)}$$

Separation typically involves the motion of individual components relative to an interface or constraining wall. For example, the electrophoresis may be measured compared to a tube wall or porous barrier, which separates the feed from the eluate. Applying an electric field to a charged surface filled with an electrolyte solution also induces motion of the fluid itself, through electroosmosis. Unlike electrophoresis which involves migration of dispersed particles, electroosmotic flow (EOF) causes bulk fluid flow due to the existence of an electric double layer near the charged channel wall (Figure 1.3). In the case of a negatively charged wall, the electroosmotic flow direction is towards the cathode electrode, and vice versa. The net velocity of a compound in an electrolyte solution that resides in a tube or porous matrix, therefore, is equal to the sum of electrophoretic and EOF velocity (Sadek et al., 2017).

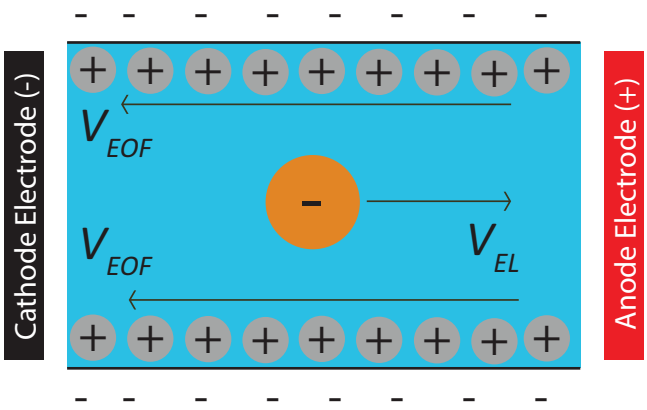

Figure 1.3: Electrophoretic migration of a negatively charged compound under an electric field, and electroosmotic migration of counter-ions attracted by the charged channel wall. V_{EL}: Electrophoretic velocity and V_{EOF}: Electroosmotic flow velocity.

Electrophoretic forces are versatile, enabling separation to be accomplished in various ways. Yet, the precondition for electrophoretic separation is the presence of compounds with distinct electrophoretic mobilities. Separation can be achieved through three primary mechanisms; (i) compounds having different electrical charge sign (positive or negative), leading to migration in opposite directions under an electric field, (ii) one of the compounds is charged and the other is neutral, leading to migration of the charged compound with the electrophoresis and migration of the neutral compounds with the electroosmotic solvent flow and (iii) both particles carry the same electrical sign (both positive or negative), but exhibit different electrophoretic mobility, allowing separation as a result of their different migration rate (Marina et al., 2005; Rudge & Monnig, 2000; Stastna, 2020).

Electrophoretic separation has broad applications in chemistry, biology, pharmaceutical, food and environmental science owing to its remarkable separation efficiency and accuracy; however it is currently mostly used for analytical purposes, for example for the genetic analysis, proteins, peptides, single-cells and metabolites. For preparative and industrial purposes, electrophoresis are often combined with membrane separation to facilitate the separation of different size and/or charge particles in larger scale applications. Electro-filtration and electrodialysis exemplify the combination of electrophoresis with membrane processing. In electro-filtration, the electrophoretic force acts perpendicular or anti-parallel to the convective solvent flow direction, and is used to eliminate/minimize cake layer formation on the membrane surface. This facilitates the permeation of smaller compounds as a result of reduced or prevented membrane fouling and enhanced permeate flux. It is commonly used to separate colloidal particles from a solution, but has not yet seen wide application in food production. In electrodialysis, electrophoresis is employed to selectively separate anionic and cationic compounds using alternatively stacked ion exchange

membranes. Here, anions and cations pass through anion exchange and cation exchange membranes, respectively and accumulate in different solutions at the end of the treatment (Khosravanipour Mostafazadeh et al., 2016; Li et al., 2023; Liu et al., 2021; Strathmann, 2004; Van der Bruggen, 2018).

Overall, the adaptability of electrophoresis provides diverse methods for separation. In food processing applications, however, the integration of electrical applications is limited by the use of ohmic heat treatment for pasteurization, pulsed electric field to enhance extraction processes, and electrodialysis for demineralization and deacidification purposes, and falls behind the use of conventional mechanical and thermal methods (Pereira et al., 2024; Wang et al., 2018). For the refinement of plant based materials, use of electrically driven processes is not yet widespread. However, the current methods of using centrifugation, precipitation and redispersion are relatively cumbersome and do not allow good resolution between different components. For example, the separation of proteins from oleosomes and of phenolic components from proteins typically requires extensive processes and the use of significant amounts of water and auxiliary chemicals (e.g. to adjust pH). The concurrent use of two driving forces, for example a pressure driven convective flow and an electric field, should allow for higher resolution in separation. This could allow us to achieve good separation between these types of constituents, while reducing the amount of water and chemicals needed.

1.4. OBJECTIVE AND THESIS OUTLINE

This thesis focuses on developing a complete, gentle and efficient fractionation process to obtain oleosomes and phenolic-free proteins from oilseeds using electrophoretic separation. Oleosomes, proteins and phenolic compounds have distinct sizes. It is hypothesized that this leads to different electrophoretic mobilities, making electro-separation possible. The use of electrophoresis can enhance their fractionation, as it can increase the resolution of the separation by acting only on charged particles proportional to their electrophoretic mobility.

To develop an electric field-assisted separation process, this thesis aims to first investigate the electrophoretic mobilities of purified oleosomes and proteins from oilseeds. Rapeseed was chosen to serve as a model oilseed.

Since the fractionation of rapeseed starts with separation of oils and proteins, **Chapter 2** explains how rapeseed oleosomes and proteins can be separated in a continuous process using electrophoresis in combination with hydrodynamic flow. For this, the electrophoretic mobilities of rapeseed oleosomes and proteins were investigated under different pH values to figure out the best moderate pH that provides the largest difference in their electrophoretic mobilities. Then, the electrophoretic separation of rapeseed oleosomes

and proteins was modelled using the Nernst – Planck equation. As a proof-of-principle, the movement of oleosomes and proteins was investigated under a fluorescent microscope, demonstrated that a combination of electrophoresis and hydrodynamic flow can indeed separate oleosomes from proteins.

In **Chapter 3**, the electro-separation of oleosomes and proteins was scaled to a bench-top size device using an electrochemical cell. Here, the concentrations of oleosomes (oil) and proteins were quantified under an increasing electric field strength and a constant flow rate. The results again confirmed that the solvent flow rate in between the electrophoresis rate of oleosomes and proteins achieves their separation. However, the separation selectivity was restricted by electrophoretic mobility differences, membrane fouling and electrolysis – based pH change.

After demonstration of the principle in the preceding chapters, **Chapter 4** focused on the separation between rapeseed proteins and the most abundant phenolic compound, sinapic acid. Rapeseed proteins (17 – 300 kDa) are much larger molecules than sinapic acid (0.22 kDa); therefore, a membrane that allows only sinapic acid electro-migration can separate them. Here, the electric field was used as a driving force for sinapic acid permeation. To investigate electro-migration of sinapic acid through various membranes, both ion exchange and ultrafiltration membranes were tested under different voltage values, and electrodialysis system was used to demonstrate the separation. Removal of sinapic acid was found to be affected by membrane surface charge and area and the applied potential difference.

In **Chapter 4**, the electro-separation of rapeseed proteins and sinapic acid was performed in a dilute stream (1.0 mg/mL soluble solid concentration dispersed in 1.0 mM potassium phosphate buffer). Nevertheless, in real protein extracts, the total soluble solid and salt concentrations are much higher. To define the limitations of electrodialysis based phenolic and protein separation, the effect of an increasing ionic strength was investigated regarding the sinapic acid removal and permeation over an anion exchange membrane in **Chapter 5**. An increasing salt concentration from 5 to 40 mM led to a decrease in the amount of removed sinapic acid. This is attributed to screening the charges by the higher ionic strength, which reduces their electrophoretic mobility. To prove that the electro-separation of rapeseed proteins and polyphenols is applicable using the electrodialysis system, a rapeseed protein extract was directly used as a sample, and 30.3 ± 4.1 wt% of sinapic acid and 14.9 ± 2.8 wt% phenolic compounds were removed in 240 min.

In **Chapter 6**, the overall results of the electrophoretic fractionation of rapeseed components were discussed and compiled into current and prospective opportunities and challenges. Furthermore, this chapter contextualizes the main findings within a broader perspective to explain future implications of the electrophoretic separation.

The general overview of the thesis is represented in Figure 1.4.

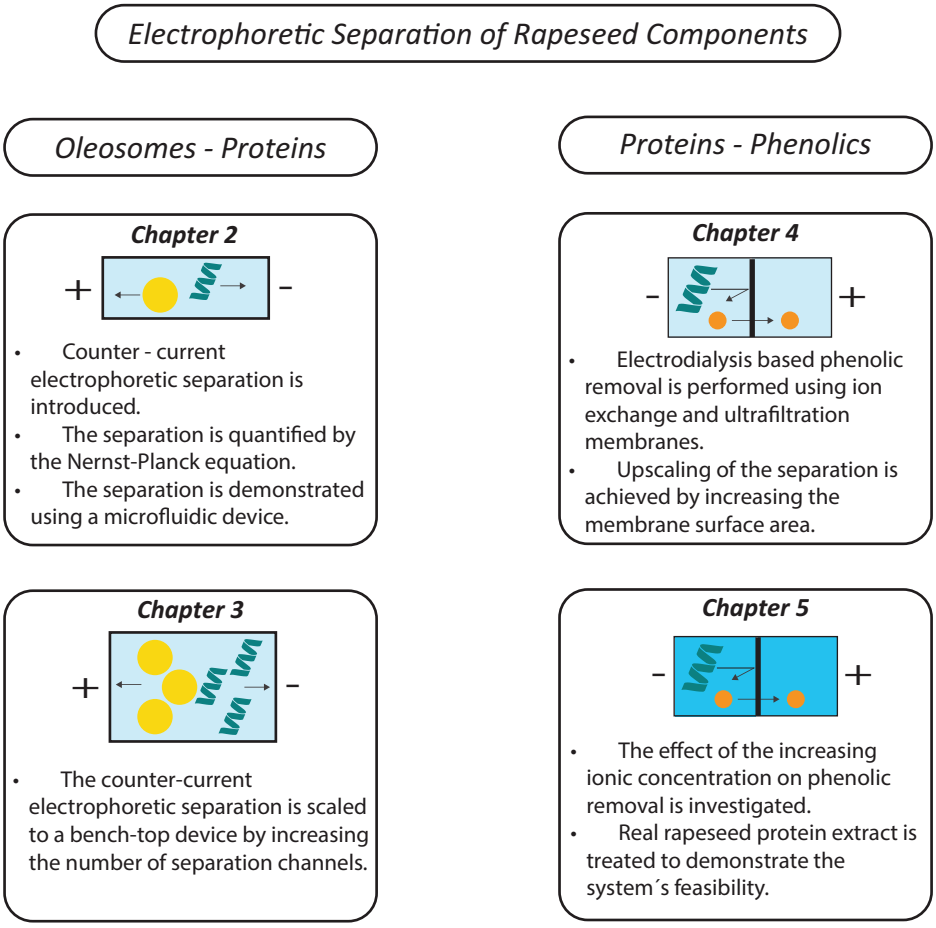

Figure 1.4: General overview of the thesis.

CHAPTER 2

Continuous counter-current electrophoretic separation of oleosomes and proteins from oilseeds

This chapter has been published as:

Ayan, K., Ganar, K., Deshpande, S., Boom, R. M., & Nikiforidis, C. V. (2023). Continuous counter-current electrophoretic separation of oleosomes and proteins from oilseeds. *Food Hydrocolloids*, 144, 109053.

ABSTRACT

Oilseeds, with their high content of oil and protein, will play an important role in the transition to plant based foods. Currently, seed oil extraction involves elevated temperatures and the use of organic solvents, which degrade the quality of both oils and proteins. To take full advantage of the oilseeds, a gentler process is needed. We here propose a mild alkaline extraction followed by a continuous electrophoretic separation process that is based on differences in electrophoretic mobility and recovers intact oleosomes and proteins from the seeds. Rapeseed oleosomes and proteins are both negatively charged at pH ≥ 5, yet exhibit significantly different electrophoretic mobility. Therefore, separation can be achieved by imposing a counter-current hydrodynamic flow rate between their electrophoresis rate. Thus, the compounds with higher mobility, oleosomes, are retained by the electric field, and the compounds with lower mobility, proteins, go along with the flow. The separation was modeled using the Nernst-Planck equation and demonstrated using a PDMS-based microfluidic system. Both the modeling and the experimental studies confirmed that the direction and rate of migration of the compounds can be steered by the electric field strength and the convective flow velocity. The proposed electrophoretic approach is feasible and scaleable, and may be a novel path to separate differently charged components under mild conditions, thereby preserving their original native properties.

2.1. INTRODUCTION

Oilseeds are valuable crops with an annual production rate exceeding 600 MT (USDA, 2022; Zhou et al., 2020). The current practices in oil extraction hinder the complete use of the oilseeds as they cause irreversible changes in the structure of both natural oil-storing organelles (oleosomes) and the remaining proteins, due to the combination of the use of organic solvents and high temperature (hot pressing and desolventizing) during the process (Fetzer et al., 2020; Ntone et al., 2020; Salazar-Villanea et al., 2016). In fact, intact oleosomes are highly stable natural oil-in-water vesicles that store triacylglycerols (TAGs) in a phospholipid–protein protective monolayer and can replace man-made emulsions used in food systems (Nikiforidis, 2019). Undenatured oilseed proteins exhibit comparable functionalities as animal proteins, such as foaming and emulsifying, which are important to create desired food structures (Tan et al., 2011). To recover intact oleosomes and undenatured proteins from oilseeds, a novel approach must be devised that avoids the use of adverse processing conditions.

As an alternative to conventional oil extraction, milder fractionation processes have been suggested, in which water is used as an extraction medium to simultaneously extract intact oleosomes and proteins (Berghout et al., 2014; Nikiforidis & Kiosseoglou, 2009; Ntone et al., 2020). The obtained extract is a mixture of oleosomes and proteins, which are then separated through a centrifugation step to collect oleosome-rich (light) and protein-rich (heavy) fractions. However, this centrifugation step is capital intensive, and requires significant maintenance and copious amounts of water when applied on industrial scales (Najjar & Abu-Shamleh, 2020; Romero-Guzmán, Jung et al., 2020; Rosenthal et al., 1996; Torres-Acosta et al., 2019).

In this work, we report on the fractionation of oleosomes and proteins with steady-state, counter-current electrophoresis. Using an electrical driving force has the advantages that (i) it is an efficient and selective driving force by acting only on individual charged particles instead of the complete suspension (Buszewski et al., 2013; Manouchehri et al., 2000), and (ii) it provides an opportunity to develop a continuous separation process when combined with a pressure-driven flow (PDF). In our case, the separation is accomplished as a net result of electrophoresis and a counter-current PDF. When the PDF velocity is set between the electrophoresis rates of the components to be separated, those with higher electrophoretic mobility are retained by the electric field, while the lower-mobility particles are taken up by the PDF (Kenyon et al., 2012; Meighan et al., 2009).

As a model system, we used rapeseed oleosomes and rapeseed storage proteins, cruciferins (12S globulins) and napins (2S albumins). Cruciferins are hexamers with a molecular weight ranging between 230 and 300 kDa and an estimated radius of 4.4 nm. On the other hand, napins are monomeric proteins with molecular weight of 12 - 17 kDa and an estimated radius

is 1.7 nm (Ntone et al., 2021; Östbring et al., 2020). The separation principle is demonstrated with a simple mathematical model using the Nernst – Planck equation that predicts the concentration change of a compound under the influence of diffusion, electrophoresis, and convection (PDF). The properties of the components are characterized, and microfluidic devices are then used to experimentally demonstrate the feasibility of the principle. We conclude with an outlook towards upscaling the principle to larger scales.

2.2. THEORY

The proposed system employs an electric field over a porous barrier, which is required to guarantee a homogeneous flow rate. We assume that the pores in the barrier are cylindrical and parallel to the electric field. At the same time, a counter – acting PDF is imposed. If the magnitude of the PDF velocity is adjusted in between the electrophoretic migration rate of two compounds, the compound with a lower electrophoresis rate will pass through the channel with the flow, while the other compound with a higher electrophoresis rate will be retained by the electric field. The electrophoresis rate ($v_{E,i}$) is equal to the product of the electrophoretic mobility (μ, µmcm/Vs equivalent to 10^{-8} m^2/Vs) and the applied electric field strength (E, V/cm) (Equation 2.1).

$$v_{E,i} = \mu_i \cdot E \qquad \text{Equation (2.1)}$$

Figure 2.1 illustrates the separation of two negatively charged particles (Particle 1 and 2) in the case of $\mu_1 > \mu_2$. The principle can be understood with the Nernst-Planck equation (Equation 2.2) that describes the transport of compounds resulting from the combined effects of convective flow (PDF), an electric field, and diffusion arising from a concentration gradient (Moshtarikhah et al., 2017). We assume that sufficient electrolytes are present and that the effects of ionic interactions between the compounds can be neglected. Further nonidealities in the system are neglected as well.

$$N_i = -D_i \frac{dC_i}{dx} - D_i \frac{C_i z_i F}{RT} \frac{d\phi}{dx} + C_i v \qquad \text{Equation (2.2)}$$

Here, N_i is the mass flux (kg/m^2·s) of component i, D_i is the diffusion coefficient of the compound i, C_i is the concentration (kg/m^3) of the compound i, x is the channel length (m), z_i is the charge number of the compound i, F is Faraday's constant, R is the universal gas constant, T is the absolute temperature (K), ϕ is the electric potential (V) and v is the flow velocity (m/s). In Equation (2.2), diffusive, electrophoretic, and convective contributions are represented by the terms of $-D_i \frac{dC_i}{dx}$, $-D_i \frac{C_i z_i F}{RT} \frac{d\phi}{dx}$ and $C_i v$, respectively.

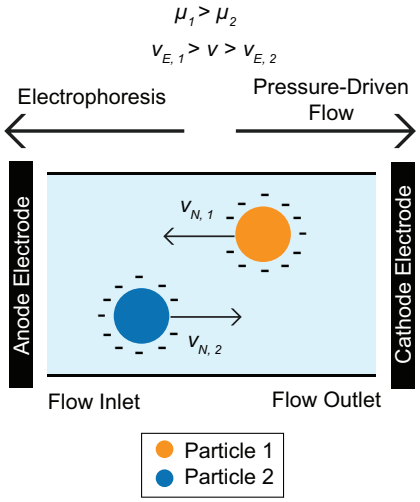

Figure 2.1: Illustration of the designed electrophoretic separation system in case of negatively charged particles exhibited different electrophoretic mobility. μ: Electrophoretic mobility, v_E: Electrophoresis rate, v: Pressure driven flow velocity, v_N: Sum of v_E and v.

Equation (2.2) can be simplified by noticing that the term of $-D_i \frac{C_i z_i F}{RT} \frac{d\phi}{dx}$ is the driving force that induces an electrophoretic migration of the component i ($v_{E,i}$), and we can use an overall mass balance as a boundary condition, given that N_i must be equal to the product of the concentration at the end of the channel (C_{iL}) and the net velocity of the component i (v_i). Therefore, Equation (2.2) can be expressed as Equation (2.3);

$$C_{iL} v_i = -D_i \frac{dC_i}{dx} + C_i (v_{E,i} + v) \qquad \text{Equation (2.3)}$$

This inhomogeneous ordinary differential equation can be solved using two boundary conditions. The first boundary condition is the concentration of the component is equal to its initial concentration ($C_i = C_{i0}$) at $x = 0$ (inlet of the separation channel), and the second one is the flux at $x = L$ (outlet of the separation channel) is equal to product of the final concentration of the component and the flow velocity ($N_i = C_{iL} \cdot v$) as the component i is captured by the solvent flow at the end of the channel. When Equation (2.3) is solved using these boundary conditions, the following relation (Equation 2.4) between the initial and the final concentration of the component i is obtained;

$$\frac{C_{iL}}{C_{i0}} = \frac{v_{E,i} + v}{v + v_{E,i} e^{\frac{-x(v_{E,i}+v)}{D_i}}} \qquad \text{Equation (2.4)}$$

Equation (2.4) gives us the concentration of the component *i* over the separation channel. The relation can be simplified by considering that the exponential term is very large when $v + v_{E,i} << 0$, and therefore the concentration of the component *i* on the downstream side will be very low. If $v + v_{E,i} >> 0$, then the exponential term is very small and can be neglected. Therefore, Equation (2.4) might be approximated by Equation (2.5);

$$\frac{C_{iL}}{C_{i0}} = \begin{cases} 0 & when \quad v + v_{E,i} < 0 \\ \dfrac{v_{E,i} + v}{v} & when \quad v + v_{E,i} > 0 \end{cases} \qquad \text{Equation (2.5)}$$

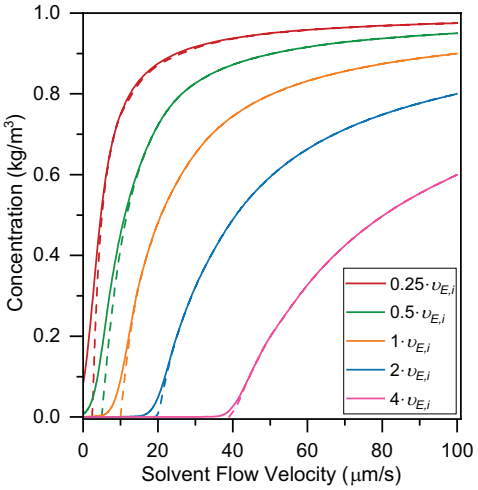

Figure 2.2: Typical concentrations in the downstrem side (C_{iL}) of the separation channel for different values of the electrophoretic velocities ($v_{E,i}$) predicted by Equation (2.4) (solid lines). The concentrations are also quite well approximated with Equation (2.5) (dashed lines).

As Equations (2.4) and (2.5) show, the separation is dominated by the relation between *v* and $v_{E,i}$, and $C_{i,L}$ can be predicted from the ratio of $v/ v_{E,i}$. When the value of *v* is larger (in absolute value) than $v_{E,i}$, the component *i* should pass the channels, but if *v* is smaller than $v_{E,i}$, then the component *i* should be retained by the electric field. Figure 2.2 shows the typical concentrations obtained for components with different $v_{E,i}$ values at the channel outlet predicted by both Equation (2.4) and Equation (2.5). Figure 2.2 indicates that Equation (2.5) provides a good approximation.

The separation of components based on their electrophoretic mobility and a counter-current flow as described in Equation (2.4) can be applied to the separation of oleosomes and proteins. Further insight into the degree of separation can be obtained by defining the selectivity of the separation as the ratio of the content of the proteins and the oleosomes in the outlet stream ($C_{proteins,L}$ and $C_{oleosomes,L}$) normalized with their initial concentrations ($C_{proteins,0}$ and $C_{oleosomes,0}$) (Equation 2.6);

$$Selectivity = \frac{\frac{C_{proteins,L}}{C_{proteins,0}}}{\frac{C_{oleosomes,L}}{C_{oleosomes,0}}} = \frac{C_{proteins,L}}{C_{proteins,0}} \cdot \frac{C_{oleosomes,0}}{C_{oleosomes,L}} \qquad \text{Equation (2.6)}$$

By regarding the system in one dimension, we neglect effects from the non-uniform Poiseuille (parabolic) flow, so we assumed the PDF velocity is the same throughout the channel. The convection term ($c_i v$) in the case of continuous electrophoresis systems is a combination of the PDF and electroosmotic flow (EOF). EOF is a bulk fluid motion caused by the surface potential of channel walls (Lim & Lam, 2021), and depends, amongst others, on the ionic strength and the properties of the channel wall. For matter of simplicity, we here neglected the EOF effects as well. Any temperature changes due to joule heating could cause alterations in the solvent viscosity and the electrophoretic mobility of the compounds, but they were also neglected.

Overall, the input parameters for the modelling of the electrophoretic separation of oleosomes and proteins are v (m/s), E (V/m), D_i (m²/s), $C_{i,0}$ (kg/m3), μ_i (m²/Vs) and z_i. The diffusivity D_i can be experimentally measured or estimated using Equation (2.7).

$$D_i = \frac{kT}{6\pi\eta R_i} \qquad \text{Equation (2.7)}$$

In which k is the Boltzmann constant (1.3806·10-23 m²·kg/ s²·K), η is the dynamic viscosity of the medium (Pa·s) and R_i is the hydrodynamic radius (m) of component i. For relatively simple ionic components the valency, z_i, will be known; for more complex components such as oleosomes, the valency can be estimated using the electrophoretic mobility and the diffusivity (Equation 2.8).

$$z_i = \frac{\mu_i RT}{D_i F} \qquad \text{Equation (2.8)}$$

2.3. MATERIALS AND METHODS

2.3.1. Materials

The rapeseeds that were used for oleosome and protein extraction were of the Alizze variant (*Brassica napus*) and were kindly provided by a seed breeder. All chemicals used were analytical grade and purchased from Sigma Aldrich (St. Louis, MO, USA). Deionized water (Milli-Q, Merck Millipore, Darmstadt, Germany) was used to prepare all solutions and dispersions.

2.3.2. Extraction of oleosomes and proteins from rapeseeds

Oleosomes and proteins were extracted from rapeseed following the methods described by Romero-Guzmán, Vardaka et al., (2020) and Ntone et al., (2021) with some modifications. Briefly, 100 g of rapeseeds were dispersed in deionized water at 1:8 (w/w) ratio and the pH of the dispersion was adjusted to 9.0 by adding 1.0 M NaOH. The dispersion was stirred at 400 rpm for 4 h at room temperature. Then, the dispersion was blended at 7200 rpm (Thermomix TM31, Utrecht, the Netherlands) for 90 s, and the slurry was collected. To remove much of the solids, a twin-screw press (Angel 7500, Naarden, the Netherlands) was used and the juice that contains the oleosomes and proteins was collected. The pH of the juice was re-adjusted to 9.0 by adding 1.0 M NaOH and it was centrifuged at 10,000 g and 4°C for 30 min (Sorvall Lynx 4000 Centrifuge, Thermo Scientific, USA). The centrifugation resulted in three layers: the oleosome – rich cream (top layer), a protein extract (middle part) and a fibre-rich residue (precipitant). To further purify the oleosomes, co-extracted proteins and other compounds were washed out twice by dispersing the oleosome cream in 0.1 M $NaHCO_3$ at 1:4 (w/w) ratio and centrifuged at 10,000 g and 4°C for 30 min to obtain the washed oleosome cream. To remove traces of $NaHCO_3$, the collected oleosome cream was washed once with deionized water in the same conditions. Finally, the purified oleosome cream was collected and stored at 4°C prior to further analysis.

To isolate cruciferins and napins from the protein extract, a combination of ultrafiltration and diafiltration systems (Vivaflow 200, Sartorius, Germany) was used. Firstly, an ultrafiltration set-up with a 100 kDa MWCO PES membrane was used, and the retentate and the filtrate were collected. The retentate was dialyzed against deionized water for 72 h at 4°C to remove any present salts, and used as a cruciferins extract. Napins and other smaller molecules (phenolics etc.) were collected in the filtrate. To remove phenolic compounds and salt, the filtrate was diafiltrated through a 5 kDa MWCO PES membrane until a transparent filtrate was obtained. The obtained retentate was used as a napins extract. Both cruciferins and napins extracts were freeze-dried (Epsilon 2-10D LSCplus, Martin Christ, Germany) and stored at -20°C prior to further analysis.

2.3.3. Chemical and physical characterization of the extracted oleosomes and proteins

2.3.3.1. Composition analysis of the extracted oleosomes and proteins

The total oil content of the oleosomes was measured using Soxhlet extraction method (B-811 Büchi Extractor, Switzerland) using petroleum ether as a solvent. First, the oleosome cream was dried at 60°C for 24 h and 1 g of dried oleosome cream was extracted for 3 h; then the extracted oil was collected and weighed. Equation (2.9) was used to calculate the total oil content on a dry basis.

$$Oil\ Content(wt\%) = \frac{Amount\ of\ extracted\ oil\ (g)}{Amount\ of\ dry\ unextracted\ sample\ (g)} \cdot 100\% \qquad \text{Equation (2.9)}$$

The total protein content in the defatted oleosome cream and protein isolates was measured using the Dumas method (Rapid N exceed, Elementar, Germany) using a nitrogen conversion factor of 5.7 to calculate the total protein content. For the analysis, aspartic acid was used as a standard, O_2 served as a blank sample and 100 – 150 mg of dried oleosome cream and protein extract were used as samples. The analysis was performed in triplicate and the results were expressed as mean ± the standard deviation.

2.3.3.2. Qualitative analysis of the protein profile

To analyze the proteins in the oleosome and protein extracts, Sodium Dodecyl Sulfate Polyacrylamide Gel Electrophoresis (SDS-PAGE) was used both under reducing and non-reducing conditions. Polypeptides are observed according to their overall molecular weight under non-reducing conditions, and subunits of the polypeptides are analyzed under reducing conditions by adding a reducing agent that acts on the disulfide bonds in protein complexes and cleaves them.

SDS-PAGE analysis was conducted as follows: Oleosome and protein samples were prepared to obtain a final protein concentration of 1 mg/mL and 100 µL of this sample was mixed with 250 µL of sample buffer (NuPAGE LDS, Thermo Fisher, the Netherlands). For reducing conditions, 100 µL of reducing agent (NuPAGE Sample Reducing Agent, Thermo Fisher, the Netherlands) was added. Then, the volume was topped to 1 mL by adding deionized water. All samples were first centrifuged at 2000 g for 1 min at room temperature and heated to 70°C for 10 min. After a final centrifugation under the same conditions, the samples (20 µL) were loaded into the SDS – PAGE gel (NuPAGE Novex 4–12% Bis-Tris Gel, Thermo Fisher, the Netherlands). A protein marker (10 µL) (PageRuler™ Prestained Protein Ladder, 10-180 kDa) was used as a standard. To run the system, MES buffer (NuPAGE MES SDS

Running Buffer, Thermo Fisher, the Netherlands) was added to the buffer chamber and the system was operated under 200 V for 30 min. After the electrophoresis, the gel was washed with deionized water for 20 min to remove any residues of the running buffer, and then the gel was dyed overnight with Bio-safe Coomassie Stain (Bio-Rad Laboratories B.V., the Netherlands). Following this, the gel was destained overnight by deionized water. The obtained bands were analyzed using a gel scanner (GS900 Gel Scanner, Bio-Rad Laboratories B.V., the Netherlands).

2.3.3.3. Particle size measurement

The droplet size distribution of the oleosomes was determined using static laser light diffraction (Mastersizer 3000, Malvern Instruments Ltd, UK). The oleosome cream was diluted in deionized water to a concentration of 1.0 wt% for the measurement. The refractive index of the oleosome cream was assumed to be 1.47 and that of water (dispersion phase) to be 1.33. The mean particle size was obtained as a result of three replicate experiments and expressed by both the surface ($d_{3,2}$) and the volume ($d_{4,3}$) weighed mean diameter ± standard deviation (µm). Besides, the particle size distribution was given as volume density (%).

To determine the particle size of the protein extracts (cruciferins and napins), dynamic light scattering (ZetaSizer Ultra, Malvern, UK) was used. Protein solutions of 0.001 wt% concentrations were prepared at different pH values (2.0 – 12.0) and all samples were stirred at 200 rpm for 4 h at room temperature prior to the measurement. The particle size distribution was obtained as a result of three replicate experiments, and the particle size was expressed as the intensity-based mean diameter ± standard deviation (nm). The particle size distributions were given as intensity (%).

2.3.3.4. ζ-Potential measurement

The ζ-potentials of the oleosomes and protein extracts were measured using electrophoretic light scattering (ELS) (ZetaSizer Ultra, Malvern, UK). The electrophoretic mobilities were collected from the same measurements using the following relation (Equation 2.10).

$$\mu = \frac{2\varepsilon\zeta f(\kappa\alpha)}{3\eta} \qquad \text{Equation (2.10)}$$

In which ε is the dielectric constant, $f(\kappa\alpha)$ is Henry's function and η is the viscosity of the suspending medium. To measure the ζ-potential, 0.01 wt% of oleosome suspension or protein solution was prepared using deionized water and the pH of the solutions was adjusted between 2.0 to 12.0 using 0.1 M NaOH and 0.1 M HCl. Then, the samples were stirred at 200 rpm for 2 h and the ζ-potential was measured at 25°C by applying 220 V potential difference. For the refractive indices, 1.47 and 1.59 were used for the oleosomes and the proteins,

respectively, and 1.33 was used for the dispersant (water). The same measurement was done using 1.0 mM potassium phosphate buffer at pH 8.0 as a dispersant. The measurements were done in triplicate using a fresh sample each time to eliminate any detrimental effect of the electric field on particles, like aggregation. The results were converted into electrophoretic mobility and given as average ± standard deviation (µmcm/Vs).

2.3.4. Fabrication of the microfluidic device for the demonstration of the electrophoretic separation

A PDMS-based microfluidic device was fabricated to serve as a micro-scale separation channel that would allow direct observation of the particle movement using a fluorescence microscope. First, a silicon wafer including the channel design was prepared using soft lithography. In brief, a silicon wafer (76 mm in diameter) was coated with SU-8 25 photoresist (Kayaku, MA, USA) to obtain 30 µm final thickness using a two-step spin coating (500 rpm for 30 s and 1800 rpm for 45 s). Then, the wafer was soft-baked overnight at 65°C and cooled down to room temperature for 15 min. Next, the design was printed on the wafer, using a micro-writer device (MicroWriter ML3, Durham Magneto Optics Ltd., Germany) with the exposure energy adjusted to 350 mJ/cm$^{2.}$ The wafer was then post-baked at 65 °C for 2 min, followed by 95°C for 10 min and cooled down to room temperature. To remove the excess uncured photoresist, the wafer was first washed with propylene glycol monomethyl ether acetate (PGMEA), followed by deionized water. To ensure strong adhesion of the printed pattern to the surface, the wafer was baked at 120°C for 20 min. Finally, the unprinted side of the wafer was glued to a petri dish to be used as a mold for microfluidic chip fabrication.

To make PDMS devices, PDMS and a curing agent (SYLGARD™ 184 Silicone Elastomer) were mixed at a 10:1 (w/w) ratio for 15 min under continuous rotation at 60° and 20 rpm. Since the mixing process traps air bubbles, a short centrifugation step at 100 rpm for 2 min at room temperature was carried out to remove the trapped air. The prepared PDMS mixture was poured onto the printed mold wafer, placed in a vacuum chamber, and degassed. After removing all air bubbles, the wafer with the PDMS was baked at 70°C for 4 h. To obtain a homogenous surface in the channels, glass slides were coated with PDMS. For this purpose, PDMS (approximately 1 - 2 g) was added at the center of the glass slide and spread by spinning at 500 rpm for 30 s and 3000 rpm for 15 s using a spin coater. Similar to the above-mentioned PDMS curing, the glass slides were also baked at 70°C for 4 h. The cured PDMS was peeled off from the wafer, and individual channels were cut out from the whole PDMS layer. Two 0.75 mm holes to serve as inlet and outlet were punched on the channels using a biopsy punch. To perform an EOF measurement, 5 mm holes were punched instead of 0.75 mm to serve as reservoirs for the buffer solution. To make a closed channel, PDMS-coated glass slides and the PDMS block with channels were covalently bonded using plasma for 15 s (Plasma Cleaner PDC – 32 G, Harrick Plasma, NY, USA). After 3 h, the channels were coated with 5 % w/v

polyvinyl alcohol (PVA) solution for 2 min to render the surface of the PDMS hydrophilic. Excess free PVA was removed by flushing the channel with nitrogen gas. Lastly, the channels were baked at 120°C for 40 min to fixate the PVA coating. The dimensions of an individual channel were 2 cm in length, 400 µm in width, and 30 µm in depth.

2.3.5. Electroosmotic flow measurement

As aforementioned, EOF is the flow of an electrolyte solution under the influence of an electric field due to the surface charge of the channel walls. To estimate the magnitude of the EOF in the fabricated PDMS channels, the current-monitoring method described by Saucedo-Espinosa & Lapizco-Encinas (2016) was used with some further modifications. This method measures the changes in the current value as a result of the exchange of electrolyte solutions that differ slightly in their ionic concentration due to EOF. Initially, the inlet reservoir and the channel were filled with low ionic concentration electrolyte solution (9.0 mM potassium phosphate buffer) and the outlet reservoir was filled with a higher ionic concentration electrolyte solution (10.0 mM potassium phosphate buffer). A stainless-steel wire was dipped into each reservoir and connected to a high-voltage power supplier (HCN 140 – 20000, Fug, Germany). When a potential difference of 600 V was applied, the current value started to increase as the lower-concentration electrolyte solution started to replace the higher-concentration electrolyte solution, and the overall conductivity in the channel increased. A stationary value indicated that the original electrolyte solution in the channel had been completely replaced. During the experiment, the current value was recorded over time and the total time to reach the plateau value was determined. The EOF velocity (v_{EOF}) was calculated by dividing the channel length (L) by the duration of the solution exchange (Δt) (Equation 2.11). The ratio of to E gives the EOF mobility (μ_{EOF}) (Equation 2.12). The measurements were performed in triplicate and the result was given as average EOF mobility ± standard deviation (µmcm/Vs).

$$v_{EOF}(\mu m / s) = \frac{L(\mu m)}{\Delta t(s)} \qquad \text{Equation (2.11)}$$

$$\mu_{EOF}(\mu mcm / Vs) = \frac{v_{EOF}(\mu m / s)}{E(V / cm)} \qquad \text{Equation (2.12)}$$

2.3.6. Electrophoretic separation of the extracted oleosomes and proteins

To investigate the particle movement under the combined influence of the electrophoresis and the PDF, a microfluidic experimental setup was used. The setup includes an inverted fluorescent microscope (Nikon-Ti2-Eclipse), a pressure pump (OB1 MK3+, Elveflow, France), and a power supply. The oleosomes and the proteins were stained by curcumin (λ_{ex} = 430 nm)

and fast green dye (λ_{ex} = 633 nm) at a ratio of 100:1 (v/v), respectively. The samples were visualized using a pE-300 ultra illumination system and a Nikon 20 x/0.75 NA air objective. All the samples were illuminated at 1–5% laser intensity and time-lapse images were acquired using a Prime BSI Express CMOS camera at an exposure time of 30 ms.

For the demonstration of the separation principle, we used 1.0 mM potassium phosphate buffer at pH 8.0 to eliminate pH fluctuations due to the electrolysis of water to some extent and the experiment duration was limited to 20 s to make sure the pH of the medium remained constant during the analysis. First of all, the samples of oleosomes and proteins were prepared at a concentration of 0.01 wt% in the buffer. Then, the sample was introduced into the micro-channel using the pressure pump connected to PDMS channel with 0.5 mm ID silicone tubing and 25 µm ID flow resistor tubing. Two metal fittings were attached to the channel inlet and outlet to serve as electrodes. Both metal fittings were connected to the power supply using crocodile clips. Once the channel was filled with the sample, the flow velocity and potential difference were adjusted to the desired values.

Before the experiment, the oleosomes and the proteins were analyzed under (i) constant pressure (50 mBar) and a stepwise increase of electric field (0 – 100 V/cm) and (ii) constant electric field (50 V/cm) and a stepwise increase of pressure (0 – 200 mBar) to reveal the movement direction and net velocity of the particles under specific conditions. The combination of the electric field and the pressure difference that caused the oleosomes and the proteins to move in opposite directions was used for the separation experiment. The movement of the particles was recorded at a rate of 1 frame per second (fps) for each experiment, and the recordings were further analyzed using the particle tracking module in ImageJ software to measure the particle velocities (Schneider et al., 2012). Particles that move near the walls were neglected to eliminate the effects of a parabolic flow profile, so only the particles at or near the center of the channel were tracked.

2.3.7. Statistical analysis

The electrophoretic mobility measurements were performed in triplicates. Statistical analysis was carried out by using SPSS version 25.0 for Windows (IBM Corp. NY, USA) to identify significant differences in the electrophoretic mobility of the oleosomes and the proteins at various pH values. For this purpose, one-way ANOVA and the Tukey test were used. Significance of the differences was assessed based on the 95% confidence limit ($P<0.05$).

2.4. RESULTS AND DISCUSSION

2.4.1. Characterization of the extracted oleosomes and proteins

After the extraction of the rapeseed oleosomes and proteins (cruciferins and napins), their composition and physicochemical properties were determined.

The composition of the oleosome cream was 92.24 ± 5.93 wt% oil and 2.59 ± 0.02 wt% proteins on a dry basis, and protein contents of the extracted cruciferins and napins were 79.19 ± 0.31 wt% and 85.25 ± 0.17 wt% on a dry basis, respectively. SDS-PAGE analysis showed that the oleosome extract was free from any co-extracted rapeseed storage proteins and was dominated by membrane-bound proteins, oleosins (Figure A.2.1, Appendix). The profiles of the protein extracts indicated that the napin isolate was free of cruciferins, however, the cruciferin isolate also included some napins (Figure A.2.1).

The size distribution of the extracted oleosomes at neutral pH is presented in Figure 2.3A. The distribution is bimodal with two peaks at around 0.6 and 5.0 µm ($d_{3,2}$: 1.18 ± 0.26 µm and $d_{4,3}$: 2.76 ± 0.94 µm). The bimodality indicates that some individual oleosomes formed aggregates, probably as a result of flocculation and/or coalescence due to electrostatic and hydrophobic attractive forces (Romero-Guzmán, Petris et al., 2020). Similar observations have been previously reported, where besides individual oleosomes with a diameter of around 1 µm, oleosome aggregates were present as well (diameter > 2.5 µm) (De Chirico et al., 2018; Romero-Guzmán, Köllmann et al., 2020).

The size distributions of the proteins at pH 8.0 are shown in Figure 2.3B. Both size distributions are bimodal as well. In the case of cruciferins, both peaks (~200 and 1200 nm) are far above their reported native size of 8.8 nm which shows the presence of larger cruciferin clusters. The napins extract showed two peaks at around 3 nm and 600 nm which implies the presence of both native napins (3.4 nm) and napin aggregates. The protein aggregation might have been induced by the extraction/purification conditions, like agitation speed, pH, pressure and freeze drying (Callahan et al., 2014; Li et al., 2020; Mahler et al., 2009). In a practical sense, the formation of larger protein particles makes the observation of the proteins under a fluorescent microscope much easier, but one has to bear in mind that these aggregates may have different mobility than molecularly dissolved proteins.

To evaluate the suitability of the proposed electrophoretic separation system for rapeseed oleosomes and proteins, their electrophoretic mobilities were measured at pH values from 2.0 to 12.0, as shown in Figure 2.4. Both the oleosomes and the proteins have very close isoelectric points, between pH values of 4.0 and 6.0, where the particles carry zero net charge, so both are charged either positively or negatively at any pH. This means that they should move in the same direction under the influence of only an electric field.

However, the electrophoretic mobility of the oleosomes is much greater than that of the proteins at pH ≥ 5.0 ($P<0.05$). The largest difference was 3.61 µmcm/Vs at pH 11.0, but the difference remains in the same range between pH 7.0 and 12.0. The larger mobility of the oleosomes may be because of their higher surface charge than proteins, but may also arise from the fact that larger particles, like oleosomes, exhibit lower hydrodynamic frictional forces relative to their volume (van Oss, 1975).

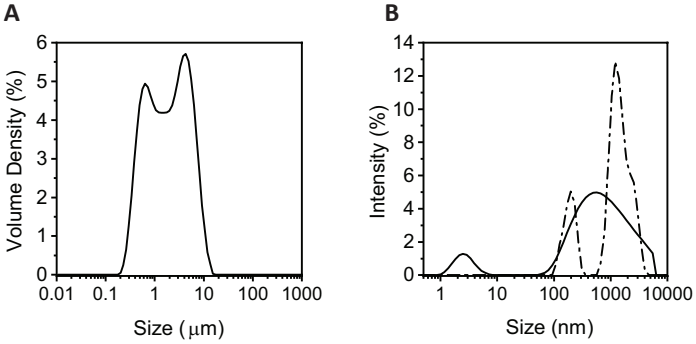

Figure 2.3: A) Size distribution of the extracted oleosomes at pH 7.0 B) Size distribution of the extracted cruciferins (dashed line) and napins (solid line) at pH 8.0.

The results indicate that the oleosomes and the proteins can be separated using the electrophoretic separation system. For example, at pH 8.0 with a 10 V/cm electric field and a 30 µm/s counter–current flow velocity, the oleosomes will move under the influence of the electric field with a net velocity of -21.9 µm/s, while the proteins have a net velocity of +13.7 µm/s and are dragged along by the solvent flow.

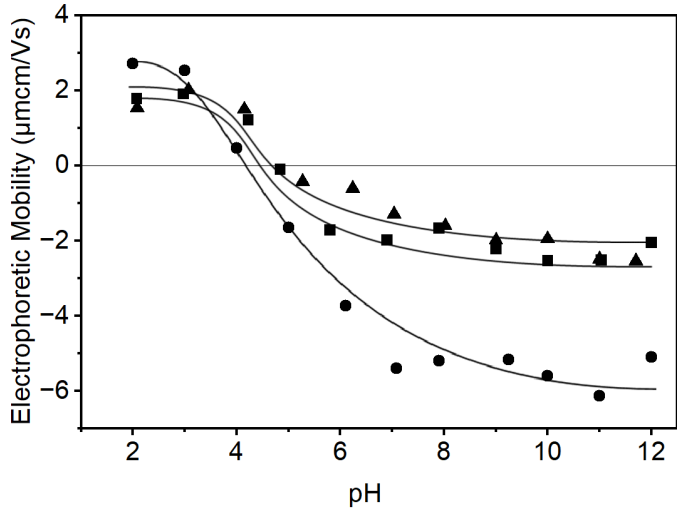

Figure 2.4: Electrophoretic mobility of oleosomes (●), cruciferins (■) and napins (▲) at pH 2.0 – 12.0. Solid lines are guide for the eyes.

For the experimental demonstration, pH 8.0 was selected since it provides a significant difference in the electrophoretic mobility and is still a mild pH. A buffer system was used to minimize the effects of electrolytic reactions during the experiment. The electrophoretic mobilities of the extracted oleosomes, cruciferins and napins in 1.0 mM potassium phosphate buffer were determined as -3.205 ± 0.136, -1.942 ± 0.169 and -1.266 ± 0.211 µmcm/Vs, respectively. The electrophoretic mobility of the oleosomes was 1.5-fold lower than when dispersed in the buffer. The main reason for this is the increasing ionic strength screening the surface charges (Semenov et al., 2010).

2.4.2. Interpretation of the experimental parameter values

The electrophoretic mobility measurements revealed that the oleosomes and the proteins have different electrophoretic mobilities at most pH values, which indicates that their electrophoretic separation is achievable. This can be further quantified by using the Nernst – Planck equation (Equation 2.4). Table 2.1 shows the data used and Figure 2.5 summarizes the findings.

Table 2.1: Electrophoretic mobility, particle size, charge number and diffusion coefficient values for oleosomes, cruciferins and napins at pH 8.0 and 1.0 mM potassium phosphate buffer.

Compound	Electrophoretic Mobility ($m^2/V \cdot s$)	Radius (m)	Charge Number (z)	Diffusion Coefficient (D_i) (m^2/s)
Oleosomes	$-3.205 \cdot 10^{-8}$	$1.38 \cdot 10^{-6}$	-5203.55	$1.58 \cdot 10^{-13}$
Cruciferins	$-1.942 \cdot 10^{-8}$	$7.60 \cdot 10^{-7}$	-1735.28	$2.87 \cdot 10^{-13}$
Napins	$-1.266 \cdot 10^{-8}$	$1.84 \cdot 10^{-7}$	-273.69	$1.19 \cdot 10^{-12}$

In Table 2.1, values of the proteins are given not for an individual protein molecule but for larger protein clusters, which probably formed during the extraction process.

In the proposed separation system, the components with low electrophoresis rate relative to the PDF velocity, are expected to flow toward the downstream side, which can be called a permeate. The original feed will become enriched in components with a high electrophoresis rate relative to the PDF velocity, and exit the system as a retentate. The former category will comprise the proteins, while the oleosomes accumulate in the retentate. To be successful, the separation requires the right balance between the applied electric field and the convective flow applied.

We can now combine the model with the values of the electrophoretic mobilities that we measured. If we assume a channel length of L = 100 µm and a PDF velocity of v = 50 µm/s, introducing the electric field leads to a reduction of the concentration of the oleosomes and the proteins in the permeate. Figure 2.5A shows the effect of increasing the electric field on

the outlet concentrations of the oleosomes and the proteins. Their full retention starts at different values of the electric field strength. The oleosomes, having higher electrophoretic mobility, are the first compounds completely retained by the electric field at 16 V/cm. Thus, separation between the oleosomes and the proteins is achieved as both cruciferins and napins are still in the permeate. However, an increase of the electric field to 27 V/cm results in the full retention of both oleosomes and cruciferins, with only napins present in the permeate. An even further increase of the electric field to 46 V/cm results in a full retention of both oleosomes and proteins. In the last case, electrophoresis dominates the hydrodynamic flow, and no separation results.

Similarly, if we set the electric field at 50 V/cm and vary the convective flow velocity, we achieve full retention of the components at low flow rates, and a breakthrough at different flow rates, depending on the individual electrophoretic migration rates of the components. Figure 2.5B shows that a flow velocity exceeding 100 µm/s initiates the separation as only the proteins are present in the permeate. To drag the oleosomes to the outlet, at least 160 µm/s solvent flow is needed. Therefore, a flow velocity between 100 and 160 µm/s ensures the separation at 50 V/cm electric field. A further increase in the flow velocity, however, blocks the separation since the electric field leads to accumulation of the oleosomes together with the proteins in the permeate. This effect is escalated at even larger flow rates. Therefore, the correct balance between the PDF and the electric field is required.

The relation between oleosome – protein separation selectivity and the solvent flow velocity can be seen in Figure 2.5C. At a lower flow rate the selectivity is very large, but the concentrations passing through to the permeate are also vanishingly small. A selectivity value approaching infinity indicates the concentration of oleosomes in the outlet stream is zero. This can be seen around 160 µm/s flow rate. An increasing solvent flow velocity decreases the selectivity, and a mixture of the oleosomes and the proteins is then collected in the downstream.

Overall, the analysis illustrates that the continuous electrophoretic separation system can indeed lead to the separation of rapeseed oleosomes and proteins.

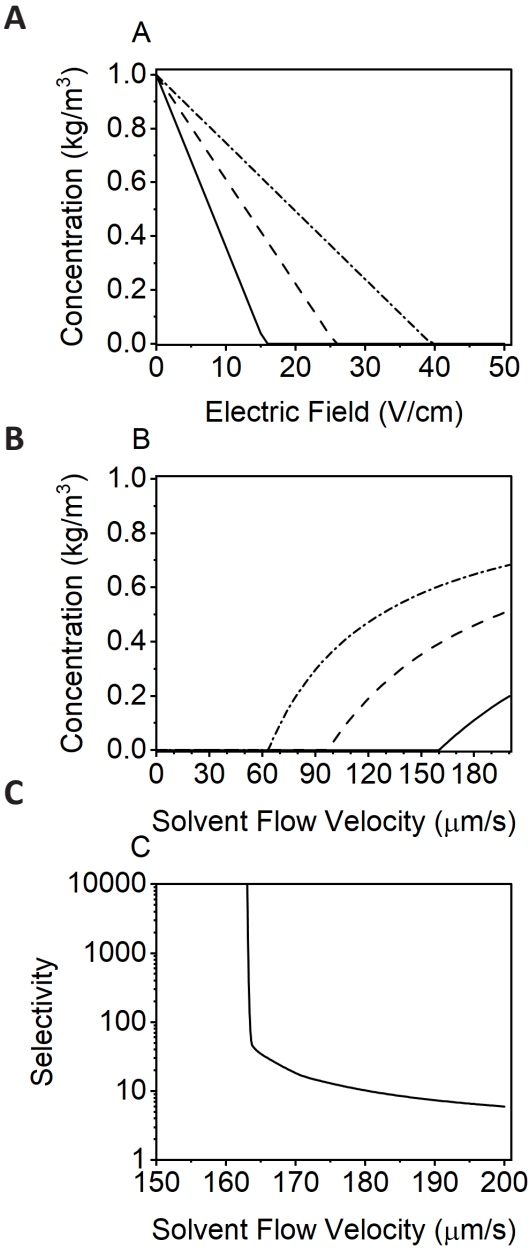

Figure 2.5: Predicted concentrations of oleosomes (—), cruciferins (- -) and napins (·-·) in the permeate under A) increasing electric field and 50 μm/s constant solvent flow velocity, and B) increasing solvent flow velocity and 50 V/cm constant electric field. C) Selectivity of the separation under increasing solvent flow velocity and 50 V/cm constant electric field.

2.4.3. Electrophoretic separation of the extracted oleosomes and proteins

The analysis above clearly indicated that the movement direction of the compounds is governed by the balance between the electric field strength and the flow velocity, and specific combinations of these two can drive the separation. To experimentally confirm this, we utilized a microfluidic device and observed the movement of the oleosomes and the proteins under the influence of the electric field and the PDF through a fluorescent microscope (Figure 2.6A).

We first determined net velocity of the oleosomes and the proteins separately as function of the applied pressure (flow rate) and the electric field strength. The net velocity of the compounds was detected experimentally by analyzing the track of the particles in the recorded movies. The experimental results were compared to the theoretical net velocity values that are predicted by summing up electrophoresis rate, PDF velocity and EOF velocity. EOF mobility was measured as 0.35 ± 0.11 µmcm/Vs, and multiplying this with the electric field gives the EOF velocity (Equation 2.12). Positive values of the velocity in Figure 2.6B and C represent the direction of the PDF, and negative values represent the electrophoresis direction.

Figure 2.6B shows the net velocity of the compounds under pressure differences ranging from 0 to 200 mBar (~0 – 160 µm/s) and a constant electric field of 50 V/cm. It can be seen that the proteins under 100 mBar pressure are dragged along by the solvent flow as they do not have enough electrophoretic velocity to counteract the convective flow. Under 100 mBar, the oleosomes have sufficient electrophoretic velocity to counteract the PDF and thus reverse their direction towards the electric field. This was also observed at 150 mBar pressure. Therefore, under 50 V/cm electric field, separation can be achieved between 100 – 150 mBar pressure, which results in 100 – 140 µm/s convective flow velocity including the EOF. The Nernst-Planck equation indicated a convective flow velocity ranging between 100 – 160 µm/s under 50 V/cm electric field ensures the separation, which is in good agreement. At a pressure of 200 mBar (total convective flow velocity: ~180 µm/s) the separation is impaired as some of the oleosomes start to get captured by the solvent flow as well.

At 200 mBar pressure, we observed unstable motion of both the oleosomes and the proteins. This may be caused by pH instabilities due to the ingression of electrolysis products, like H^+ ions, from the anode electrode into the separation channel (Agostino et al., 2014; Rudge & Monnig, 2000). The electrophoretic mobility of the oleosomes is more sensitive to pH changes than that of the proteins (Figure 2.4). To avoid these complications, the pressure difference was limited to 150 mBar. In a larger – scale separator, care can be taken that no electrolysis products are added to the system, for example by using flushed electrodes. However, as the microfluidic system was only meant to demonstrate the principle, this was not implemented; nor would it have been practically feasible. Therefore, we only employed moderate electric fields, allowing separation without introducing significant pH differences.

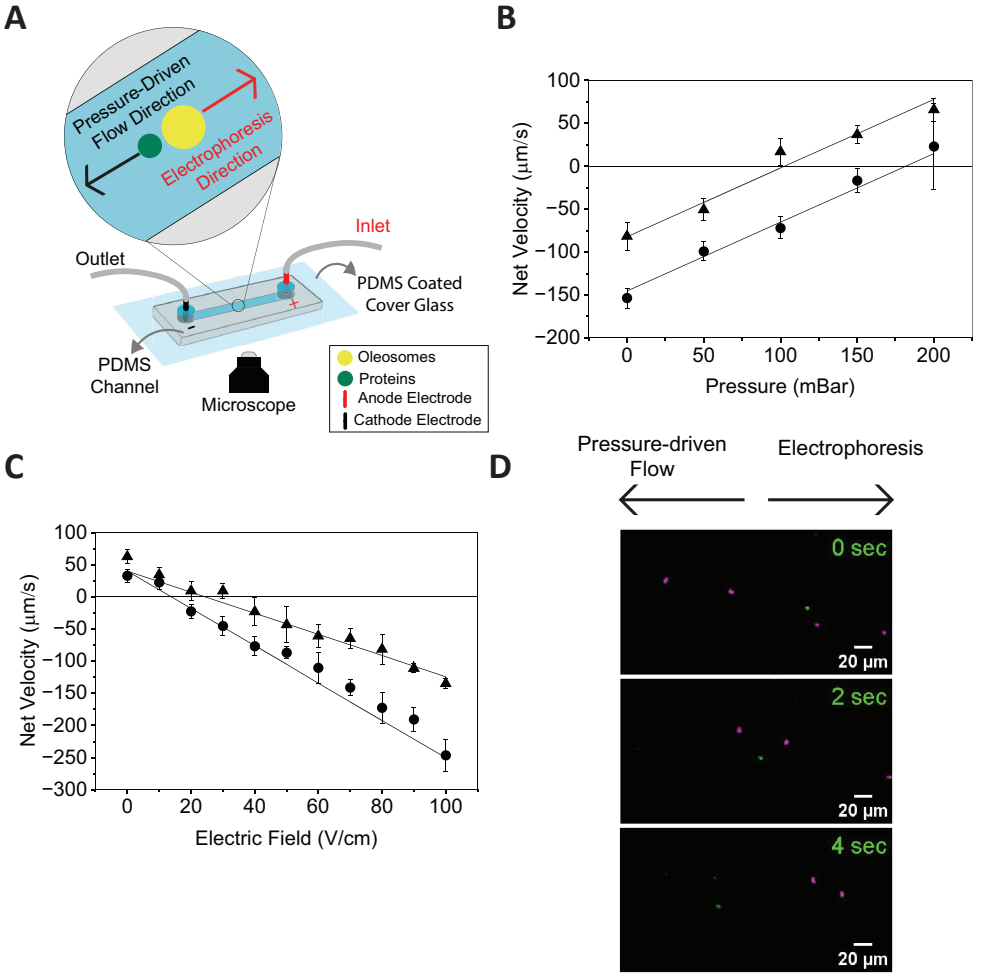

Figure 2.6: A) Schematic of the experimental setup B) Net velocity of the oleosomes (●) and the proteins (▲) under increasing pressure and constant electric field of 50 V/cm and C) increasing electric field and constant pressure of 50 mBar. Lines represents the predicted net velocity taking into account electrophoresis, pressure-driven flow and electroosmotic flow. Positive and negative values represent direction of pressure-driven flow and electrophoresis, respectively. D) Movement of the oleosomes and the proteins under 120 mBar pressure and 50 V/cm electric field at time 0, 2 and 4 s. Oleosomes (magenta) and proteins (green) were visualized by curcumin (λ_{ex}= 430 nm) and fast green dye (λ_{ex}= 633 nm), respectively. Electrophoresis (right) and pressure-driven flow (left) are acting in the opposite direction.

Besides the effects of increasing convective flow velocity, a variation of the net velocity under increasing electric field strength under constant pressure of 50 mBar can be seen in Figure 2.6C. Separation can be observed under an electric field value of 20 – 30 V/cm and a flow velocity of approximately 50 µm/s. This finding is also in good accordance with the Nernst-Planck equation, which predicted separation with an electric field of 16 – 27 V/cm in case of 50 µm/s convective flow velocity. The equation can therefore adequately estimate the necessary electric field strength and convective flow velocity for the separation.

The experimental demonstrations highlight that the convective flow velocity is actually a combination of PDF and EOF. The fact that EOF generally results in a stronger plug flow than pressure driven Poiseuille flow (parabolic flow profile) may make the prediction by the Nernst-Planck equation and the experimental realization better than with pure PDF. In a larger-scale separator, the EOF may be utilized to generate flow without applying pressure; otherwise, their combination should be adjusted to achieve the right convective flow velocity. In our microchannel, we experimentally set the pressure such that the right convective flow is generated. The alignment between the calculated lines and the experimental data points in Figure 2.6B and C indicated this was done properly.

To directly observe the separation in the microchannel, a pressure difference of 120 mBar and an electric field strength of 50 V/cm were chosen as this combination caused the oleosomes and the proteins to move in the opposite direction with similar velocities. The separation was visualized using a fluorescent microscope and time-lapse images are presented in Figure 2.6D. The directions of solvent flow and electrophoresis are to the left (cathode electrode) and to the right (anode electrode), respectively. The initial positions of the compounds are shown at t = 0 s, and the changing positions are given at the 2^{nd} and 4^{th} seconds. Figure 2.6D shows the oleosomes moving in the direction of electrophoresis and the proteins moving in the direction of convective flow. During the separation, the net velocity of the oleosomes was detected as -37.29 ± 5.29 µm/s, and the net velocity of the single protein particle was 22.99 µm/s.

Overall, we proposed a new mechanism for separation of rapeseed oleosomes and proteins with a relatively simple model and could microscopically observe the separation itself using a microfluidic channel. We expect that the principle can be scaled up to larger processes by using a larger array of channels, for instance using a porous barrier. In an upscaled version, electrodes can be positioned on both sides of the porous medium to form an electric field. And, a convective flow can be introduced either using the pressure difference between the sides of the porous barrier or taking advantage of the electroosmotic flow. Given this approach, the electrophoretic separation system can be upgraded by utilizing electrochemical cells or electrodialysis systems. By retaining the balance between the electric field and

the PDF, but increasing their absolute values, one can improve the specific throughput of the system. An important practical issue is the formation of a pH gradient between the anode and cathode electrodes due to electrolysis, which may alter the movement of the oleosomes and proteins. In our microfluidic experiment, we maintained the pH by limiting the recording time to 20 s. Over this short time, the electrolysis products have not yet reached the location of observation. In a larger system, one will have to mitigate the effects, for example by using flushed electrodes, as is often used in electrodialysis.

In practice, the electrophoretic separation system was proposed as an alternative to the centrifuge-based final separation for mild alkaline extraction products of rapeseed. This study utilized purified oleosomes and proteins to demonstrate the separation principle. However, in a real case, multiple compounds, like carbohydrates and phenolics, are present, and a multi-stage separation would be required to recover oleosomes and proteins. To perform the separation with real-life systems, the electrophoretic mobility of each species must be determined. Besides, further investigation is also needed to understand the interactions between oleosomes and proteins or other extracts at varying concentrations.

2.5. CONCLUSIONS

We demonstrated the principle of separating components with different electrophoretic mobilities in a steady state system by using an electric field antiparallel to the convective flow, creating a counter-current system. This can be best achieved in flow channels or with a porous barrier on larger scales, effectively providing a very large number of channels. The principle was introduced and demonstrated using a simple model based on the Nernst-Planck equation, which shows that separation can be obtained when the convective flow is in between the electrophoretic migration rates of the components to be separated. Measurements of the electrophoretic mobilities of rapeseed oleosomes and proteins revealed that the separation should indeed be possible. The separation was then confirmed by direct observation of the migration of individual components by microscopy and using a microfluidic channel. Also in this device, the differences in electrophoretic migration rates were confirmed. Finally, the separation between the oleosomes and the proteins could be directly observed. The principle of the continuous electrophoretic separation is suitable for upscaling. The number of channels can be increased using a porous barrier containing many individual channels, which also provides higher overall productivity. Since the separation rests on the balance between the convective flow rate and the applied electric field strength through the channel, increasing the latter will also allow for larger flow rates and hence productivity. The current work demonstrates that counter-current electrophoretic separation is possible and feasible with practically relevant systems, such as proteins and oleosomes from rapeseed.

2.6. APPENDIX

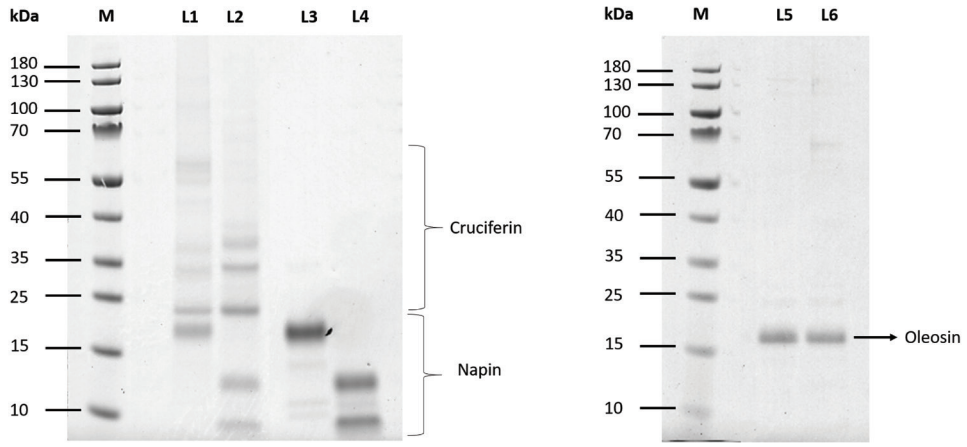

Figure A.2.1: SDS – PAGE electropherograms for the protein isolates and the oleosomes. Lane 1 (L1) – Cruciferins (non-reducing), L2 – Cruciferins (reducing), L3 – Napins (non-reducing), L4 – Napins (reducing), L5 – Oleosomes (non-reducing) and L6 – Oleosomes (reducing). Results: Cruciferins gives various bands ranging from 22 to 60 kDa under non-reducing conditions, and 22, 33 and 37 kDa bands under reducing conditions which are attributed to cruciferin sub-units (Akbari & Wu 2015; Wanasundara 2011). Additionally, cruciferins isolate also includes a band around 17 kDa which dissociates to 12 and 5 kDa under reducing conditions that represents the napins (Ntone et al., 2020). This can also be confirmed by observation of the same bands in napins isolate. For the oleosomes cream, there is one major band around 18 kDa under both non-reducing and reducing conditions. These bands represent oleosin proteins and the single oleosin band is considered as an indicator for purified oleosomes as it proves there is no co-extracted rapeseed storage proteins (Romero-Guzmán, Köllmann et al., 2020).

- The recording belong to Figure 2.6 D can be found through the following link;

https://www.sciencedirect.com/science/article/pii/S0268005X23005994#appsec1

CHAPTER 3

Scaling the electrophoretic separation of rapeseed proteins and oleosomes

This chapter has been published as:

Ayan, K., Boom, R. M., & Nikiforidis, C. V. (2024). Scaling the electrophoretic separation of rapeseed proteins and oleosomes. *Journal of Food Engineering*, 381, 112188.

ABSTRACT

Gentle extraction of ingredients from raw materials is essential for high-quality food ingredients and can lead to reducing the use of water, chemicals, and energy in the extraction. For example, a simple aqueous extraction can yield a mixture of oil, in the form of a natural oil-in-water oleosome emulsion, and proteins. The oleosomes and proteins can then be further separated in a next step. We explored a continuous counter-current electrophoretic process that separates oleosomes and proteins based on their electrophoretic mobility by balancing an electric field with an opposing solvent flow. The separation is accomplished through the retention of the component with the higher electrophoretic mobility, the oleosomes, and the passage of the proteins, having lower mobility. The fluxes of oleosomes and proteins from rapeseed, after aqueous extraction, were analyzed as a function of the electric field (0 - 75 V/cm) and 1.2 ± 0.1 mL/min solvent flow rate. At 50 V/cm, the permeation flux of proteins was 10-fold higher than that of oleosomes, as shown by the selectivity increasing to 9.84 from 1.90 at 25 V/cm. The difference in their flux promises to become more pronounced under an increasing treatment duration, but two main technical limitations, electrolysis-based pH alteration and membrane fouling, restrict further separation. We expect the listed challenges can be mitigated with the addition of electrode rinse chambers and the use of larger pore size membranes.

3.1. INTRODUCTION

Mitigation of the environmental impact of food manufacturing by replacing animal-based ingredients with plant-based ones has become increasingly significant (Knorr et al., 2020). In this perspective, technologies for the extraction and isolation of valuable constituents like proteins from plant matrices are key (Herrero et al., 2015; Munialo, 2023; Pouliot et al., 2014). Current industrial practices generally prioritize the production of highly purified ingredients, leading to unsustainable processing and, in some cases, degraded techno-functional properties such as low solubility due to, for example, denaturation (Ma et al., 2022). Hence, efficient separation processes should be developed that maximize the functionality of the components by preserving their native structure while minimizing the use of hazardous chemicals, water, and energy (Chemat et al., 2020; Liang et al., 2023; Lie-Piang et al., 2023).

As oilseeds are sources of both oils and proteins, an efficient fractionation of oilseeds should be aimed at obtaining both oil - rich (oleosome cream) and protein - rich fractions. Instead of a sequential extraction process which first isolates the oils through mechanical expression and subsequent extraction with an organic solvent, and then solubilizes the protein into an alkaline solution, this can be achieved via a single aqueous extraction that extracts both oils and proteins simultaneously. Oleosomes and proteins can then be separated from each other by centrifugation (Ntone et al., 2020). Although aqueous fractionation allows better use of oilseeds, this approach must be improved regarding resource efficiency as it is still quite intensive in water and energy. Therefore, our focus is on improving the final centrifugation-based separation, as it demands a significant capital investment, requires substantial water and energy consumption, due to high rotational speed, and may require significant operational maintenance. These factors present challenges in the industrial implementation of aqueous fractionation of oilseeds (Berghout et al., 2015; Guzman, 2020; Najjar & Abu-Shamleh, 2020; Szepessy & Thorwid, 2018; Tamborrino et al., 2019).

To develop an enhanced separation process, we investigated the possibility of an electric field-based process as electrical driving forces are more efficient when compared to mechanical and thermal forces (Ptasinski & Kerkhof, 1992). To create the electrical fractionation process, it is necessary to comprehend how an electric field can separate oleosomes and proteins. In a previous paper (Ayan et al., 2023), we demonstrated that a combination of electrophoresis and a solvent flow in the opposite direction of the electrophoresis can separate compounds with distinct electrophoretic mobility, like oleosomes and proteins. The separation makes use of differences in the electrophoresis rate between oleosomes and proteins, which is strongly depended on the pH of the dispersion medium. By using an electric field antiparallel to the flow at pH 8.0, the components with a higher electrophoresis rate (oleosomes) are dragged by the electric field against the flow, while the components with a lower electrophoresis rate (proteins) follow the flow. This principle was shown with a simple mass transfer model,

and was demonstrated practically in a microfluidic device. Here, we bring the micro-scale proof-of-principle to a lab-scale system to show the proposed separation mechanism can be scaled. We used a standard electrochemical cell that contains a sample (retentate) and a buffer (permeate) chamber separated from each other with a porous frit that acts as flow field stabilizer and has large pores to avoid separation by size exclusion. An electrode is placed on each side of the membrane. The fluxes of oleosomes and proteins and selectivity over the frit are evaluated under different combinations of electric field and solvent flow rate, and the selectivity is used to indicate the degree of separation obtained.

3.2. MATERIALS AND METHODS

3.2.1. Materials

The Alizze variant of rapeseeds (*Brassica napus*) was utilized as a source of oleosomes and proteins, and was kindly provided by a seed breeder. All chemicals used were analytical grade and purchased from Sigma Aldrich (St. Louis, MO, USA). All solutions and dispersions were prepared using deionized water (Milli-Q, Merck Millipore, Darmstadt, Germany).

3.2.2. Extraction of rapeseed oleosomes and proteins

Oleosomes and proteins were extracted from rapeseed through an aqueous extraction method described by Ntone et al. (2020) with some modifications. First, crushed rapeseeds were mixed with deionized water at 1:10 (w/w) ratio and the pH was adjusted to 9.0 by adding 1.0 M NaOH. This mixture was agitated at 400 rpm for 4 h at room temperature to extract both oleosomes and proteins into the aqueous phase. Subsequently, the mixture was blended at 7200 rpm (Thermomix TM31, Utrecht, the Netherlands) for 90 s. Then, a twin-screw press (Angel 7500, Naarden, the Netherlands) was used to separate the aqueous phase that contains the extracted oleosomes and proteins from insoluble solids. The collected juice was centrifuged at 10,000 g and 4°C for 30 min (Sorvall Lynx 4000 Centrifuge, Thermo Scientific, USA) after readjusting the pH to 9.0 by adding 1.0 M NaOH. This step was necessary to prevent pH changes due to releasing or removal of some species during pressing. After the centrifugation, the extracted oleosomes accumulate on the top cream layer and the extracted proteins are present in the supernatant part. Besides, a fiber-rich residue is collected as a precipitant.

To purify the extracted oleosomes removing co-extracted storage proteins and other compounds, the oleosome cream was dispersed in 0.1 M $NaHCO_3$ at 1:4 (w/w) ratio and centrifuged at 10,000 g and 4°C for 30 min. The collected oleosome cream was initially spread onto a filter paper to eliminate excess sodium bicarbonate solution, followed by a

single washing step with excess deionized water under the same centrifugation conditions to remove any remaining trace of sodium bicarbonate. Subsequently, the purified oleosome cream was collected and again spread onto filter paper to remove excess water. The purified oleosome cream was then stored at 4°C for further analysis.

The extracted rapeseed proteins were further purified using a cross-flow filtration setup equipped with a 5 kDa MWCO PES membrane (Vivaflow 200, Sartorius, Germany) to remove co-extracted phenolic compounds. The concentrated protein extract was then desalted using a diafiltration setup (5 kDa MWCO, Vivaflow 200, Sartorius, Germany) until a stable conductivity level was achieved. To remove any remaining salt, the collected retentate was dialyzed against deionized water for 72 h at 4°C using a 3.5 kDa MWCO dialysis bag. The desalted protein extract was freeze-dried (Epsilon 2-10D LSCplus, Martin Christ, Germany) and stored at -20°C for further analysis.

3.2.3. Characterization of the extracted oleosomes and proteins

3.2.3.1. Composition analysis

The extracted oleosome cream was analyzed for its moisture, oil, and protein content. To determine the moisture content, a known amount of oleosome cream was dried at 60°C for 24 h. Then, the moisture content is determined using the weight difference between the wet and the dried samples (Equation 3.1). The dried oleosome cream was used for oil content quantification. Oil was extracted from around 1.0 g of dried sample using petroleum ether in a Soxhlet extractor (B-811 Buchi Extractor, Switzerland) for 3 h. The total oil content was calculated by dividing the extracted oil content by the dried sample weight (Equation 3.2).

$$Moisture\ Content\ (wt\%) = \cdot \frac{Amount\ of\ initial\ sample\ (g) - Amount\ of\ dried\ sample\ (g)}{Amount\ of\ initial\ sample\ (g)} \cdot 100\% \quad \text{Equation (3.1)}$$

$$Oil\ Content\ (wt\%) = \frac{Amount\ of\ extracted\ oil\ (g)}{Amount\ of\ dry\ sample\ (g)} \cdot 100\% \quad \text{Equation (3.2)}$$

To determine the total protein content in the defatted oleosome cream and the dried protein extract, the Dumas method (Rapid N exceed, Elementar, Germany) was used. For the analysis, aspartic acid was used as a standard, O_2 served as a blank sample and around 100 mg of the defatted oleosome cream and the dried protein extract were used as samples. To calculate the protein content, a nitrogen conversion factor of 5.7 was used. All analyses were performed in triplicate and the results were expressed as mean ± standard deviation.

3.2.3.2. Qualitative analysis of the protein profile

To qualitatively evaluate the purity of the extracted oleosomes and proteins, Sodium Dodecyl Sulfate Polyacrylamide Gel Electrophoresis (SDS-PAGE) was performed. The present polypeptides and their subunits were analyzed according to their molecular weight under non-reducing and reducing conditions, respectively. The reducing condition involves adding a reducing agent (mercaptoethanol) that cleaves disulfide bonds in the protein structure and reveals the subunits.

Oleosome and protein samples were diluted using deionized water to achieve a protein concentration of approximately 1 mg/mL. Next, 40 µL of sample and 40 µL of sample buffer (2x Laemmli Sample Buffer, Bio-Rad B.V., the Netherlands) (1:10 v/v mixture of mercaptoethanol and the sample buffer for the reducing condition) were mixed. The mixed samples were heated to 95°C for 10 min, and the samples were cooled down to room temperature. 20 µL of the samples were loaded into the SDS – PAGE gel (4–20% Mini-PROTEAN® TGX™ Precast Protein Gels, Bio-Rad B.V., the Netherlands). Besides, 10 µL of a protein marker (Precision Plus Protein™ Dual Xtra, Bio-Rad B.V., the Netherlands) was also loaded into the gel and served as a standard for molecular weights. Finally, SDS buffer (10x Tris/Glycine/SDS Electrophoresis Buffer, Bio-Rad B.V., the Netherlands) was added to the buffer chamber and the system was operated under 200 V for 40 min. When the SDS-PAGE run was completed, the gel was washed with deionized water for 10 min twice to remove any residues of SDS, and then the gel was dyed with Bio-safe Coomassie Stain (Bio-Rad Laboratories B.V., the Netherlands) for 2 h. To remove the background color of the dye, the gel was washed with deionized water overnight under continuous agitation. The obtained bands were analyzed using a gel scanner (GS900 Gel Scanner, Bio-Rad Laboratories B.V., the Netherlands).

3.2.3.3. Particle size measurement

The particle size distribution of the extracted oleosomes was determined using laser light diffraction (Mastersizer 3000, Malvern Instruments Ltd., UK). For the measurement, 1.0 wt% oleosome cream dispersion was prepared using deionized water, and the sample was stirred at 200 rpm for 1 h. Refractive indices of 1.47 and 1.33 were used for the oleosomes (dispersed phase) and water (continuous phase), respectively. The differential particle size distribution of the oleosomes is given as function of the volume density (%/µm).

To determine the particle size distribution of the protein extract, dynamic light scattering method (ZetaSizer Ultra, Malvern, UK) was used. The extracted proteins were dispersed in 1.0 mM potassium phosphate buffer (pH 8.0) to obtain a 0.001 wt% final concentration, and the samples were stirred at 400 rpm for 2 h at room temperature. The measurement was

done in triplicate and *Z* - average particle size was expressed as mean diameter ± standard deviation (nm). The particle size distribution was expressed as intensity (%/nm).

3.2.3.4. Determination of electrophoretic mobility

The electrophoretic mobility was measured using the dynamic light scattering method (ZetaSizer Ultra, Malvern, UK). The extracted oleosomes and the proteins were dispersed in 1.0 mM potassium phosphate buffer (pH: 8.0) at a concentration of 0.01 wt%. Then, the samples were stirred at 400 rpm for 2 h and the measurement was done at 25°C by applying 220 V potential difference. The analysis was performed in triplicate, and each measurement was performed with a fresh sample to eliminate any adverse effect of the electric field on the particles, such as aggregation. The results were expressed as the mean electrophoretic mobility ± standard deviation (μmcm/Vs).

3.2.4. Operation of the electrophoretic separation system

A continuous electrophoretic separation apparatus was developed in-house by adapting an electrochemical cell. The two parts of the cell are the retentate (sample) and the permeate (buffer) cells (OD: 55 mm, ID: 49 mm, Height: 55 mm) which were connected on either side of a glass frit (ID: 15 mm, OD: 30 mm, pore size: 16 - 40 μm). The membrane was equipped with titanium mesh electrodes (anode and cathode) on each side, which were attached to a wire to maintain electrical connection. To prevent any leakage, the perimeter of the membrane was covered by silicone grease. Fluid flow through the membrane was provided by a hydrostatic pressure difference between the cells, and the electric field strength (E) was calculated using the current density (*J*) and the conductivity (*C*) (Equation 3.3). The electric field strength is then used to calculate the electrophoretic velocity (v_E) of the compounds according to their electrophoretic mobility (μ) (Equation 3.4).

$$E\,(V/cm) = J\,(A/cm^2)\,/\,C\,(S/cm) \qquad \text{Equation (3.3)}$$

$$v_E(\mu m/s) = \mu\,(\mu mcm/Vs)\cdot E\,(V/cm) \qquad \text{Equation (3.4)}$$

To visually observe the retention-permeation mechanism, only rapeseed proteins dispersed in 1.0 mM potassium phosphate buffer (pH 8.0) were used as a sample. The proteins were dyed with fast green dye at a 1:1000 v/v ratio to facilitate the observation. The retentate and permeate cells were filled with dyed protein solution (100 mL) and buffer (50 mL), respectively. Then, the migration of the proteins was monitored for 10 min under 50, 25 and 0 V/cm electric field and photographed.

For the separation experiments, 0.02 wt% oleosome and protein dispersions were prepared using 1.0 mM potassium phosphate buffer at pH 8.0, and they were mixed at 1:1 v/v ratio

to be used as a sample. The retentate cell was filled with 100 mL of the prepared sample, and the permeate cell was filled with 50 - 65 mL (depending on the desired flow rate) of the buffer solution. The level of the liquids was kept constant over the experiments by collecting the excess amount of liquid transferred to the permeate cell and adding the same amount of liquid to the retentate cell after 10 min of operation. Before and after each experiment, the pH, conductivity, temperature and volume of the retentate and the permeate cells were measured and recorded. Each separation experiment lasted 20 minutes and was performed in triplicate at room temperature.

For further analysis, the samples from the retentate and permeate cells were collected and 1.0 mL of samples were separated for protein content quantification. The rest of the samples were freeze dried for oil content quantification.

3.2.5. Evaluation of the electrophoretic separation of rapeseed oleosomes and proteins

3.2.5.1. Determination of the total protein content

The initial and final protein concentrations in both compartments of the separation unit were quantified using high performance size exclusion chromatography (HPSEC) (Ultimate 3000 UHPLC system, Thermo Scientific, MA, U.S.A.). For the analysis, a combination of a TSKgel G3000SWxl column (7.8 mm × 300 mm) and a TSKgel G2000SWxl column (7.8 mm × 300 mm) (Tosoh Bioscience LLC, King of Prussia, PA, U.S.A.) was used. The experimental conditions were as specified; the flow rate of the mobile phase (30% acetonitrile in deionized water and 0.1% trifluoroacetic) was 1.5 mL/min, the column temperature was 30˚C, the UV detector was at 214 nm and the injection volume was 10 µL. The system was calibrated using purified rapeseed proteins for 0·01 – 0·30 mg/mL range. The total protein content (mg) and the average protein flux (mg/m^{2}s) were calculated using Equations (3.5) and (3.6), respectively. All samples were analyzed in triplicate, and the results were given as average ± standard deviation·

$$Protein\ content\ (mg) = Protein\ concentration\ (mg/mL) \cdot Sample\ volume\ (mL)$$

Equation (3.5)

$$Protein\ \ flux\ (mg/m^2 s) = \frac{Protein\ content\ in\ the\ \ permeate\ (mg)}{Membrane\ surface\ area\ (m^2) \times Duration\ (s)}$$

Equation (3.6)

3.2.5.2. Determination of oil (triacylglycerols) content

The total oil content was determined through total triacylglycerols (TAGs) content using proton nuclear magnetic resonance (HNMR) spectroscopy. The analysis was conducted with a Bruker Ascend standard-bore 700 MHz spectrometer equipped with a broadband inverse (BBI) probe (Bruker, Billerica, MA, USA). First, oil was extracted from the dried samples using petroleum ether. The dried samples were taken into Eppendorf tubes and 1.0 mL of petroleum ether was added and the suspension was mixed at 1000 rpm for 1 h at room temperature. Then, the suspension was centrifuged at 15000 g for 10 min. After separating the solvent and the precipitated solids, the same procedure was repeated two more times using the solid residue. All solvents from the three rounds of oil extraction were collected and evaporated under nitrogen gas. The extracted oils were then analyzed for their TAG content. For this purpose, the extracted oils were dispersed in d - chloroform solvent, including 0.03 v% TMS as an internal standard, and NMR readings were performed with 32 scans. The NMR spectrum was acquired at 295 K and further analyzed for TAGs quantification by integration of the internal standard peak and TAGs peaks (chemical shift: 4.10 - 4.32 ppm) (Guillén & Ruiz, 2003) using TopSpin software (Version 3.6.5, Bruker BioSpin, 2021). The oleosome flux (mg/m^{2}s) was calculated using an equation analogous to the one for protein (Equation 3.7):

$$Oleosome\ \ flux\ (mg\ /\ m^2 s) = \frac{Triglyceride\ content\ in\ the\ \ permeate\ (mg)}{Membrane\ surface\ area\ (m^2\ ) \times Duration\ (s)}$$

Equation (3.7)

To assess the separation between oleosomes and protein, the selectivity was determined using Equation (3.8).

$$Selectivity = \frac{\dfrac{Final\ \ protein\ concentration\ \text{in}\ the\ \ permeate\ (mg\ /\ mL)}{Initial\ \ protein\ concentration\ (mg\ /\ mL)}}{\dfrac{Final\ oleosome\ concentration\ \text{in}\ the\ \ permeate\ (mg\ /\ mL)}{Initial\ oleosome\ concentration\ (mg\ /\ mL)}}$$

Equation (3.8)

3.2.6. Statistical analysis

Statistical analysis was carried out with SPSS version 25.0 for windows (IBM Corp. NY, USA) to determine any significant differences between the treatments. For this purpose, one-way ANOVA and Tukey tests were used, and the results were assessed at both 95% and 98% confidence level.

3.3. RESULTS AND DISCUSSION

3.3.1. Characterization of the extracted rapeseed oleosomes and proteins

The extracted oleosomes and proteins from rapeseeds were first characterized regarding their composition, protein profile, particle size and electrophoretic mobility in aqueous dispersion.

The oleosomes were obtained as a cream after centrifugation, which contained 31.83 ± 0.53 wt% water, 61.39 ± 0.98 wt% oil and 3.81 ± 0.03 wt% proteins. The proteins were collected from the liquid phase below the cream and their purity was 79.19 ± 0.32 wt%. The qualitative analysis of the protein profile of both the obtained oleosomes and proteins took place using gel electrophoresis. In the protein extract, bands appeared at around 15, 20, 25, 30 and 50 kDa indicating the presence of cruciferins and napins, which are the major storage proteins in rapeseeds (Akbari & Wu, 2015; Wanasundara, 2011) (Figure A.3.1, Appendix). The electropherogram of the oleosome cream showed a band at around 18 kDa, which could be attributed to oleosins, the main proteins on the oleosome interface (Romero-Guzmán, Köllmann, et al., 2020). The oleosin protein dominated oleosome-cream protein profile indicated the sufficient purification of the oleosomes.

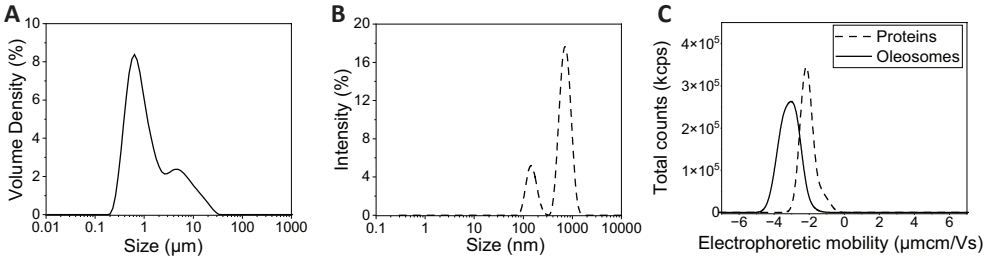

Figure 3.1: A,B) Size distribution of the extracted oleosomes at neutral pH and proteins at pH 8.0, respectively C) Electrophoretic mobility distribution of the extracted oleosomes (—) and proteins (- -) in 1.0 mM potassium phosphate buffer at pH 8.0.

To understand the physical state of the obtained oleosome cream, the size distribution was analyzed. Figure 3.1A shows that the oleosomes have a bimodal size distribution. The presence of native oleosomes was indicated by a peak at around 0.6 µm, while the peak at around 5.0 µm implied the formation of larger particles. Application of 1.0 wt% SDS made the larger peak disappear; hence this peak may be due to intermolecular forces like hydrophobic interactions (De Chirico et al., 2018; Romero-Guzmán, Petris, et al., 2020). However, SDS was not applied during the electrophoresis experiments, hence the bimodal distribution is relevant.

Similar to oleosomes, the extracted rapeseed proteins also have a bimodal size distribution pattern (Figure 3.1B). However, in case of the proteins, the peaks are located approximately at 150 and 700 nm. This implies that the proteins already formed larger clusters during the isolation and/or dehydration process due to electrostatic and/or hydrophobic interactions (Callahan et al., 2014; Roy & Gupta, 2004). The proteins have a Z - average particle size of 1.54 ± 0.23 µm.

To determine the processing conditions of the electrophoretic separation, electric field strength and solvent flow velocity, the average electrophoretic mobilities of the extracted oleosomes and proteins were measured using 1.0 mM potassium phosphate buffer at pH 8.0 as a dispersant. The average electrophoretic mobilities were -3.128 ± 0.123 µmcm/Vs and -2.105 ± 0.061 µmcm/Vs for the oleosomes and the proteins, respectively. The results confirm that the electrophoretic mobility of the oleosomes is greater than that of proteins and that it should be possible to separate them using electrophoretic separation. Nevertheless, the electrophoretic mobility depends on the surface charge density (combined effect of size and surface charge) of the particles (Fukasawa et al., 2020; Srinivas, 2012). Since both the oleosomes and the proteins form aggregates, a size range of particles with various electrophoretic mobilities coexist in the same sample. Figure 3.1C represents the electrophoretic mobility distributions of the extracted oleosomes and proteins. Besides the differences, there is also an overlapping area, which means some oleosomes and proteins have the same mobility. The electrophoretic separation of oleosomes and proteins may therefore not yield very sharp separation in this case. The selectivity may be enhanced by using a different dispersion medium that eliminates the aggregates. For instance, addition of some salt can break down the aggregates; however, it would also impair the electrophoretic mobilities of the compounds due to shielding (Galli et al., 2020; Semenov et al., 2010). 1.0 mM potassium phosphate buffer was chosen here as it experimentally provided the most significant difference in the mobility of oleosomes and proteins among the other buffers tried.

3.3.2. Electrophoretic separation

3.3.2.1. The working principle of the developed electrophoretic separator

The experimental setup includes three parts; a sample (retention) cell, a macroporous layer (a glass frit) to provide the flow and a buffer (permeate) cell (Figure 3.2A). As the electrodes are placed on the porous layer, the electric field is formed inside the porous structure. A component is retained when its electrophoretic velocity exceeds the solvent flow velocity by preventing it from passing through the membrane. In contrast, the compound is captured by the solvent flow and accumulates in the permeate cell due to its insufficient electrophoresis.

To visualize this pattern, dyed rapeseed proteins were used, and their movement was monitored under 0, 25, 50 V/cm electric field and 0.5 mL/min average flow rate (flow velocity: 47.2 µm/s) for 10 min. Figure 3.2B shows that the dyed proteins started to appear in the permeate cell within 10 min without electric field. The migration rate of the dyed proteins decreased when 25 V/cm electric field was applied (Figure 3.2C), and no dyed compounds in the permeate cell were observed under the influence of 50 V/cm electric field (Figure 3.2D). This straightforward experiment demonstrates the fundamental working principle of the electrophoretic separation cell.

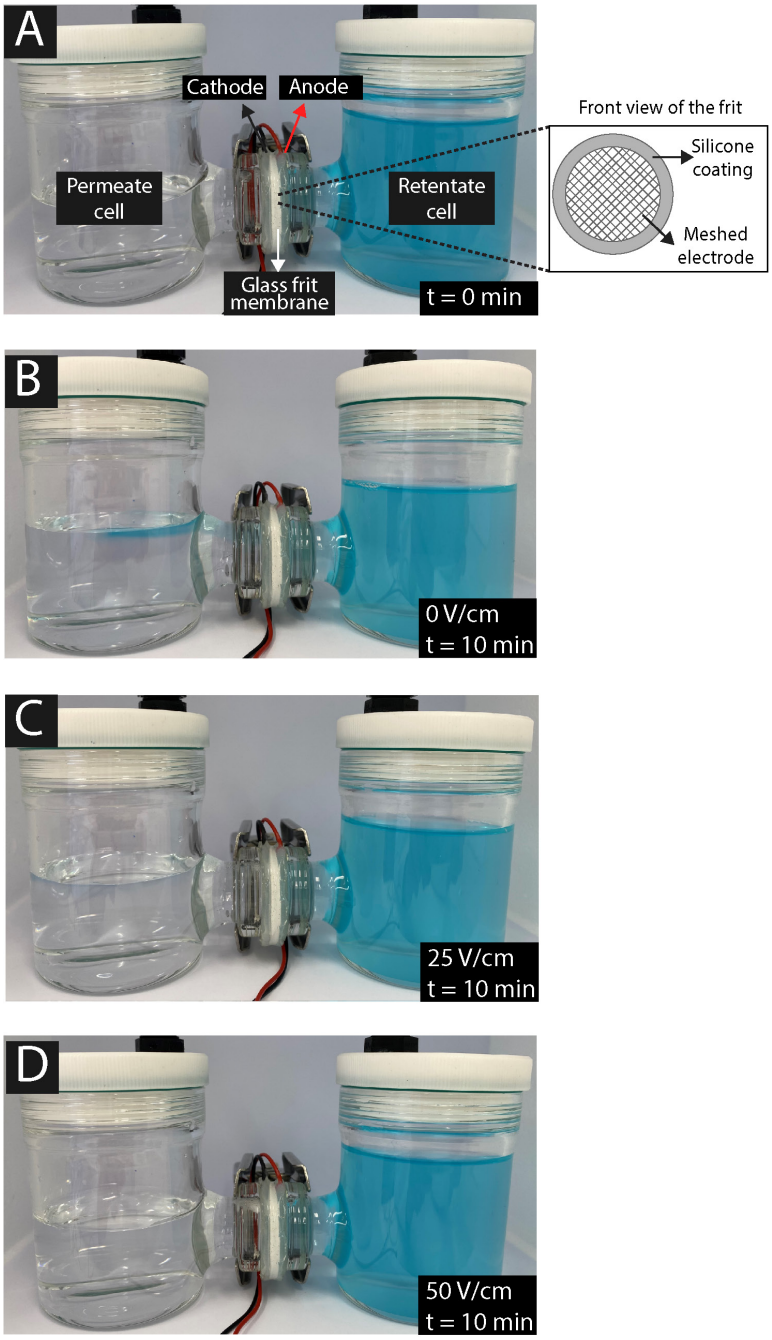

Figure 3.2: A) The developed electrophoretic separator and the initial state of the sample. Retention and permeation of dyed rapeseed proteins in 1.0 mM potassium phosphate buffer (pH 8.0) under 0 (B), 25 (C) and 50 V/cm (D) electric field strength and 0.5 ± 0.1 mL/min flow rate (~40 µm/s flow velocity) in 10 minutes. *Electrophoretic mobility of the proteins is -2.105 ± 0.061 µmcm/Vs.

3.3.2.2. Electrophoretic separation of rapeseed oleosomes and proteins

To explore the electrophoretic separation of the oleosomes from the proteins, the average solvent flow rate was set to 1.2 ± 0.1 mL/min (linear velocity: 113.2 ± 9.4 µm/s), as it is expected that an electric field within the range of 36.1 and 53.6 V/cm should accomplish their separation. An experiment with no electric field was used as a control experiment. Three different electric field strengths (25, 50 and 75 V/cm) were used. To evaluate the stability of the operational conditions during the experiments, the pH, conductivity and temperature were recorded before and after the experiments. The detailed data is available in Table A.3.1.

The pH is critical in such a separation, as it directly influences the electrophoretic mobility; nevertheless, alterations in pH are inevitable in electric field-assisted systems due to electrolysis reactions on the electrodes without the use of electrode rinse chambers (Obata et al., 2020; Semenov et al., 2010). The pH is expected to decrease in the retentate cell (anode electrode) and increase in the permeate cell (cathode electrode) over time. Indeed, the initial pH of 8.01 ± 0.03 gradually dropped to 7.96 ± 0.05, 7.82 ± 0.11 and 7.63 ± 0.02 in the retentate cell, and the initial pH of 8.01 ± 0.02 increased to 8.11 ± 0.03, 8.15 ± 0.07, and 9.65 ± 0.17 in the permeate cell under 25, 50 and 75 V/cm electric field applications. Applications of 25 and 50 V/cm resulted in smaller pH deviations than 75 V/cm throughout the experiments.

To evaluate the stability of the applied electric field strength, the conductivities of the feed solution and the buffer were monitored. Even though some fluctuations were found, these were too small to significantly affect the electric field strength. Similarly, no significant change was observed in the temperature, in the range of applied current values (1.8 to 6.0 mA), remaining at 22.4 ± 0.5˚C.

The electromigration of the oleosomes and the proteins can be understood by examining their permeation fluxes across the membrane where the separation takes place. The flux is the product of the compound concentration and the net velocity, which in turn is the sum of the (negative) electrophoretic velocity and the (positive) counter-current solvent velocity ($Flux_i = c_i \cdot (v_E + v_s)$). Therefore, an increment in the electric field should reduce the flux of charged particles due to lower net velocity. Figure 3.3A represents the flux of the oleosomes and the proteins under 0 - 75 V/cm electric field. Under zero electric field, their migration is governed by the solvent flow and both oleosomes and proteins have their highest flux; 9.90 ± 1.30 mg/m^{2}s and 24.50 ± 1.90 mg/m^{2}s, respectively. The disparity in the flux of oleosomes and proteins is attributed to some large oleosome aggregates in addition to the native oleosomes, which are likely to be trapped inside the frit. In contrast, the proteins are free from that large aggregates. Introducing of 25 V/cm electric field caused a slight decrease in their flux due to the weakened effect of the solvent flow by electrophoresis. However,

the most evident effect was visible at 50 V/cm electric field, where the oleosome flux approached zero (1.6 ± 0.7 mg/m^{2}s). In contrast, the protein flux decreased by 30.3% and reached 17.1 ± 1.6 mg/m^{2}s. This implies that while most of the oleosomes were retained by the electric field and only a small fraction of the oleosomes (ones that exhibit similar electrophoretic mobility to the proteins) are allowed to pass through the membrane, the migration of the proteins was still primarily driven by the solvent flow. To put this into perspective, the protein flux is 10 times larger than the oleosome flux, while this ratio was 2.5 without electric field. Thus, the migration rates were indeed influenced by the electric field strength in accordance to their electrophoretic mobility.

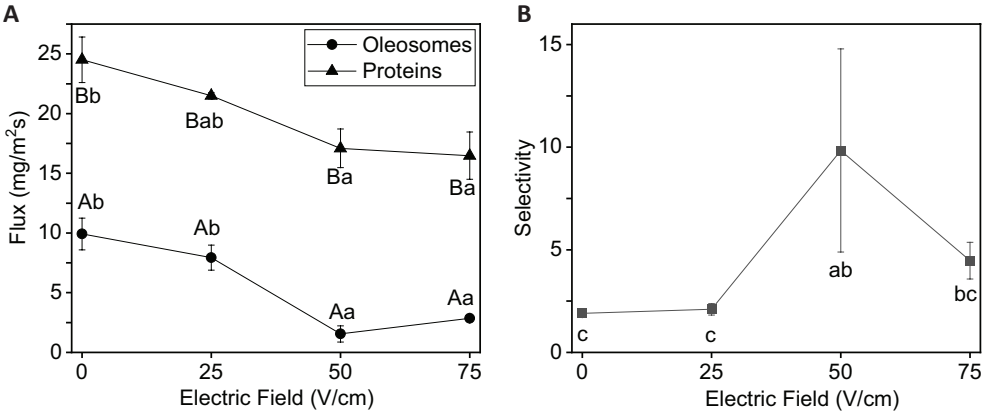

Figure 3.3: A) Flux (mg/m^{2}s) of oleosomes and proteins under an increasing electric field strength. B) Electrophoretic separation selectivity under an increasing electric field. *Uppercase letters indicate significant differences between the samples (oleosomes and proteins) and lowercase letters show the differences between the electric field treatments (P<0.05). Solid lines are guide for the eyes.

The permeation flux of the compounds were also tested at 75 V/cm electric field, which should retain both oleosomes and proteins as their electrophoretic velocity is then greater than the flow velocity. Nevertheless, the flux values reached a plateau, and there is no further decrease (P>0.05). This may stem from pH changes and from inhomogeneities in the electric field inside the frit pores. As mentioned before, the pH value dropped to 7.63 ± 0.02 in the retentate cell, and this effect may have been stronger near the anode electrode (Obata et al., 2020). It is known that the mobilities of rapeseed oleosomes and proteins decrease when the pH approaches their isoelectric point (pH 4.0 - 6.0) (Ayan et al., 2023). Consequently, their electrophoresis rate may have not increased with higher electric field, given the possible reduction in their mobility. The pH can be adjusted by titration with alkali and acid, like NaOH and HCl, but addition of these electrolytes would lead to a decline in the electric field strength due to increased conductivity (Equation 3.3). The use of electrode rinse chambers would alleviate this problem, but were outside the scope of this study. A second possibility is that the electric field was not completely homogeneous inside the frit, due to the positioning of the electrodes close to the frit. This would leave parts of the

frit with a lower electric field and hence would still allow permeation of the proteins and oleosomes.

The differences in the flux of oleosomes and proteins under the electric field indicated that the separation is indeed possible. Further insights into the separation can be gained by analyzing the selectivity. The selectivity characterizes the efficiency of the process to separate target compounds from each other (Wang et al., 2022), expressed as a ratio of permeated compounds concentration in respect to their initial concentration in the feed (Equation 3.8). A higher selectivity value corresponds to a better mutual separation. Figure 3.3B shows that the selectivity value increased significantly from 1.90 ± 0.11 to 9.84 ± 4.95 under 50 V/cm ($P<0.05$). This highlights that the electric field indeed acts on oleosomes and proteins based on their electrophoretic mobility and their separation is driven by the electrophoretic mobility differences. The larger deviation at 50 V/cm stems at least partly from the low oleosome concentration, which makes the quantification of its concentration difficult, so we expect that this is mainly because of the analyses. One can clearly see that an electric field that is too large (75 V/cm) results in poor separation, so it is important to set the correct balance between flow and electric field.

Overall, lab - scale electrophoretic separation of rapeseed oleosomes and proteins was performed under a constant flow rate of 1.2 ± 0.1 mg/mL for 20 min. However, the set-up used is relatively simple, which may have caused the unexpectedly large fluxes at very high field strengths (75 V/cm) due to inhomogeneities and perhaps even flow instabilities formed by the high electric field. Moreover, a flow rate decrease of 25.0% and 43.5% was observed between the 20^{th} to 30^{th} min of the operation under zero and 50 V/cm. We expect that this is due to membrane fouling (data not shown). To regain the initial flow rate, the membrane had to be washed with 0.5 M NaOH and deionized water. To avoid these flow rate reductions, the experiment was operated for 20 min at most. This fouling may have been caused by larger oleosomes aggregates and the lower local pH near the electrode, which may have caused local aggregation of the protein and/or oleosomes. These aggregates may then have blocked the frit pores. These problems can be overcome by using larger pore size frit and electrode rinse chambers, which physically separate the electrodes from the dispersion to be separated. They can also eliminate pH changes over time (Moura Bernardes et al., 2013).

3.4. CONCLUSIONS

We investigated a benchtop electrophoretic separator for the electrophoretic separation of oleosomes and proteins from rapeseed. At the correct combination of the electric field strength (50 V/cm) and counter-current flow rate (1.2 ± 0.1 mL/min), separation occurred with an average selectivity of around 10 over 20 minutes of operation. While we showed that the separation takes place, the separation was not yet optimal since both oleosomes and proteins were partially aggregated, and had overlapping distributions of the electrophoretic mobility. This can be improved by minimizing the aggregation before separation. The relatively simple experimental set-up gave rise to some technical challenges, such as membrane fouling and electrolysis-based pH shift. These can be mitigated by increasing the pore size of the membrane, more optimal placement of the electrodes and using electrode rinse chambers, which are standard in electrodialysis but were outside the scope of this work.

3.5. APPENDIX

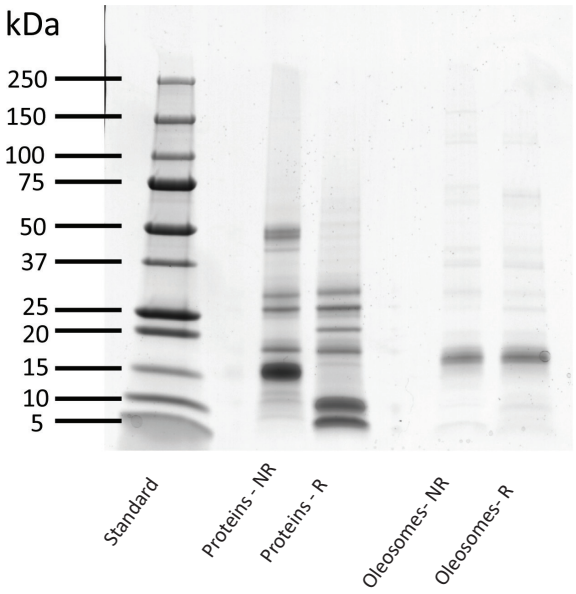

Figure A.3.1: SDS – PAGE electropherograms for the extracted rapeseed oleosomes and proteins. NR: Non-reducing condition and R: Reducing condition.

Results: The protein extract includes broad range of bands ranging from around 15 to 50 kDa under non-reducing conditions, and 5 to 33 kDa under reducing conditions. The peak at ~15 kDa which dissociates into two bands at ~10 and ~5 kDa under reducing conditions represents the napin fraction, and the bands intensified around 20, 25, 30 and 50 attributed to cruciferin sub-units (Akbari & Wu 2015; Wanasundara 2011). In the oleosomes, there is one major band at 18 kDa under both non-reducing and reducing conditions. These bands represent oleosin protein used a biomarker for oleosome purification, thereby proving the absence of co-extracted rapeseed storage proteins (Romero-Guzmán, Köllmann, et al., 2020).

Table A.3.1: pH, conductivity and temperature of the samples before and after the conducted experiments

Sample	pH	Conductivity (µS/cm)	Temperature (˚C)
0.2 mg/mL oleosome - protein mixture	8.01 ± 0.03	245.7 ± 14.9	23.0 ± 1.1
1 mM potassium phosphate buffer	8.01 ± 0.02	244.8 ± 6.8	22.2 ± 0.4
0 V/cm - Retentate	7.97 ± 0.06	263.0 ± 11.4	23.3 ± 0.8
0 V/cm - Permeate	8.00 ± 0.00	250.0 ± 2.0	22.5 ± 0.2
25 V/cm - Retentate	7.96 ± 0.05	238.3 ± 5.1	22.0 ± 0.3
25 V/cm - Permeate	8.11 ± 0.03	241.3 ± 2.9	21.7 ± 0.5
50 V/cm - Retentate	7.82 ± 0.11	250.7 ± 9.3	22.3 ± 0.4
50 V/cm - Permeate	8.15 ± 0.07	248.7 ± 4.9	22.2 ± 0.4
75 V/cm - Retentate	7.63 ± 0.02	236.7 ± 2.1	22.6 ± 0.3
75 V/cm - Permeate	9.65 ± 0.17	256.0 ± 2.6	22.5 ± 0.1

CHAPTER 4

Electrophoretic removal of sinapic acid from rapeseed protein extract

This chapter has been submitted as:

Ayan, K., Boom, R. M., & Nikiforidis, C. V. (2024). Electrophoretic removal of sinapic acid from rapeseed protein extract

ABSTRACT

Isolation of proteins from oilseeds to supply functional proteins for the food industry is essential but challenging due to the presence of anti-nutrients such as phenolic compounds. To deliver proteins, the removal of phenolic compounds is crucial. Conventionally, this is accomplished by alcohol washing; however, this is resource-intensive, may be unacceptable for some and does not provide proteins with good techno-functional properties since it alters the native protein structure. To overcome such drawbacks, gentle processing methods must be developed. In this work, we investigated the electro-separation of sinapic acid from rapeseed protein extract. A porous medium (ion exchange or ultrafiltration membrane) permitting electromigration of only sinapic acid and retaining the proteins was utilized under two different potential differences. The electro-separation of sinapic acid relied on electrostatic and electrophoretic forces, which cause their adsorption and permeation. Among the treatments, 1.5 V over an anion exchange membrane showed the best performance, providing considerable sinapic acid removal (34.0 ± 4.0 wt%) while maintaining the protein content and pH stability. A larger system with a larger membrane surface area yielded as high as 90.3 ± 3.8 wt% of sinapic acid removal within 240 min while retaining 88.8 ± 7.6 wt% of the proteins.

4.1. INTRODUCTION

The emergence of plant materials as an alternative protein source is a result of the nutritional needs of the growing world population and the environmental impact of the livestock industry (Banach et al., 2023; Lamberg-Allardt et al., 2023). Besides, changes in dietary preferences due to health or moral issues also significantly impact this development (Lamberg-Allardt et al., 2023). On the other hand, transitioning to plant-origin proteins is not a trivial task, as it requires an understanding of the characteristics of different plant proteins and availability of suitable protein extraction methods, considering that plant matrices are complex in structure and comprise a range of non-protein materials (Munialo, 2023).

Various plant sources from leaves to legumes have been proposed as a protein source (Banach et al., 2023). Oilseeds are outstanding vegetative protein sources with an annual production volume of more than 650 MT (USDA, 2024). Industrially, their primary utilization is oil extraction; however, oilseeds also contain 20 – 30 wt% proteins, which are currently underutilized or even discarded. The main challenge in the extraction of proteins from oilseeds is the presence of anti-nutrients like phenolic compounds that interact with the proteins and form protein-phenolic complexes characterized by low solubility, reduced functionality, and indigestibility (Arrutia et al., 2020; Hadidi et al., 2024). Besides, the presence of phenolic compounds affects the sensory properties by inducing a bitter–astringent taste, and a darker colour (Banach et al., 2023). To obtain oilseed proteins of good quality and functionality, the removal of phenolic compounds, or dephenolization, is therefore crucial.

Phenolic compounds are generally eliminated using solvent extraction with high-polarity solvents like methanol and ethanol. Solvent extraction is a mature technology and is widely applied as it is simple and cost-effective (Alara et al., 2021). However, it has some drawbacks regarding the obtained protein quality and efficiency. The use of alcoholic solvents alters the structure of the proteins and sometimes causes their denaturation (Yılmaz & Gultekin Subasi, 2023; Shao et al., 2012; Peng et al., 2020). Additionally, heat is often used to improve the extraction yield, and this can also degrade the proteins (Gironi & Piemonte, 2011). The conventional solvent extraction requires a large amount of solvents and recycling of the solvent, which requires long processing times and may release a residual amount of these greenhouse gases into the environment (Shi et al., 2022). Finally, the use of ethanol may not be culturally acceptable to a sizable group of consumers. To mitigate the listed drawbacks and to deliver phenolic-free oilseed proteins, gentler and resource-efficient separation processes must be developed.

Electric field can be utilized for gentle separation as it can be more effective than mechanical or thermal gradients and may contribute to improved selectivity by acting only on charged compounds (Ptasinski & Kerkhof, 1992; Wang & Weatherley, 2023). The use of electric field

has already been investigated for the removal of tobacco polyphenols using electrodialysis (Bazinet et al. 2005) and for enhanced solvent extraction of polyphenols from various sources using high-voltage electric discharge (Boussetta et al., 2011; Rajha et al., 2014; Roselló-Soto et al., 2015). Nevertheless, to the best of the authors' knowledge, there is no study yet on electrophoretic dephenolization of oilseed protein extracts.

In this work, separation using an electric field over an ion exchange membrane and/or ultrafiltration membrane was used to remove sinapic acid (SA), the most abundant phenolic compound in rapeseeds, from rapeseed proteins (Nandasiri et al., 2020). Under the influence of an external electric field, charged compounds, SA and the proteins in this case, electromigrate towards the oppositely charged electrode. Both SA and the proteins carry a negative charge under alkaline conditions; however, the rapeseed proteins are much larger molecules (12 – 300 kDa) than SA (0.224 kDa) (Ayan et al., 2023; Precupas & Popa, 2024). Thus, separation can be obtained using a membrane that only allows the electromigration of SA and retains the proteins. The retention and permeation of SA and its removal were evaluated under various conditions. Additionally, the protein loss and pH stability was investigated.

4.2. MATERIALS AND METHODS

4.2.1. Materials

Alizze variant (*Brassica napus*) rapeseeds were kindly provided by a seed breeder to be used for protein extraction. Sinapic acid (purity ≥ 99.0) and all chemicals used were of analytical grade and purchased from Sigma Aldrich (St. Louis, MO, USA). Deionized water (Milli-Q, Merck Millipore, Darmstadt, Germany) was used to prepare all solutions and dispersions.

4.2.2. Extraction of rapeseed proteins

Rapeseed proteins were extracted from dehulled and defatted rapeseed meal by dispersing 100 g of rapeseed meal in deionized water at a ratio of 1:10 (w/w). The pH of the dispersion was then adjusted to 9.0 by adding 1.0 M NaOH. The dispersion was stirred at 400 rpm for 4h at room temperature. Subsequently, the dispersion was centrifuged at 10,000 g and 4°C for 30 min (Sorvall Lynx 4000 Centrifuge, Thermo Scientific, USA). The supernatant containing the extracted proteins was collected and freeze-dried (Epsilon 2-10D LSCplus, Martin Christ, Germany). To remove the co-extracted phenolic compounds, the dried protein extract was washed four times for 1h with excess methanol under constant agitation. At the end of each cycle, the mixture of methanol and protein extract was centrifuged at 10,000 g and 4°C for 30 min, and the pellet was collected and redispersed in methanol until the four

washing cycles were completed. Finally, the dephenolized rapeseed protein extract was dried overnight under a fume hood and stored at -20 °C for further analysis.

4.2.3. Protein content of the extracted proteins

The total protein content of the obtained rapeseed protein extract was measured using the Dumas method (Rapid N exceed, Elementar, Germany). For the analysis, aspartic acid was used as a standard and oxygen (O_2) served as a blank sample. To quantify the total protein content, nitrogen conversion factor of 5.7 was applied. The analysis was conducted in triplicate, and the results were expressed as mean ± the standard deviation (wt%).

4.2.4. Total phenolic content of the extracted proteins

The total phenolic content was determined using the Folin Ciocalteu assay. For the analysis, 1.0 mL of sample was mixed with 5.0 mL of deionized water, and 0.5 mL of Folin Ciocalteu reagent was added. The mixture was vortexed, and 1.0 mL of 20 wt% Na_2CO_3 solution was added. Finally, the volume of the mixture was completed to 10.0 mL by adding deionized water. The samples were incubated in dark for 1h, and their absorbance was measured at 725 nm using an UV-Vis Spectrophometer (DR6000, Hach, Colorado, U.S.A). Tannic acid was used as a standard for the quantification. All analyses were done in triplicate and the results were given as the mean ± standard deviation (wt%).

4.2.5. Sinapic acid content of the extracted proteins

To determine the SA content, high-performance liquid chromatography (Ultimate 3000 RS UHPLC system, Thermo Scientific, MA, U.S.A.) equipped with a UV-Vis detector was used. As a stationary phase, Gemini® 3µm C18 110 Å column (150 x 4.6 mm, Phenomenex, CA, U.S.A) was used. The mobile phase consisted of eluent A (0.1% trifluoroacetic acid in deionized water) and eluent B (0.1% trifluoroacetic in acetonitrile), introduced to the column at a flow rate of 1.0 mL/min. For the analysis, a gradient elution program was applied. The program started with 95.0% A and 5.0% B and gradually transitioned, first to 85.0% A and 15.0% B over 4 min, followed by a change to 80.0% A and 20.0% B within the next 10 min, then to 50.0% A and 50.0% B over the following 10 min, and finally, returned to the initial composition in the last 3 min of analysis. The column temperature was maintained at 35 °C, the UV detector was set to 220 and 325 nm and the injection volume was 10 µL. The system was calibrated using sinapic acid (purity ≥ 99.0) with different concentrations between 0.01 – 0.2 mg/mL for the quantification. All analyses were done in triplicate, and the results were given mean ± standard deviation (wt%).

4.2.6. Electrophoretic removal of sinapic acid from the rapeseed protein extract

4.2.6.1. Electrodialysis cell configuration

Electro-separation of SA from the rapeseed proteins was performed using an electrodialysis (ED) system. The system includes an ED cell (length 20 cm, width 10 cm, 84 cm^2 of effective surface area), three peristaltic pumps to circulate the solutions (flow rate: 2.0 L/h), buffer solution (1.0 mM potassium phosphate buffer at pH 8.0, flow rate: 2.0 L/h) and electrolyte solution (0.5 M Na_2SO_4, flow rate: 20.0 L/h), and a power supply (PLH250 DC Power Supply, AimTTi, Huntingdon, U.K.) connected to the electrodes on both sides of the ED cell. The ED cell contains stacked ion exchange membranes (IEM) (Shandong Tianwei Membrane Technology Co., Ltd., Shandong, China) separated with specific flow spacers to form separate compartments for the electrodes, the sample (retentate) and the buffer (permeate). Both electrodes (anode and cathode) were separated from the sample and the buffer solution using cation exchange membranes (CEM), and the retentate and the permeate cells were separated using either an anion exchange membrane (AEM) or an ultrafiltration membrane (UFM) (VT, Synder, CA, U.S.A). Further details regarding the specifications of the used membranes are provided in Table 4.1.

Table 4.1: Specifications of ion exchange and ultrafiltration membranes used in the experiments

Property	Anion Exchange Membrane (AEM)	Cation Exchange Membrane (CEM)	Ultrafiltration Membrane (UFM)
Ion exchange capacity (mmol/g)	0.90 – 1.10	0.90 – 1.10	-
Thickness (wet) (µm)	40 – 50	40 – 50	-
Water Uptake (25°C) (wt%)	15 – 20	15 – 20	-
Electrical resistance (Ωcm^2)	≤2.50	≤3.00	-
pH stability	1 – 12	1 – 12	1.8 – 11
Temperature stability (°C)	15 – 40	15 – 40	Up to 55
Material	Polystyrene	Polystyrene	Polyethersulfone
Molecular weight cut-off (kDa)	-	-	3
Surface charge sign	Positive	Negative	Negative

4.2.6.2. Sample preparation

To prepare the sample solution, dephenolized rapeseed protein extract and SA were mixed at a ratio of 20:1 w/w and dispersed in 1.0 mM potassium phosphate buffer (pH 8.0). Since the addition of SA decreased the pH, this was adjusted to 8.0 prior to the separation experiment using 0.1 M NaOH and 0.1 M HCl solutions.

4.2.6.3. Measurement of the limiting current density

The limiting current density (LCD) is an important parameter that determines the highest current value to maintain an Ohmic linear relation between the current and potential difference for electrodialysis processes. To measure the LCD, the method by Isaacson and Sonin was used (Isaacson & Sonin, 1976; Knežević et al., 2022). To do so, the potential difference was incrementally increased from 1.0 to 3.0 V, and the corresponding current value was recorded for each potential difference. Then, the current density (A/m^2) and the potential difference (V) values were plotted to determine the LCD value, marking the point where the relation between voltage and current density changes. The LCD value was determined for the sample solution (dispersed rapeseed proteins and SA) and the buffer solution.

4.2.6.4. Operation of the electrophoretic separation

Electrophoretic removal of SA from the prepared mixture was performed both below and above the LCD using AEM and UFM as separating membranes. The experiments lasted for 240 min, and samples from the retentate and permeate cells were collected at certain time points (0, 30, 60, 120, 180 and 240 min). Besides, pH and conductivity were measured using a multimeter (HQ440d multi, Hach, Tiel, Netherlands) at the specified time points to monitor the changes, while the volume and temperature of the retentate and permeate were measured at the beginning and end of the experiments.

4.2.6.5. Evaluation of the electrophoretic separation of sinapic acid from rapeseed protein extract

The electromigration of SA through the membranes was quantified by measuring both the retained and permeated SA content. For this, the HPLC method specified in Section 4.2.5 was used. The SA content, flux and removal (wt%) were calculated using Equation (4.1), (4.2) and (4.3), respectively.

$$Sinapic\ acid\ content\ (mg) = Sinapic\ acid\ concentration\ (mg/mL) \cdot Sample\ volume\ (mL) \quad \text{Equation (4.1)}$$

$$Sinapic\ acid\ flux\ (mg/m^2 h) = \frac{Permeated\ sinapic\ acid\ content\ (mg)}{Surface\ area\ of\ membrane\ (m^2) \cdot Duration(h)} \quad \text{Equation (4.2)}$$

$$Sinapic\ acid\ removal\ (wt\%) = \frac{Initial\ sin.\ acid\ content\ (mg) - final\ \sin.\ acid\ content\ (mg)}{Initial\ sin.\ acid\ content\ (mg)} \cdot 100\% \quad \text{Equation (4.3)}$$

The protein concentration in the collected samples was also quantified to assess the loss during the process. For this purpose, again High-Performance Size Exclusion Chromatography (HPSEC) (Ultimate 3000 UHPLC system, Thermo Scientific, MA, U.S.A.) equipped with a UV detector was used. A combination of a TSKgel G3000S (WxL 7.8 mm × 300 mm) and a TSKgel G2000S (WxL 7.8 mm × 300 mm) (Tosoh Bioscience LLC, King of Prussia, PA, U.S.A.) served as a stationary phase, and 30% acetonitrile in deionized water and 0.1% trifluoroacetic at a constant flow rate of 1.5 mL/min was used as a mobile phase. The column temperature was kept at 30˚C, the UV detector was set at 214 nm and the injection volume was 10 µL. The system was calibrated using purified rapeseed protein in the range of 0.03 – 2.0 mg/mL range. The total protein content (mg) was calculated using Equation (4.4):

$$Total\ protein\ content\ (mg) = Protein\ concentration\ (mg/mL) \cdot Sample\ volume\ (mL) \quad \text{Equation (4.4)}$$

After evaluating the separation, the most optimal condition, which yielded the highest SA removal, the lowest protein loss and stable pH, was studied for complete SA removal from the mixture.

4.2.7. Statistical analysis

Statistical analysis was carried out by using SPSS version 25.0 for Windows (IBM Corp. NY, USA) to assess the significance of differences in SA and protein content throughout the processing and among different treatments. For this purpose, one-way ANOVA and Tukey test were used. The results were evaluated at a 95% confidence level.

4.3. RESULTS AND DISCUSSION

4.3.1. Characterization of the rapeseed protein extract

Proteins were extracted from defatted rapeseed meal and dephenolized to be used as a protein fraction in the electrophoretic separation experiments. For their characterization, the total protein content, total phenolic content and SA content were determined. The dephenolized rapeseed proteins contained 69.76 ± 0.41 wt% of proteins. To evaluate the efficiency of methanol washing, the total phenolic content (TPC) and SA content were determined before and after the dephenolization step. The initial TPC of 5.35 ± 0.13 wt% decreased to 2.43 ± 0.10 wt% after four-fold washing with methanol. SA, on the other hand, was almost completely removed (0.01 ± 0.00 wt%) from the protein extract, indicating that the treatment was effective in obtaining a SA-free protein extract. It should be noted that the Folin Ciocalteu method may not be entirely accurate in measuring the total phenolic content, as some amino acids like tyrosine can also react with the Folin reagent and interfere with the results (Everette et al., 2010; Salazar-Villanea et al., 2016).

The mixture of SA and proteins was prepared based on TPC in the unwashed protein extract to achieve a similar composition for the electrophoretic separation experiments. Therefore, the original ratio of TPC to the protein extract of 1:18.7 w/w was rounded up 1:20 w/w to prepare the mixture of SA and dephenolized protein extract. Here, SA represented phenolic compounds originally found in the rapeseed protein extract.

4.3.2. Electrophoretic sinapic acid removal from the rapeseed protein extract

Electrophoretic removal of SA from the rapeseed protein extract was performed using an electrodialysis (ED) device equipped with ion exchange and/or ultrafiltration membranes. For the separation, both electrophoresis and size differences between SA and the rapeseed proteins were utilized. The mixture of SA and proteins was introduced to the ED cell near the cathode (negatively charged) electrode, causing their electrophoresis direction towards the anode (positively charged) electrode. Due to their size differences, only SA passed through the membrane and was thus removed (Figure 4.1).

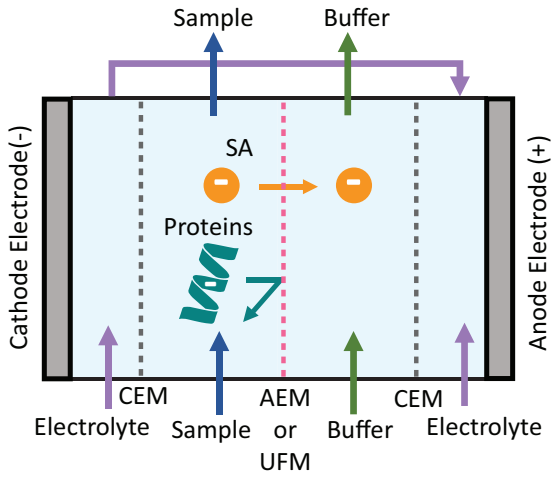

Figure 4.1: The schematic design of the electrodialysis device for electrophoretic sinapic acid – rapeseed proteins separation. Blue, orange and green arrows indicate the path of the electrolyte, sample and buffer solution in the electrodialysis cell. CEM: Cation exchange membrane, AEM: Anion exchange membrane, UFM: Ultrafiltration membrane, SA: Sinapic acid

To assess their separation under different conditions, both AEM and UFM were tested below and above the LCD, which was 0.40 ± 0.10 A/m^2 with the corresponding potential difference of 1.8 ± 0.2 V for AEM and 0.03 ± 0.00 A/m^2 with the corresponding potential difference of 2.0 ± 0.0 V for UFM (Figure A.4.1 and 2, Appendix). Therefore, 1.5 V was chosen to represent the separation below the LCD for both membranes. 1.0 V per membrane (3.0 V in total) was used for the measurement above the LCD, which was also the maximum allowed potential difference for the ED cell. Using the listed four different combinations (1.5 V AEM and UFM, and 3.0 V AEM and UFM), SA retention and permeation were analyzed. Figure 4.2 summarizes the changes in SA content in the retentate (A), permeate (B) and membrane (C), respectively. Furthermore, Figure 4.2D shows the permeation flux and total removal of SA from the mixture.

In the case of using 1.5 V potential difference (0.11 ± 0.02 A/m^2 average current density) with an AEM, the highest SA reduction was observed within the first 120 min, after which the reduction rate decreased. This may stem from the adsorption of SA in the AEM. Figure 4.2C indicates that the maximum adsorption of SA also took place at 120th min, after which the adsorption of SA began to decrease, due to the continuing extraction towards the positive electrode. The charged compound (SA) was initially adsorbed by the membrane as a result of electrostatic attraction due to the opposite electrical charge of SA (-) and the membrane surface (+), along with the electrophoretic forces. Then, the adsorbed SA permeated into the buffer. Adsorption occurred faster than permeation as the electrophoresis rate of a charged compound is faster in an aqueous environment than in a porous membrane (Franck et al.,

2024; Rudge & Monnig, 2000). This demonstrates that the adsorption in the AEM does not impede the continuing removal of SA. Even though the electrophoretic and electrostatic forces were the most significant forces in the SA migration, co-current electroosmotic flow, which occurs as a result of the migration of attracted counter-ions by the membrane toward the anode electrode, and diffusion could also contribute to the SA migration.

The observed mechanism below the LCD using 1.5 V and an AEM, however, changed when the LCD was exceeded. At 3.0 V (0.68 ± 0.10 A/m² average current density), adsorption due to the enhanced electrophoretic force played a more significant role than electromigration in SA removal. This can be attributed to the decrease in transport number of SA. The transport number (t_i) defines the ratio of the current carried by ion to the overall current (i_t) carried by all ions through the membrane. Its value depends on the fraction of the ion i (a_i) and the total current ($t_i = a_i \cdot i_t$). Given that, the transport number decreases when the fraction of the ion decreases under the constant current. When surpassing the LCD, the salt flux across the membrane increases, accelerating desalination. A more rapid desalination was indeed observed during the experiments (Table A.4.1). This leads to a decrease of the fraction of the other compounds migrating through the membrane, such as SA. Hence, the permeability of SA decreased. Besides, formation of H^+ and OH^- ions from water splitting reactions might have also contributed to the decrease in the transport number of SA (Nikonenko et al., 2014; Rodrigues et al., 2022; Strathmann, 2004; Van der Bruggen, 2018). In addition to the potential decrease in SA transport number, its enhanced electrostatic interactions with the charged groups in the membrane due to the increasing pH could influence its adsorption. Due to the complexity of an ED system operating under over-limiting current conditions, revealing the exact underlying causes is challenging. In general, operating the system below the LCD is advised.

When a UFM instead of an AEM was used, a different permeation mechanism was observed. With 1.5 V (0.02 ± 0.00 A/m² average current density), no significant change in SA content was obtained. Only a small fraction of SA passed through the membrane, and there was almost no discernable sorption. This highlights the importance of the electrostatic interaction between the compounds to be transferred and the membrane. The surface charge of the UFM is negative, giving rejection of negatively charged compounds like SA when other forces, diffusive and electrophoretic forces, are not sufficient. Besides, the use of a negatively charged membrane caused a counter-current electroosmotic flow, which may also have impaired the electromigration of SA. As a result of these effects, SA was rejected by the membrane even though its size (0.24 kDa) is much smaller than that of the molecular weight cut-off of the membrane (3 kDa). Similar to the SA migration, no significant desalination in the retentate was observed (Table A.4.1). Here, one should note that the average current density in the case of 1.5 V UFM was much lower due to its higher resistance compared to the case of 1.5 V AEM, which could also cause low SA permeation.

SA permeation through the UFM was, however, visible with an increased potential difference of 3.0 V (2.65 ± 0.90 A/m² average current density). The electrophoretic force now overcame the electrostatic repulsion and electroosmosis. Consequently, SA could be adsorbed by the membrane and enter the permeate. Doyen et al. (2013) reported an increasing permeation of charged compounds through a UFM when exposed to a higher electric field due to their enhanced electrophoresis rate. It is assumed that the different reactions to the overpotential state in AEM and UFM are due to their permeability and selectivity. The generated OH^- ions and other anionic compounds were transferred through the AEM as long as their size was small enough; however, not all OH^- ions produced in the retentate cell were carried to the permeate cell when using the UFM, which resulted in an increasing pH and conductivity in both compartments (Table A.4.1 and 2). This observation may indicate that the repulsion forces between OH^- or anionic salt ions and the UFM were stronger than those between SA and UFM. Therefore, the majority of the current may still be carried by SA, resulting in a higher permeability.

In general, the results demonstrate that a significant reduction in SA content at the end of 240 min ($P<0.05$) under all treatments except application of 1.5 V UFM. While all three treatments yielded comparable SA removal ($P>0.05$), they exhibited different SA permeation profiles and fluxes. In ED, SA removal was achieved by adsorption and permeation. The highest permeation flux (59.5 ± 9.7 mg/m²h) was observed at 3.0 V using a UFM as a result of the increased electrophoretic forces dominating the electrostatic repulsion and electroosmosis. The second highest SA flux (39.9 ± 4.2 mg/m²h) was observed with an AEM using 1.5 V. In this case, the flux was enhanced by the electrostatic attraction forces between SA and the membrane, as well as by the electroosmotic flow.

The lowest flux values were observed with 3.0 V using an AEM (20.1 ± 7.8 mg/m²h) and with 1.5 V using a UFM (19.3 ± 5.1 mg/m²h). When the AEM was used, exceeding the LCD enhanced salt and OH^- ions transport through the membrane led to a reduction in the transport number of SA and its permeation. For the UFM, the electrostatic repulsion forces and reverse electroosmotic flow prevented adsorption of SA and its permeation due to inadequate electrophoretic forces generated by 1.5 V potential difference.

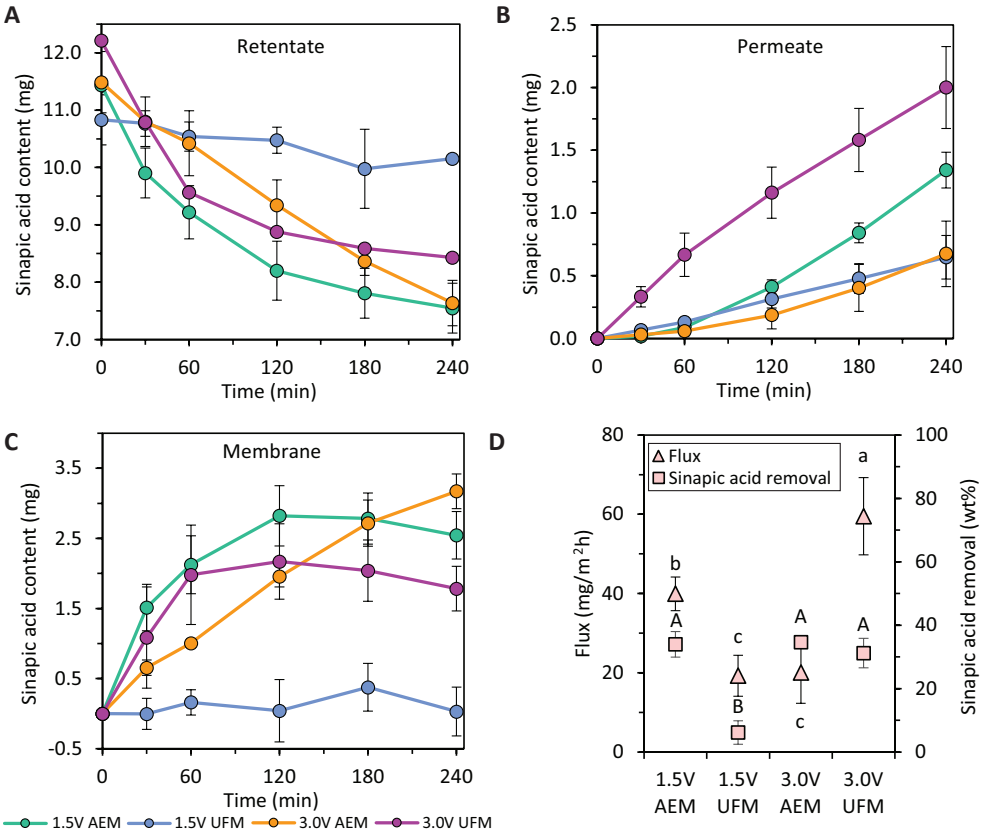

Figure 4.2: Sinapic acid content in the retentate (A), permeate (B) and in the membrane (C), and flux and sinapic acid removal (wt%) (D) under the treatments of 1.5 V AEM, 1.5 V UFM, 3.0 V AEM and 3.0 V UFM. AEM: Anion exchange membrane, UFM: Ultrafiltration membrane. Small letters indicate significance between the flux values and the capital letters indicate significance between the sinapic acid removal under different treatments ($P<0.05$).

In addition to SA removal, the retention of the protein in the feed is important. The protein content was tracked throughout the process for each applications, and the results were represented in Figure 4.3. Only the application of 3.0 V with an AEM caused a significant protein loss ($P<0.05$). The initial protein content of 148.6 ± 16.1 mg decreased to 117.9 ± 4.6 mg at the end of 240 min. This is consistent with the increasing SA adsorption by the membrane due to the increasing electrophoretic forces. Like SA, rapeseed proteins were also negatively charged under alkaline conditions. Therefore, they also migrate toward the anode electrode and adsorb to the positively charged membrane surface. This effect was also observed with 1.5 V using an AEM; nevertheless, here the protein loss was not significant within 240 min ($P>0.05$). In UFM applications, there was almost no protein loss as a result of the electrostatic repulsion between the proteins and the membrane surface ($P>0.05$).

The protein content data also reveals that the initial protein content (time = 0 min) varied, and there were considerable level of standard deviation even within the same treatment, like 1.5 V AEM. This variation occurred because the dried protein extract after methanol wash contained some stiff flocculates, preventing the collection of a uniformly dispersed protein sample for each analysis.

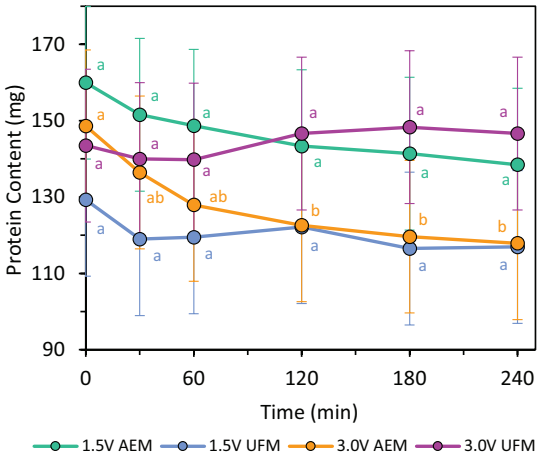

Figure 4.3: Changes in the protein content under different treatments throughout the process. Time = 0 min indicates the initial protein content. AEM: Anion exchange membrane, UFM: Ultrafiltration membrane. The letters indicate significant difference in the protein content during 240 min for each treatment (P<0.05).

Lastly, all treatments were assessed on their pH stability. As a general rule, water splitting reaction takes place when the current exceeds the LCD, leading to pH changes as a result of generated H^+ and OH^- ions (Kniaginicheva et al., 2015). The results confirmed this. The initial pH of 8.0 was stable throughout the process when the UFM was used at 1.5 V, while a small deviation was observed when the AEM was used; the final pH was 7.77 ± 0.11 in the retentate and 7.64 ± 0.14 in the permeate cells. The reason of this is the transport of anions through the AEM, which was not visible with the UFM due to the electrostatic repulsion.

On the other hand, strong pH changes were observed with both AEM and UFM as soon as the LCD was exceeded. In AEM, the H^+ and OH^- ions produced in the retentate cell migrated through the CEM and AEM (Figure 4.1), and the pH decreased to 6.14 ± 0.45 in the retentate cell. However, the passage of OH^- ions through the AEM caused the pH to increase to 9.78 ± 0.64 in the permeate cell. As mentioned earlier, ion transport through the UFM was not that efficient; therefore, OH^- ions accumulated in both retentate and permeate cells, which caused an increasing pH in both compartments. The final pH was recorded as 10.49 ± 0.30 in the retentate and 10.62 ± 0.63 in the permeate cells. The detailed pH information can be found in Table A.4.2.

Overall, four different configurations were tested to reveal the most optimal treatment for performing the electrophoretic SA separation from rapeseed protein extract. Regarding the total SA removal, protein loss and pH stability; the treatment of 1.5 V AEM is the most promising condition. To demonstrate an enhanced SA removal under this condition, the approach was upscaled using five AEMs.

Changes in the mixture composition when treated by five AEMs and 1·5 V can be seen in Figure 4·4A. The majority (84·5 ± 2·7 wt%) of SA was removed within the first 120 min, and the total removal was 90·3 ± 3·8 wt% at the end of 240 min. Besides, no significant protein loss was observed during the processing and 88·8 ± 7·6 wt% of proteins was retained in the sample solution ($P>0.05$). Nonetheless, when using five AEMs, the SA flux decreased to 12·9 ± 3·8 mg/m^{2}h from 39.9 ± 4·2 mg/m^{2}h when a single AEM was used. This reduction in flux is attributed to the reduced potential difference per membrane. The overall potential difference was kept constant at 1.5 V to show the effect of the increased surface area, resulting in less electrophoretic forces and impaired permeation. However, the increasing SA content in the permeate indicated that the separation obtained was not based solely on adsorption but both (transient) adsorption and permeation of SA (Figure 4.4B).

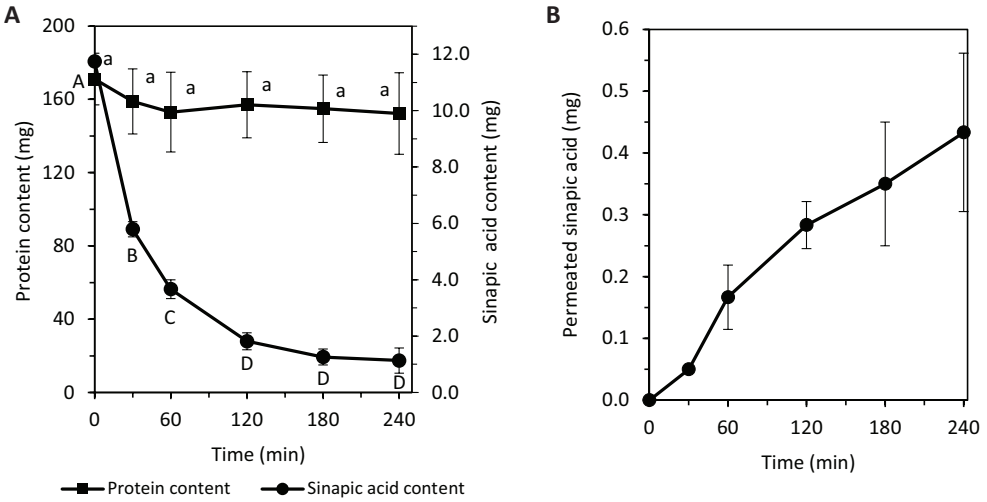

Figure 4.4: A) Changes in the protein (bars) and sinapic acid content (line) of the sample when treated by 1.5 V and five anion exchange membranes. Time = 0 indicates the initial protein and sinapic acid content. Small letters indicate significance in the protein content and the capital letters indicate the significance in sinapic acid content during the processing B) Permeated sinapic acid content.

4.4. CONCLUSIONS

We investigated electrophoretic sinapic acid (SA) removal from rapeseed proteins to explore the potential of an electric field assisted separation. We utilized both anion exchange (AEM) and ultrafiltration membranes (UFM). The separation was studied at 1.5 and 3.0 V potential difference, to investigate the separation below and above the limiting current density (LCD). The treatments were evaluated regarding total SA removal, protein loss, and pH stability.

The electrophoretic removal of SA relied on transient adsorption in the membrane and continuous permeation into the permeate chamber, driven by electrophoretic and electrostatic forces. The electrostatic forces enhanced the separation when positively charged AEM was used, but impaired the SA electromigration in the UFM due to its negatively charged surface under the influence of 1.5V. Consequently, 34.0 wt% and 6.2 wt% SA removal were recorded in AEM and UFM, respectively. This situation changed under the over potential situation. Exceeding the LCD enhanced the desalination rate, reducing the SA transport. Nevertheless, a similar level of SA removal (33.5 wt%) with 1.5 V was obtained, highlighting the effect of enhanced electrophoretic forces. Under 3.0 V UFM treatment, both SA migration and adsorption increased due to the suppressed electrostatic repulsion forces, and 31.0 wt% SA was removed.

The treatments were further evaluated regarding the protein loss and the pH stability. Only the application of 3.0 V AEM induced a notable protein loss due the combination of the electrophoretic and electrostatic attraction forces. Additionally, the pH was maintained stable only when the system was run under the LCD, both 3.0 V AEM and UFM applications resulted in dramatic pH changes due to water splitting reactions and transport of OH^- ions.

To demonstrate the improved SA separation, an AEM was chosen with 1.5 V as it provided a significant decrease in SA content, almost no protein loss and a stable pH. To upscale this approach, five AEMs were stacked to form five flow channels and increase the membrane surface area. With this configuration, 90.3 wt% SA was removed in 240 min.

Overall, the principle of electrophoretic SA removal was demonstrated utilizing an electrodialysis device. The results indicate that electric field-driven separation of SA from the proteins as a result of electrostatic and electrophoretic forces is possible and can be scaled up by increasing the surface area of the membrane.

4.5. APPENDIX

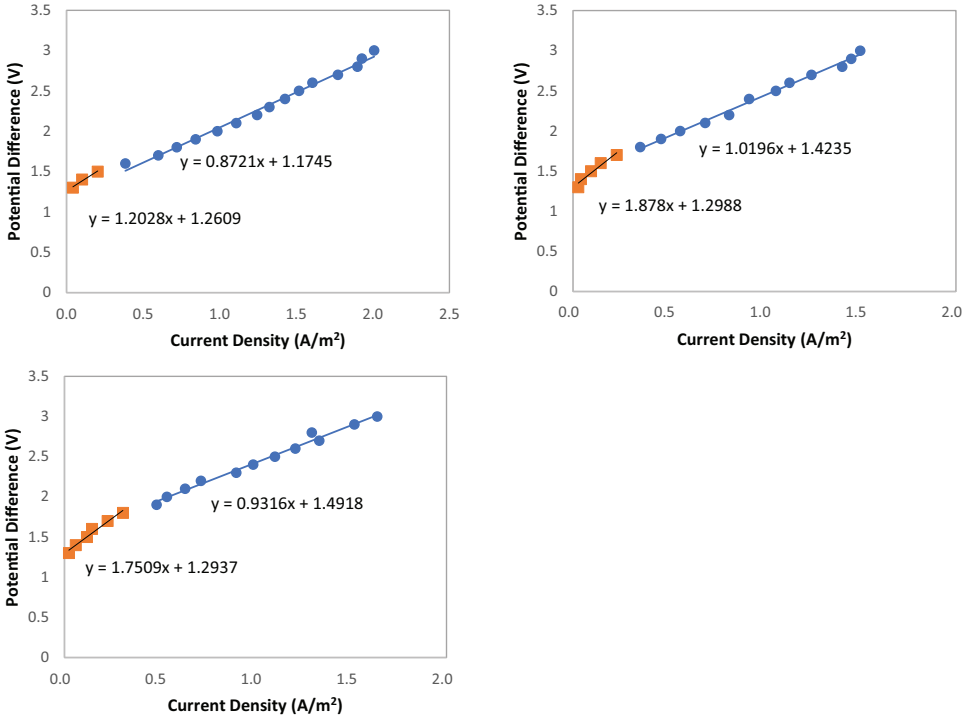

Figure A.4.1: Limiting current density measurement data for the anion exchange membrane.

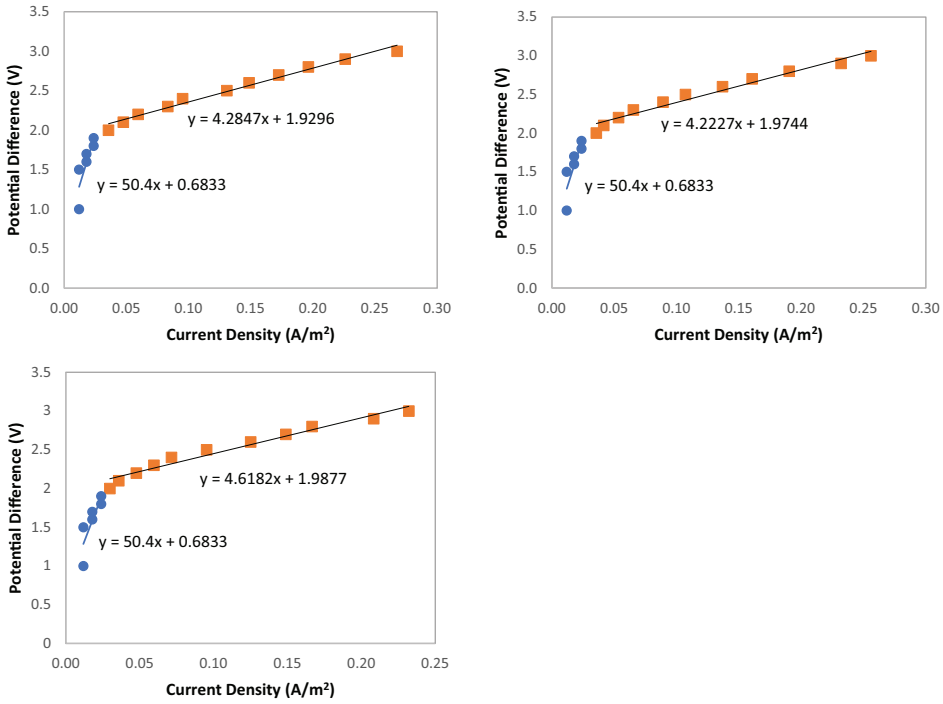

Figure A.4.2: Limiting current density measurement data for the ultrafiltration membrane (3 kDa pore size).

Table A.4.1: Changes in the conductivity of retentate and permeate samples during the electrodialysis treatment. Conductivity unit: µS/cm, AEM: Anion exchange membrane and UFM: Ultrafiltration membrane

Sample	1.5 V AEM	1.5 V UFM	3.0 V AEM	3.0 V UFM
Retentate (0 min)	386.3 ± 30.4	370.3 ± 9.0	363.3 ± 2.3	358.7 ± 6.1
Permeate (0 min)	248.0 ± 4.6	253.7 ± 9.8	246.3 ± 7.5	244.3 ± 0.6
Retentate (30 min)	373.7 ± 42.8	374.3 ± 15.0	315.0 ± 13.5	347.3 ± 21.9
Permeate (30 min)	237.0 ± 4.6	252.0 ± 7.0	299.3 ± 16.2	249.3 ± 8.6
Retentate (60 min)	374.7 ± 57.5	378.3 ± 19.1	276.0 ± 24.8	351.7 ± 31.5
Permeate (60 min)	237.3 ± 3.2	250.3 ± 9.1	349.3 ± 24.5	275.3 ± 15.9
Retentate (120 min)	389.7 ± 100.0	388.3 ± 23.2	216.7 ± 35.6	389.7 ± 53.5
Permeate (120 min)	250.7 ± 3.2	253.0 ± 5.3	443.0 ± 51.4	370.0 ± 59.9
Retentate (180 min)	404.0 ± 152.7	403.0 ± 30.1	174.7 ± 42.2	425.7 ± 68.1
Permeate (180 min)	265.0 ± 7.0	261.3 ± 4.0	521.0 ± 66.3	529.0 ± 145.5
Retentate (240 min)	415.0 ± 208.4	420.0 ± 47.5	147.5 ± 47.1	463.7 ± 93.5
Permeate (240 min)	277.7 ± 13.3	271.0 ± 4.0	599.0 ± 81.0	746.0 ± 265

Table A.4.2: Changes in the pH of retentate and permeate samples during the electrodialysis treatment. AEM: Anion exchange membrane and UFM: Ultrafiltration membrane

Sample	1.5 V AEM	1.5 V UFM	3.0 V AEM	3.0 V UFM
Retentate (0 min)	8.02 ± 0.01	8.01 ± 0.01	8.02 ± 0.01	8.01 ± 0.01
Permeate (0 min)	8.03 ± 0.02	8.02 ± 0.03	8.02 ± 0.01	8.02 ± 0.02
Retentate (30 min)	8.00 ± 0.01	8.03 ± 0.03	7.82 ± 0.08	8.60 ± 0.42
Permeate (30 min)	7.90 ± 0.12	8.01 ± 0.01	8.28 ± 0.14	8.37 ± 0.05
Retentate (60 min)	8.00 ± 0.01	8.01 ± 0.01	7.69 ± 0.21	9.39 ± 0.40
Permeate (60 min)	7.89 ± 0.13	8.02 ± 0.01	8.88 ± 0.50	8.72 ± 0.21
Retentate (120 min)	7.98 ± 0.02	8.01 ± 0.02	7.18 ± 0.29	10.02 ± 0.40
Permeate (120 min)	7.84 ± 0.17	8.03 ± 0.04	9.42 ± 0.53	9.55 ± 0.70
Retentate (180 min)	7.91 ± 0.08	8.04 ± 0.04	6.76 ± 0.36	10.33 ± 0.29
Permeate (180 min)	7.79 ± 0.18	8.02 ± 0.02	9.63 ± 0.65	10.28 ± 0.65
Retentate (240 min)	7.77 ± 0.11	8.00 ± 0.07	6.14 ± 0.45	10.49 ± 0.30
Permeate (240 min)	7.64 ± 0.14	8.00 ± 0.02	9.78 ± 0.64	10.62 ± 0.63

CHAPTER 5

Electrophoretic dephenolization of rapeseed proteins: The influence of ionic strength on sinapic acid electromigration

This chapter has been submitted as:

Ayan, K., Nikiforidis, C. V., Boom, R. M., (2024). Electrophoretic dephenolization of rapeseed proteins: The influence of ionic strength on sinapic acid electromigration

ABSTRACT

Next to the oil, proteins are the other most valuable constituent of oil bearing seeds, such as rapeseed. Current recovery methods often employ conditions (temperature, pH, use of solvents) that degrade the functionality of the proteins. Electrophoretic processes that utilize the electrical charge of the components as additional driving force, offer an alternative. Sinapic acid (SA), the predominant phenolic compound in rapeseed, can be removed by electrophoretic permeation through a membrane. As the raw juice from the rapeseeds may have differing ionic strength, it is important to analyze its effect on SA electromigration and removal under changing ionic concentrations. We examined SA solutions with five different ion concentrations (5, 10, 20, 30 and 40 mM). The highest SA removal of 57.2 ± 3.4 wt% was achieved at 5 mM buffer, which decreased between 5 and 20 mM, and then reached a plateau. The feasibility of the dephenolization principle was then demonstrated with a practical rapeseed protein extract. 30.3 ± 4.1 wt% of SA and 14.9 ± 2.8 wt% of the natural phenolics were removed in 4h of operation while retaining 96.5 ± 0.9 wt% of the proteins. The principle is expected to be easily extended towards full removal of SA and other phenols.

5.1. INTRODUCTION

Rapeseeds are the second most cultivated oil bearing crop in the worldwide due to their high oil content. The majority of the rapeseed oil can be extracted with the well-developed solvent-based industrial oil extraction process. However, this process also degrades the quality of the proteins, which nowadays emerge as valuable fraction in itself. Thus, co-extraction that preserves the quality of both the oil and the proteins is an important issue (Tan et al., 2011; Zhang et al., 2023).

The use of rapeseed protein is, however, limited by the presence of anti-nutrient compounds like phenolic compounds. These can bind to the proteins covalently or non-covalently and interfere with their proper extraction by reducing their solubility. Besides, the phenolic – protein complex impairs the digestibility and the functionality of the proteins (Alu'datt et al., 2013; Sharma et al., 2023). Dephenolized rapeseed proteins have higher solubility, which is regarded as a prerequisite for many applications (Tian et al., 2023). Thus, it is relevant to remove the phenolics during the fractionation of rapeseeds to eliminate the undesired consequences and improve the quality of the rapeseed proteins. Dephenolization can be performed using solvent extraction, with ethanol, the most common solvent employed for this purpose. Again, this technique is not environmentally benign, requires a complicated process (solubilization, solid-liquid separation, desolventizing) (Santos-Buelga et al., 2012), and leads to degradation of the proteins as well (Peng et al., 2020; Wagner et al., 2021).

For a gentler process not requiring any auxiliary solvents, we earlier proposed an electric field driven separation that makes use of electrophoretic migration of the phenolics, represented in this study by sinapic acid (SA), the most abundant phenolic compound in rapeseed (Chapter 4). The principle was demonstrated by the electrophoretic removal of SA from rapeseed protein extract, using an electrodialysis (ED) system. In an aqueous solution at pH 8.0, SA dissociates (pKa: 4.19 – 4.47) and carries a negative charge due to its carboxyl group (Nićiforović & Abramovič, 2014). Under an external electric field, SA migrates toward the anode (positively charged) electrode by permeating though a porous membrane that retains larger proteins.

The previous study was done using a very dilute system containing 1.0 mg/mL solid dispersed in 1.0 mM buffer solution. Real protein extracts are more concentrated which may affect the efficiency of the electrical separation by affecting the electromigration of the compounds. The present study therefore investigates the effect of the ionic strength on SA electromigration and removal. To limit the complexity, only pure SA dispersed in a various buffer concentrations (5, 10, 20, 30 and 40 mM) was used as a model system. Next to this model system, a real rapeseed protein extract was used to demonstrate the practical feasibility of the electrophoretic dephenolization process.

5.2. MATERIALS AND METHODS

5.2.1. Materials

Sinapic acid (purity ≥ 99.0) was obtained from Sigma Aldrich (St. Louis, MO, USA). Rapeseeds of Alizze variant (*Brassica napus*) were kindly provided by a seed breeder for protein extraction. All solutions and dispersions were prepared using deionized water (Milli-Q, Merck Millipore, Darmstadt, Germany). All other chemicals were of analytical grade and purchased from Sigma Aldrich (St. Louis, MO, USA).

5.2.2. Electrophoretic removal of sinapic acid

5.2.2.1. Electrodialysis cell configuration

An electrodialysis (ED) system was employed to investigate the effect of the ionic strength on the electrophoretic removal of SA. The ED cell (length 20 cm, width 10 cm, 84 cm^2 of effective surface area) was equipped with three peristaltic pumps to circulate the feed (retentate), permeate (flow rate: 2.0 L/h) and electrolyte solutions (0.5 M Na_2SO_4, flow rate: 20.0 L/h), and a power supply (PLH250 DC Power Supply, AimTTi, Huntingdon, U.K.) to generate the electric field. In the ED cell, electrolyte solution was separated from the retentate and permeate cells using cation exchange membranes (CEM) on both anode and cathode side, and the retentate and the permeate cells were separated using an anion exchange membrane (AEM) (Shandong Tianwei Membrane Technology Co., Ltd., Shandong, China). Specifications of the ion exchange membranes are provided in Table 5.1.

Table 5.1: Specifications of ion exchange membranes used in the experiments.

Property	Anion Exchange Membrane (AEM)	Cation Exchange Membrane (CEM)
Ion exchange capacity (mmol/g)	0.90 – 1.10	0.90 – 1.10
Thickness (wet) (µm)	70 – 80	70 – 80
Water Content (25°C) (wt%)	20 – 25	20 – 25
Electrical resistance (Ωcm^2)	4.50 – 5.50	4.50 – 5.50
pH stability	1 – 14	1 – 14
Temperature stability (°C)	15 – 40	15 – 40
Material	Polystyrene	Polystyrene
Surface charge sign	Positive	Negative

5.2.2.2. Measurement of the limiting current density

The limiting current density (LCD) determines the highest current value to maintain an Ohmic linear relation between the current and potential difference in the ED system. It was measured for different buffer solutions using the method proposed by Isaacson and Sonin (Isaacson & Sonin, 1976; Knežević et al., 2022). For the measurement, the current was incrementally increased and the corresponding voltages were recorded. Then, the current density (A/m^2) and the potential difference (V) values were plotted to determine the LCD value, marking the point where the relation between voltage and current density diverges. The measurements were done in duplicates and the results are given as average LCD ± difference between the measurements (A/m^2).

5.2.2.3. Operation of the electrophoretic sinapic acid removal experiments

To operate the system, the SA solution with different buffer concentrations (ionic strength of 5, 10, 20, 30 and 40 mM at pH: 8.0) was first prepared to obtain a concentration of 0.05 mg/mL SA. The volume of the feed (retentate) and permeate solutions were 250 mL. Before the experiment, the pH, conductivity and temperature of the solutions were measured using a multimeter (HQ440d multi, Hach, Tiel, Netherlands). The pH and conductivity were monitored during 240 min of operation at certain points in time (0, 30, 60, 120, 180 and 240 min). Besides, samples from the retentate and permeate were collected at the same specified times to analyze the SA content. At the end of the operation, the volume and temperature of the retentate and permeate were measured as well.

5.2.2.4. Determination of sinapic acid content

The SA contents of the retentate and permeate solutions were analyzed from the collected samples using a high-performance liquid chromatography system (Ultimate 3000 RS UHPLC system, Thermo Scientific, MA, U.S.A.) equipped with a UV-Vis detector. A Gemini® 3µm C18 110 Å column (150 x 4.6 mm, Phenomenex, CA, U.S.A) served as a stationary phase, with the mobile phase containing eluent A (0.1% trifluoroacetic acid in deionized water) and eluent B (0.1% trifluoroacetic in acetonitrile), delivered to the column at a flow rate of 1.0 mL/min. A gradient elution program was used for the analysis. The program started with 95.0% A and 5.0% B transitioning to 85.0% A and 15.0% B over 4 min, then to 80.0% A and 20.0% B over the next 10 min, followed by a shift to 50.0% A and 50.0% B over the next 10 min, and finally reverted to the initial composition in the last 3 minutes of the analysis. The column temperature was set at 35 ˚C, the UV detector was set to 220 and 325 nm and the injection volume was 10 µL. Calibration of the system was performed using SA (purity ≥ 99.0) with different concentrations between 0.01 – 0.2 mg/mL. All analyses were done in triplicate, and the results were given as mean ± standard deviation (mg/mL).

The electrophoretic removal of SA from the feed solution and the electro-migration of SA through the membrane were quantified using Equation (5.1), (5.2), (5.3) and (5.4).

$$Sinapic\ acid\ content\ (mg) = Sinapic\ acid\ concentration\ (mg/mL) \cdot Sample\ volume\ (mL) \quad \text{Equation (5.1)}$$

$$Sinapic\ acid\ removal\ (wt\%) = \frac{Initial\ sin.acid\ content\ (mg) - final\ \sin.acid\ content\ (mg)}{Initial\ sin.acid\ content\ (mg)} \cdot 100\% \quad \text{Equation (5.2)}$$

$$Sinapic\ acid\ removal\ flux\ (mg/m^2 h) = \frac{Removed\ sinapic\ acid\ content\ (mg)}{Surface\ area\ of\ membrane\ (m^2) \cdot Duration(h)} \quad \text{Equation (5.3)}$$

$$Sinapic\ acid\ permeation\ flux\ (mg/m^2 h) = \frac{Permeated\ sinapic\ acid\ content\ (mg)}{Surface\ area\ of\ membrane\ (m^2) \cdot Duration(h)} \quad \text{Equation (5.4)}$$

5.2.2.5. Approximation of the desalination rate in the feed solution

In ED systems, ions migrate towards the opposite electrode by passing through a CEM or AEM depending on their charge. To determine the degree of desalination of the feed solution (retentate), the initial and the final conductivity values were used (Equation 5.5).

$$Total\ desalting\ (\%) = \frac{Initial\ conductivity\ of\ feed\ solution}{Final\ conductivity\ of\ feed\ solution} \cdot 100\% \quad \text{Equation (5.5)}$$

5.2.3. Electrophoretic dephenolization of rapeseed protein extract

5.2.3.1. Extraction of rapeseed proteins

Rapeseed proteins were extracted from full-fat rapeseeds by dispersing the seeds in deionized water at a ratio of 1:7 (w/w). The pH of the dispersion was then adjusted to 8.0 by adding 10.0 M NaOH. The dispersion steeped while stirred at 400 rpm for 4 h at room temperature. Subsequently, the seeds were blended at high shear rate for 90 s (Thermomix TM31, Utrecht, the Netherlands) and the resulting slurry was passed through a twin-screw press (Angel 7500, Naarden, the Netherlands) to release the juice from the seed fiber. The collected dispersion was centrifuged at 10,000 g and 4°C for 30

min (Sorvall Lynx 4000 Centrifuge, Thermo Scientific, USA). The cream layer containing the oleosomes was scooped out and the supernatant containing the extracted proteins was collected. To remove the residual oleosomes from the supernatant, the supernatant was vacuum-filtered over a 2.5 µm pore size filter paper (Whatman Grade 5, GE Healthcare Life Sciences, Little Chalfont, UK). The collected extract was stored at 4 °C for electrodialysis experiments. Some of the extract was freeze dried (Epsilon 2-10D LSCplus, Martin Christ, Germany) to determine its total solid content.

5.2.3.2. Characterization of the rapeseed protein extract

5.2.3.2.1. Determination of total solid content in the rapeseed protein extract

To determine the total solid content of the rapeseed protein extract, a known amount of liquid extract was poured into containers, and then freeze dried. The freeze dried protein extract will still contain some moisture, so to remove the remaining moisture the freeze-dried protein extract was then dried in an infrared moisture analyzer (MA 35, Sartorius, Germany) at 105 ˚C until a constant weight was observed. The total solid content was determined using Equation (5.6). The samples were analyzed in triplicate and the results were given as mean ± standard deviation (wt%).

$$Total\ solid\ content\ (wt\%) = \frac{Amount\ of\ the\ dried\ extract\ (g)}{Amount\ of\ the\ undried\ extract\ (g)} \cdot 100\%$$

Equation (5.6)

5.2.3.2.2. Determination of rapeseed storage proteins content

The protein concentration in the collected samples was quantified to assess the protein loss during the electroseparation process. For this purpose, High-Performance Size Exclusion Chromatography (HPSEC) (Ultimate 3000 UHPLC system, Thermo Scientific, MA, U.S.A.) equipped with a UV detector was used. A combination of a TSKgel G3000S column (WxL 7.8 mm × 300 mm) and a TSKgel G2000S column (WxL 7.8 mm × 300 mm) (Tosoh Bioscience LLC, King of Prussia, PA, U.S.A.) served as stationary phase, and 30% acetonitrile in deionized water and 0.1% trifluoroacetic at a constant flow rate of 1.5 mL/min was used as mobile phase. The column temperature was kept at 30˚C, the UV detector was set at 214 nm and the injection volume was 10 µL.

The system was calibrated using purified rapeseed proteins (cruciferins and napins) in the range of 0.03 – 2.0 mg/mL range. Both standards and the samples were analyzed in triplicate. The total protein content (mg) and protein retention were calculated using Equation (5.7) and (5.8), and the results were given as mean ± standard deviation (wt%).

$$Total\ protein\ content\ (mg) = Protein\ concentration\ (mg/mL) \cdot Sample\ volume\ (mL)$$

Equation (5.7)

$$Protein\ retention\ (wt\%) = \frac{Initial\ protein\ content\ in\ the\ feed\ solution\ (mg)}{Final\ protein\ content\ in\ the\ feed\ solution\ (mg)} \cdot 100\%$$

Equation (5.8)

5.2.3.2.3. Total phenolic content of the rapeseed protein extract

The total phenolic content was determined using the Folin Ciocalteu assay. For the analysis, 1.0 mL of sample was mixed with 5.0 mL of deionized water, and 0.5 mL of Folin Ciocalteu reagent was added. The mixture was vortexed, and 1.0 mL of 20 wt% Na_2CO_3 solution was added. The volume of the mixture was completed to 10.0 mL by adding deionized water. The samples were then incubated in darkness for 1h, and their absorbance was measured at 725 nm using an UV-Vis Spectrophometer (DR6000, Hach, Colorado, U.S.A). Tannic acid (TA) was used as a standard for the quantification. The standard TA samples were analyzed in duplicate, while the rapeseed protein extract samples were analyzed in triplicate. The total phenolic content and total dephenolization were calculated using Equation (5.9) and (5.10), and the results were given as the mean ± standard deviation.

$$Phenolic\ content\ (mg) = Phenolic\ concentration\ (mg/mL) \cdot Sample\ volume\ (mL)$$

Equation (5.9)

$$Total\ dephenolization\ (wt\%) = \frac{Initial\ phenolic\ content\ (mg) - Final\ phenolic\ content\ (mg)}{Initial\ phenolic\ content\ (mg)} \cdot 100\%$$

Equation (5.10)

5.2.3.2.4. Sinapic acid content of the rapeseed protein extract

The SA content in the retentate and permeate, SA flux and SA removal were determined as described in Section 5.2.2.4.

5.2.3.3. Operation of the electrophoretic dephenolization

For the electrophoretic dephenolization of the rapeseed protein extract, the same ED device and the procedure described in the Section 5.2.2.1 and 5.2.2.3 were used with some modifications. To increase the surface area of the membrane and to assess more solutions within a given period of time, five AEMs instead of one were used, and flow rate of retentate and permeate solutions were set at 5.0 L/h. Then, the LCD was determined as explained in the Section 5.2.2.2. To treat the rapeseed protein extract, an identical conductivity buffer solution was used in the permeate cell, which was 10 mM potassium phosphate buffer at pH: 8.0. Before starting the experiment, the pH of the rapeseed protein extract was re-adjusted to pH 8.0 when necessary.

5.2.4. Energy consumption by the electrodialysis and joule heating

The energy consumed by the electrodialysis process is calculated using the applied potential difference (*U*, *V*), current (*i*, *mA*) and treatment duration (*t, h*) (Equation 5.11), and the use of buffers with varying ionic concentration was compared with each other. Besides, the total energy consumed to treat the rapeseed protein extract was also calculated.

As the use of electrical energy can cause joule heating, the initial and final temperature differences (T - T_0) in the sample solutions due to the joule heating were quantified using the Equation (5.12) to evaluate the effect of electric field on the temperature. Here, i (*A*) is current, t (*s*) is time, m is sample mass (*kg*) and C_p is water specific heat capacity (4182 *J/kg°C*).

$$Energy\ consumption\ (mWh) = U \cdot i \cdot t \qquad \text{Equation (5.11)}$$

$$U \cdot i \cdot t = m \cdot C_p \cdot (T - T_0) \qquad \text{Equation (5.12)}$$

5.2.5 Statistical analysis

SPSS version 25.0 for Windows (IBM Corp. NY, USA) was used to assess the significance of differences among different treatments. For this purpose, one-way ANOVA and Tukey test were used. The results were evaluated at a 95% confidence level.

5.3. RESULTS AND DISCUSSION

5.3.1. Determination of the limiting current densities for various buffer concentrations

The LCDs were measured for 5, 10, 20, 30 and 40 mM buffer concentrations. It increases with higher flow rate, temperature, and ionic strength. In the present study, only the ionic strength of the solution was varied; thus, the change in LCD was solely based on the ionic strength. Figure 5.1 shows the linear dependence of the LCD and the conductivity on the ionic strength of the solution. Above the LCD, the counter ions near the ion exchange membranes are depleted and water molecules dissociate into H^+ and OH^-. This does not contribute to further separation while using more electric energy, and compromises the membrane perm-selectivity. It is therefore generally advised to operate ED systems at up to 80% of LCD (Knežević et al., 2022; Zimmermann et al., 2023). The measured LCDs and the current values for the system operation for each buffer concentration are shown in Table 5.2, and the detailed date are represented in Figure A.5.1-5 and Table A.5.1 (Appendix).

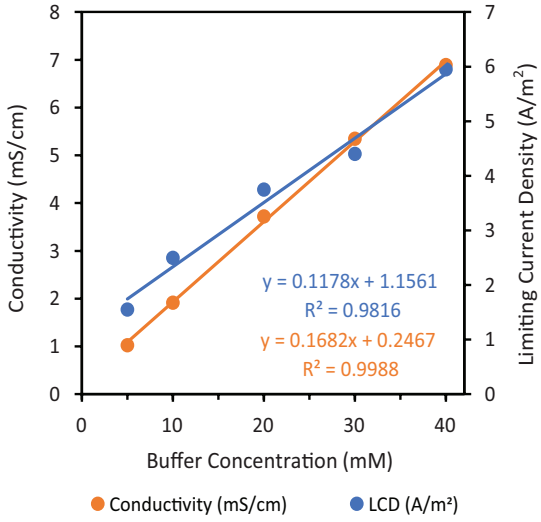

Figure 5.1: Conductivity and limiting current density values according to the increasing ionic strength of potassium phosphate buffer solutions at pH: 8.0. Solid lines represent the regression.

Table 5.2: The measured limiting current density values for various buffer concentrations and the current values used for the electrodialysis operations.

Buffer Concentration (mM)	Limiting Current Density (A/m^2)	Operation Current Values (mA)
5	1.55 ± 0.00	9.6
10	2.50 ± 0.00	16.8
20	3.75 ± 0.08	24.8
30	4.40 ± 0.00	30.0
40	5.95 ± 0.00	40.0

5.3.2 Electrophoretic sinapic acid removal under increasing ionic strength

In an ED system, the migration of a charged compound is governed by the combination of diffusion, electrophoresis and convection (solvent flow). The significance of these factors depends on the location and conditions in the ED cell. In the bulk solutions of the retentate and permeate, the migration of the compound is provided by its electro-migration and convective liquid flow. In the membrane, electrophoretic migration of the charged components takes place, plus electro-osmotic flow of the complete solution. In our case, we do not employ a pressure difference over the membrane, and therefore there is no contribution of pressure driven flow. The diffusive transfer in the boundary layers near the membrane is neglected as the feed solution is mixed continuously and the system is operated below the LCD (Tekinalp et al., 2023). In the current system, we neglected the electro-osmotic flow too because no significant volume change due to liquid transfer was observed between the retentate and the permeate cell after operation (data not shown). Therefore, we assumed that the migration of SA in the bulk solution was achieved by only electrophoresis. It is expected that a larger ionic strength causes a reduction of the electrophoretic migration rate (u_i) by affecting the electrophoretic mobility (μ_i) and electric field strength (E).

$$u_i(m/s) = \mu_i(m^2/Vs) \cdot E\,(V/m) \qquad \text{Equation (5.13)}$$

$$E\,(V/m) = Current\ density\,(A/m^2) \Big/ Conductivity\,(S/m) \qquad \text{Equation (5.14)}$$

Figures 5.2A and D represent the retained SA content, total SA removal and SA removal flux, respectively. The removal of SA initiated by its adsorption by the membrane, which is mainly triggered by the electrophoresis. The results show that the lowest final SA content and highest SA removal (57.2 ± 3.4 wt% with 207.9 ± 15.0 mg/m^{2}s removal flux) were achieved with 5 mM buffer ($P<0.05$). Using 10 and 20 mM buffer solutions then gave decreasing SA removal. Above 20 mM, the SA removal flux did not change significantly ($P>0.05$). This indicates that the electrophoretic migration rate reached a plateau.

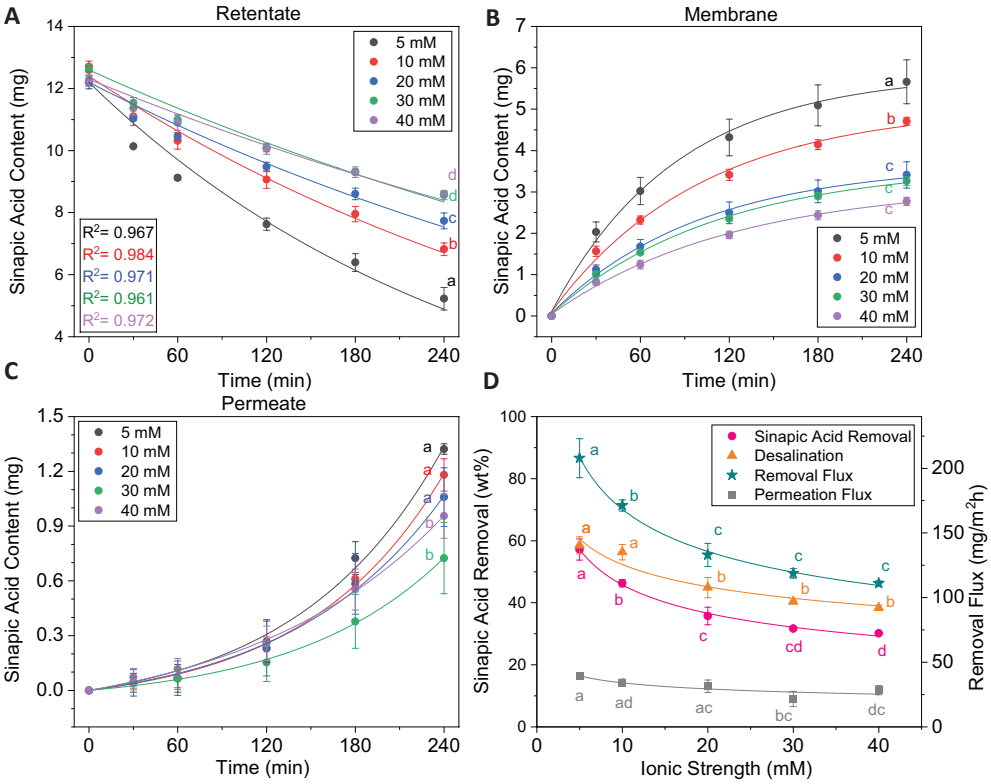

Figure 5.2: Sinapic acid content in the A) retentate solution, B) membrane and C) permeate solution during the processing. D) Total desalination, sinapic acid removal, removal and permeate fluxes according to the increasing ionic strength. The letters indicate significant differences between the different buffer concentrations (P<0.05). Solid lines in A are the fitted model equation based on ($C_{outlet} = C_{inlet} \cdot exp\ (-u_e \cdot t / W)$), and solid lines in B,C and D are guide for the eyes.

The electrophoretic migration rate is calculated by multiplying the electrophoretic mobility and the electric field strength (Equation 5.13 and 5.14). Since SA is molecularly dissolved in water, it was not possible to directly measure its mobility using electrophoretic light scattering. Thus, the electrophoretic mobility of SA in different buffer solutions was predicted based on its content in inlet (C_{inlet}) and outlet (C_{outlet}) retentate solutions, process time (t) and channel thickness (W) (Equation 5.15) (Sun et al., 2020). The average electric field strength was estimated using the current density and the average conductivity (Equation 5.14). The equation described the experimental results well, indicating that the process could be further extended to achieve quantitative removal of the SA (Figure 5.2A and Figure A.5.7). The electrophoretic mobilities and electrophoresis rates of SA are shown in Table 5.3. The highest electrophoretic mobility was indeed observed in 5 mM buffer; increasing the ionic strength of buffer reduced the electrophoretic mobility. There was no further significant reduction in the electrophoretic mobility above 10 mM, and 40 mM provided the lowest SA electrophoretic mobility. The results also indicated that the reduced

electric field strength due to the increasing ionic concentration caused the further decrease in the electro-migration rate of SA.

$$C_{outlet} = C_{inlet} \cdot exp\left(\frac{-u_e \cdot t}{W}\right) \quad \text{Equation (5.15)}$$

The observed relation between the ionic strength and the electrophoretic mobility is typical for the molecular interaction between the SA and the electrolytes (Koval et al., 2005; Stellwagen & Stellwagen, 2020). When a charged compound is dispersed/dissolved in an electrolyte solution, it attracts counter-ions from the electrolyte, which forms an ionic 'cloud' around the compound. An increasing ionic strength shields the solute´s charge (SA in the present case). Nevertheless, the charge screening reaches a saturation point where the attracted counter-ions is too dense and cannot cause a further decrease in the electrophoretic mobility (Bahga et al., 2010; Gopmandal & Duval, 2022). In our case, the electrophoretic mobility of SA reached this value at 10 mM.

Following SA adsorption, its removal continues by permeation, as soon as the concentration gradient reaches the permeate side of the membrane. Diffusive forces cannot be disregarded in the membrane, as it is the limiting layer in the system, and forms a concentration gradient. Thus, both diffusion and electrophoresis determine the SA migration through the membrane. In the membrane, diffusion is slower than in a bulk solution as the available space for diffusion is smaller. The diffusion coefficient (D_i) and the electrophoretic mobility (μ_i) are related through the Einstein equation (Equation 5.16), in which R is the universal gas constant ($J/mol{\cdot}K$) and T is the temperature ($^{\circ}K$). The diffusion coefficient inside the membrane pores is related to the diffusion coefficient in bulk solution and water fraction of the membrane (φ_w) (Equation 5.17) (Liu & She, 2022).

$$\mu_i = \frac{z_i D_i}{RT} \quad \text{Equation (5.16)}$$

$$D_{i,\,membrane} = D_{i,\,free\,solution} \cdot \left(\frac{\varphi w}{2-\varphi w}\right)^2 \quad \text{Equation (5.17)}$$

Table 5.3: The estimated electrophoretic mobility of sinapic acid in the bulk solution, average electric field strength, the estimated electrophoretic migration rate in the bulk solution, and the estimated electrophoretic mobility and diffusion coefficient inside the anion exchange membrane. The letters indicate the significant differences between different buffer concentrations (P<0.05).

Buffer Concentration (mM)	Electrophoretic Mobility in free solution (µmcm/Vs)	Average Electric Field (V/m)	Electrophoretic Velocity in bulk solution (µm/s)	Electrophoretic Mobility in the membrane (µmcm/Vs)	Diffusion Coefficient in the membrane (m^2/s)
5	-0.289 ± 0.035[a]	11.0 ± 0.5[a]	-0.032 ± 0.003[a]	-0.0046 ± 0.0006[a]	$1.2 \cdot 10^{-12} \pm 1.5 \cdot 10^{-13}$[a]
10	-0.213 ± 0.009[b]	10.6 ± 0.8[a]	-0.023 ± 0.001[b]	-0.0034 ± 0.0001[b]	$8.5 \cdot 10^{-13} \pm 3.6 \cdot 10^{-14}$[b]
20	-0.212 ± 0.020[b]	7.9 ± 0.2[b]	-0.017 ± 0.001[c]	-0.0034 ± 0.0003[b]	$8.8 \cdot 10^{-13} \pm 6.9 \cdot 10^{-14}$[b]
30	-0.197 ± 0.002[b]	7.3 ± 0.1[b]	-0.014 ± 0.000[cd]	-0.0032 ± 0.0000[b]	$7.4 \cdot 10^{-13} \pm 2.1 \cdot 10^{-14}$[b]
40	-0.188 ± 0.001[b]	6.9 ± 0.0[b]	-0.013 ± 0.000[d]	-0.0030 ± 0.0000[b]	$7.6 \cdot 10^{-13} \pm 4.1 \cdot 10^{-14}$[b]

Figure 5.2A, B and C indicates that the SA that is removed from feed solution does not immediately permeate but first accumulates in the membrane due to its interaction with the membrane's charged groups, and the low mobility (both diffusive and electrophoretic). To put this into a perspective, the electrophoretic mobility and the diffusion coefficient of SA in the membrane was estimated. The electrophoretic mobility of SA in the membrane was more than 60 times lower than the bulk value (Table 5.3). Again, 5 mM buffer provided the highest electrophoretic mobility and diffusion coefficient in the membrane. However, 5, 10 and 20 mM provided a similar level of SA permeation through the membrane (P>0.05), while 30 and 40 mM provided the lowest SA permeation. The ionic strengths inside the membrane are affected by Donnan interaction and therefore are more constant than the bulk ionic strengths, leading to diffusivities and electrophoretic mobilities inside the membrane that depend less on the bulk ionic strength. The permeation flux values represented in Figure 5.2D also indicated the similarities between the different buffer concentrations. No significant differences were observed between 20, 30 and 40 mM buffer concentrations and 5, 10 and 20 mM buffer concentrations (P>0.05).

The transport numbers (t_i) provide additional insight to the transfer through the membrane. The transport number is defined as the fraction of the current carried by a certain ion, relative to the overall current in the system (Equation 5.18). In this study potassium phosphate buffer was used and dissociation of the buffer components at pH 8.0 gives various anionic compounds ($H_2PO_4^-$ and HPO_4^{-2}) with different valences. An average valence (z_i) (-1.5) and flux (N_i) values were used for $H_2PO_4^-$ and HPO_4^{-2} to avoid unnecessary complications. Table 5.4 shows the estimated transport numbers. The transport of the buffer ions always dominates the transport through the AEM. This is reasonable because under low current density values, the ion exchange membrane is more selective to divalent ions like HPO_4^{-2} (Kim et al., 2012). The higher $H_2PO_4^-$ transport number over SA can be explained by its higher diffusivity due to its lower molecular weight. Besides, the buffer concentration (5 – 40 mM)

is always much higher than that of SA (0.22 mM), which affects adsorption of salt ions as well (Honarparvar & Reible, 2020). The increasing ionic strength of the buffer causes a decrease in the SA transport number until 20 mM, but above this value did not change significantly ($P>0.05$). This is explained by the Donnan exclusion due to the fixed charge groups in the membrane. It is clear that a lower ion concentration provides more efficient SA permeation and removal from the feed solution. One should realise that over time the ionic strength of the feed solution will be reduced (Table A.5.3), due to the larger transport numbers of the buffer ions, which may create a synergistic effect for an enhanced SA removal under extended treatment duration (or when using larger membrane surface areas).

$$t_i = \frac{z_i N_i}{\sum_i z_i N_i} \qquad \text{Equation (5.18)}$$

Table 5.4: Estimated transport numbers of sinapic acid and anionic salt components.

Buffer Concentration (mM)	Sinapic acid transport number	Anionic salt ions transport number
5	0.0193 ± 0.0022[a]	0.9807 ± 0.0022[a]
10	0.0081 ± 0.0023[b]	0.9919 ± 0.0023[b]
20	0.0035 ± 0.0014[b]	0.9965 ± 0.0014[b]
30	0.0052 ± 0.0024[b]	0.9948 ± 0.0024[b]
40	0.0034 ± 0.0006[b]	0.9966 ± 0.0006[b]

In addition to SA and buffer ion transport, pH and temperature were tracked to determine the system stability during the operation. As the ED system was operated below the LCD, it was not expected to observe strong pH changes in the retentate and the permeate solutions, and the obtained results confirmed that the pH was stable at around pH 8.0 without any significant deviation (Table A.5.2). The temperature increased with 1.0 - 4.0˚C over 240 minutes, which is attributed to the energy introduced by pumping and other agitation since only minor contributions from joule heating (0.4 ± 0.2 °C) was observed. The maximum temperature recorded 25.0 ± 1.4 ˚C was still in the range of room temperature. Thus, no detrimental thermal effect was observed. The detailed information is represented in Table A.5.4.

5.3.3 Electrophoretic dephenolization of rapeseed protein extract

We showed that the ionic strength of the solution affects SA electro-migration and overall removal; however, the SA removal reached a plateau above 10 mM ionic strength. To demonstrate the practical relevance of this approach, we used a rapeseed protein extract with 8.1 ± 0.3 wt% solid content. The ionic strength was 10 mM, and therefore a 10 mM buffer solution was used in the permeate stream to avoid any effects of a difference in osmotic pressure. Five AEMs were used instead to achieve sufficient separation. The changes made in the ED system do affect the LCD; thus, it was measured again and determined to be 0.66 ± 0.08 A/m^2 (Figure A.5.6). The ED system was operated as previously stated, and SA content, total phenolic content and protein content were analyzed together with pH, conductivity and temperature.

Figure 5.3 summarizes the overall results. After 240 min of operation, 30.3 ± 4.1 wt% of SA and 14.9 ± 2.8 wt% of phenolics were removed while retaining 96.5 ± 0.9 wt% of the proteins. In the previous section, a SA-only solution in 10 mM buffer with a single AEM resulted in 46.3 ± 1.2 wt% SA removal. The slower SA removal with the complete extract can be caused by various factors;

(i) Operation of the ED system below the LCD of 0.66 A/m2 provides a lower electric field strength (2.1 ± 0.1 V/m) when compared to 10 mM buffer application (10.6 ± 0.8 V/m).

(ii) The rapeseed extract contains proteins, soluble fibers, sugars, salt ions and different phenolic compounds, which also interact with the AEM, and may influence the adsorption and permeation of the phenolics, while the permeation of a mixture of phenolics may behave differently from only SA.

The influence by other components was confirmed by the observation that the use of a more complex mixture lead to slower desalting as well. The conductivity of the feed solution decreased by only 4.1 ± 0.8% after 240 min of operation (Table A.5.5), while with the SA-only solution this was 56.3± 2.5%. However, since the rapeseed extract does behave quite similar qualitatively to the SA solutions, we are therefore confident that the process can give much further removal of the phenolics. To extend the removal of SA and other small compounds like salts and phenolics, the system can be operated for longer times, or larger surface area AEMs can be used. In addition, electrodialysis reversal (EDR) can be employed. EDR improves the process performance by altering the electrode polarity during the process to minimize membrane fouling (Chao & Liang, 2008).

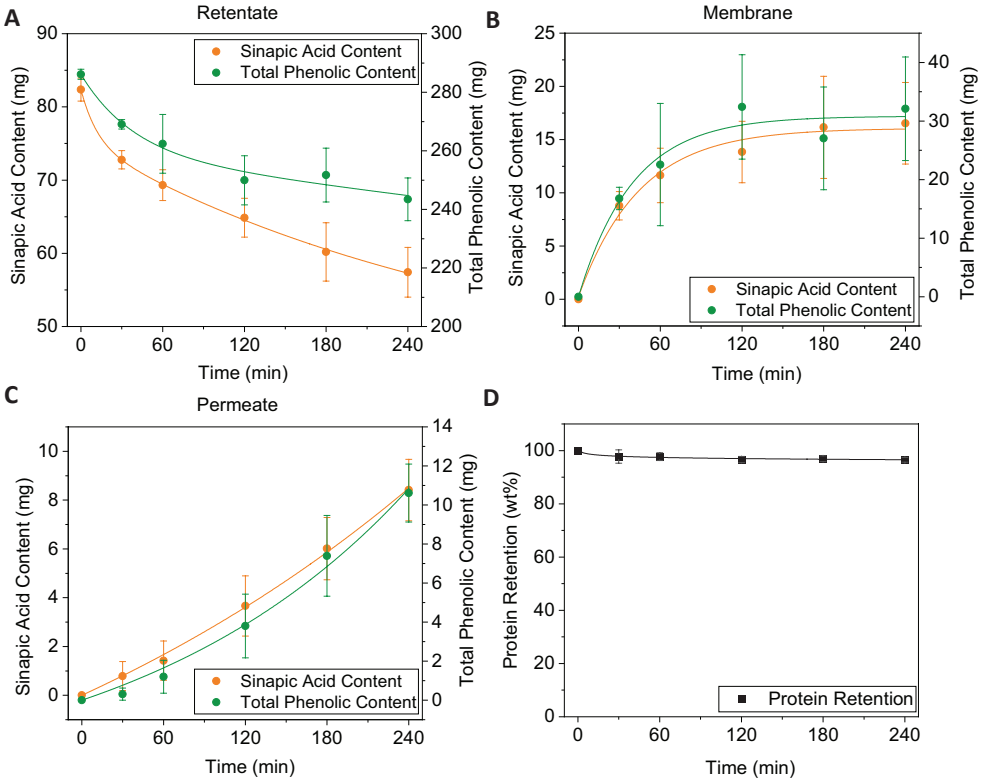

Figure 5.3: Sinapic acid and total phenolic content in the A) retentate solution, B) membrane and C) permeate solution during the operation. D) Protein retention in the retentate solution during the operation. Solid lines are guide for the eyes.

5

Similar outcomes were obtained with pH and temperature measurements. The detailed information can be found in Table A.5.5.

5.3.4 Energy consumption during electrodialysis

The energy consumption as function of the ionic strength was calculated with Equation (5.11). Figure 5.4 shows an almost linear dependence on the ionic strength. The reason of the deviation between 20 and 30 mM is the higher potential difference (3.0 ± 0.3 V) observed in the case of 20 mM when compared to 30 mM (2.4 ± 0.0 V). Additionally, Figure 5.4 compares the energy consumption with the permeation and removal fluxes of SA, and the increasing energy consumption did not enhance SA removal or permeation since it is primarily used for buffer ions transportation (desalination), as previously explained. Thus, ionic concentration not only influences SA electro-migration but also affects the energy consumption. Optimal selection of ionic concentration is necessary to design an energy efficient process.

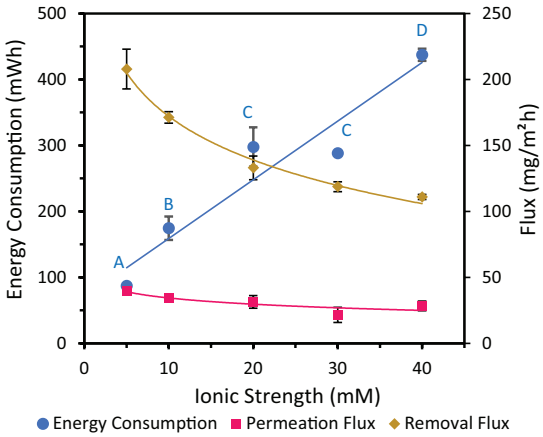

Figure 5.4: Energy consumption by the electrodialysis treatment, permeation flux and removal flux on sinapic acid under an increasing ionic strength. The letters indicate significant differences between the energy consumption values ($P<0.05$). Solid lines are guide for the eyes.

The energy required for treating the rapeseed protein extract was determined at 40.5 ± 1·8 mWh, which is significantly lower than with the SA-only solutions. We attribute that to the lower current (4.4 mA) used in that experiment.

This study demonstrates the feasibility of electric field based separation of rapeseed proteins and phenolics. Nevertheless, an ED system is a complex system and will require further investigation to optimize. Further research is needed to optimize the membrane affinity to the various phenolic compounds, adapt the process to the presence of a range of ions in the background electrolyte, and select optimal anion exchange membranes (material, water content, thickness, charge density) (Mubita et al., 2022).

5.4. CONCLUSIONS

We investigated the effect of the ionic strength (5 mM to 40 mM) on the electrophoretic removal of sinapic acid (SA) from plant protein extracts. The electro-migration of SA was affected by a higher ionic strength in two ways; (i) it reduced SA's electrophoretic mobility and (ii) it reduced the electric field strength. The highest SA removal was recorded with the use of 5 mM buffer, and SA removal decreased with 10, 20, 30 and 40 mM buffers.

During the process, SA first accumulates in the anion exchange membrane (AEM), and only after some time permeates into the permeate, moving towards steady state over time. This is due to the lower mobility of SA in the membrane due to lower diffusivity and higher affinity to the membrane's charged groups.

A full rapeseed protein extract, with 10 mM ionic strength, was used to demonstrate the feasibility of the process for practical systems. The phenolics removal were lower than with the SA-only solutions, even though the membrane surface area was five times larger than with the SA-only solutions. We expect that this is due to matrix effects and polarization of co-migrating components. While we here show the feasibility of the process, further research is required to optimize the system for industrial application.

5.5. APPENDIX

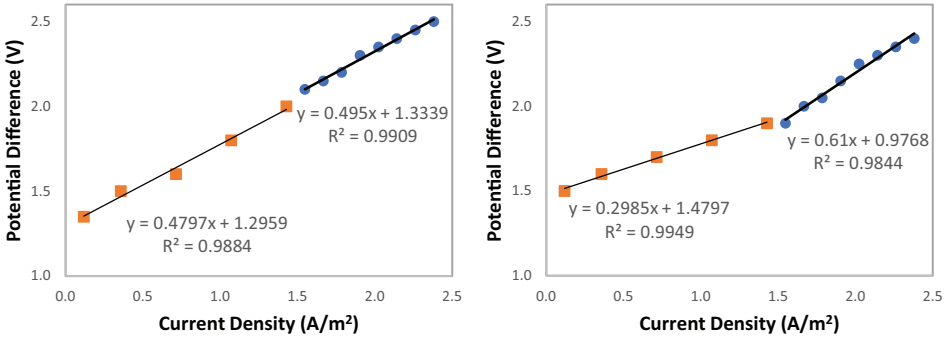

Figure A.5.1: Limiting current density measurement data for 5 mM potassium phosphate buffer.

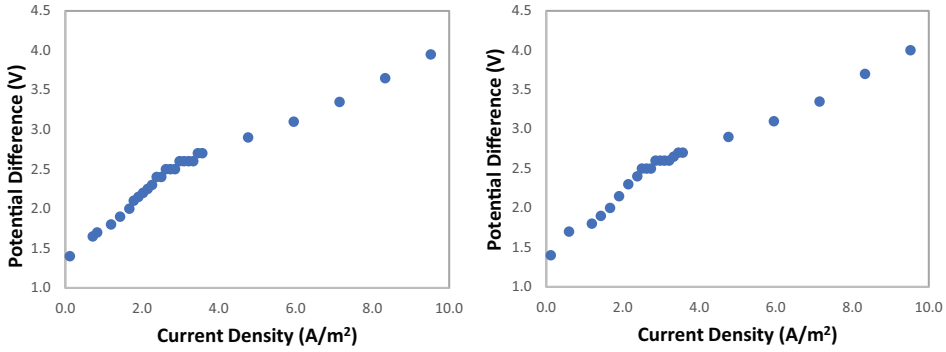

Figure A.5.2: Limiting current density measurement data for 10 mM potassium phosphate buffer.

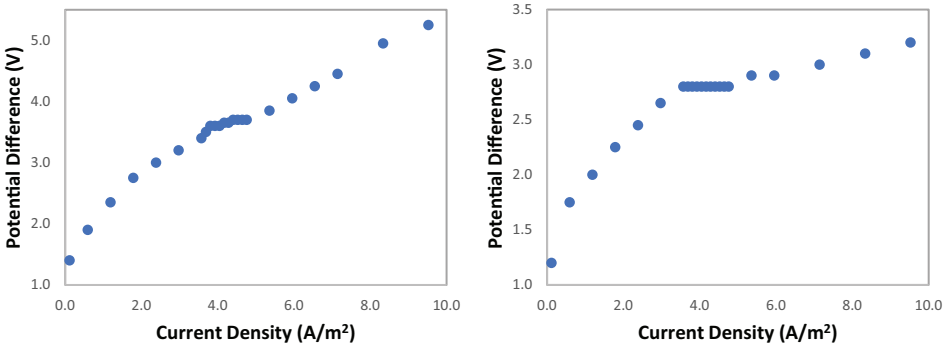

Figure A.5.3: Limiting current density measurement data for 20 mM potassium phosphate buffer.

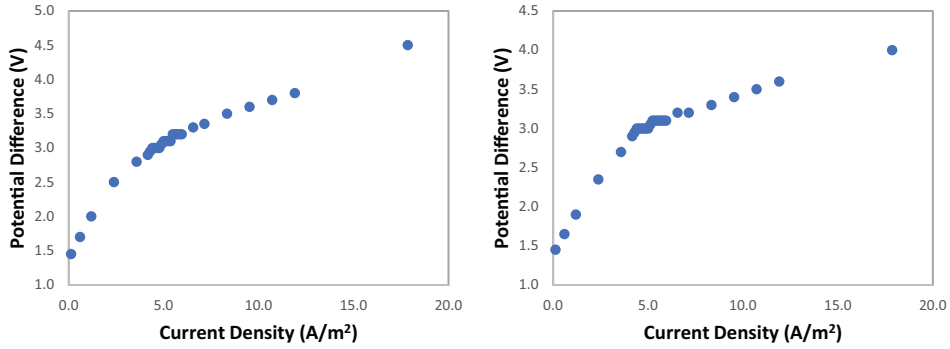

Figure A.5.4: Limiting current density measurement data for 30 mM potassium phosphate buffer.

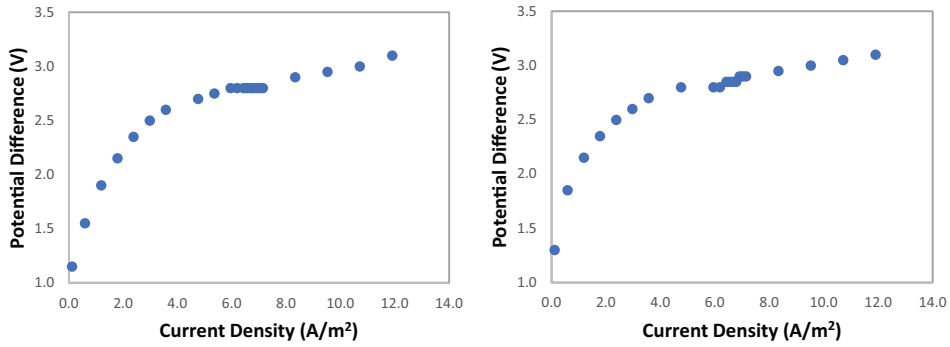

Figure A.5.5: Limiting current density measurement data for 40 mM potassium phosphate buffer.

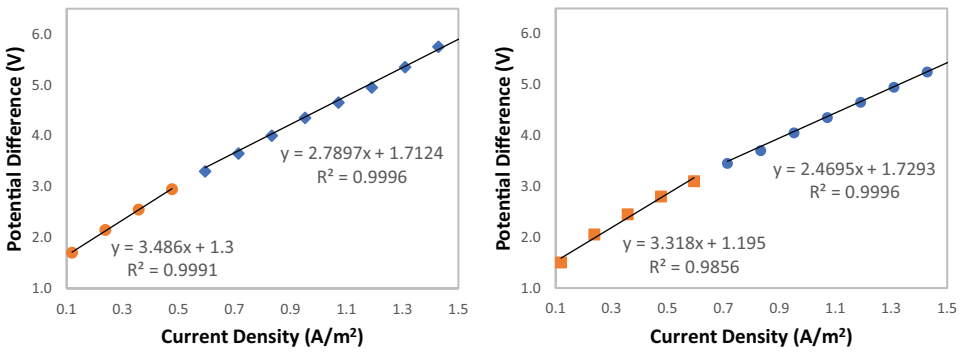

Figure A.5.6: Limiting current density measurement data for rapeseed protein extract.

Table A.5.1: Limiting current densities for potassium phosphate buffer at varying concentrations.

Sample	LCD in Measurement 1 (A/m^2)	LCD in Measurement 2 (A/m^2)	Average LCD (A/m^2)
5 mM Buffer	1.55	1.55	1.55 ± 0.00
10 mM Buffer	2.50	2.50	2.50 ± 0.00
20 mM Buffer	3.81	3.69	3.75 ± 0.08
30 mM Buffer	4.40	4.40	4.40 ± 0.00
40 mM Buffer	5.95	5.95	5.95 ± 0.00
Rapeseed Protein Extract	0.60	0.71	0.66 ± 0.08

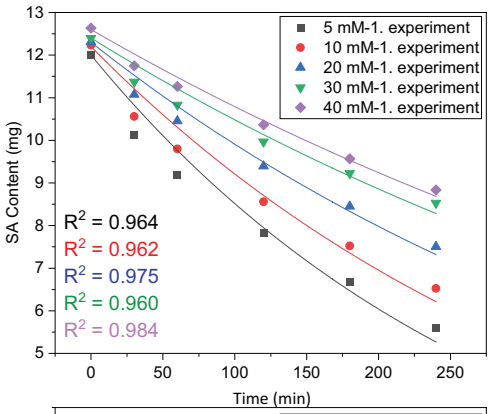

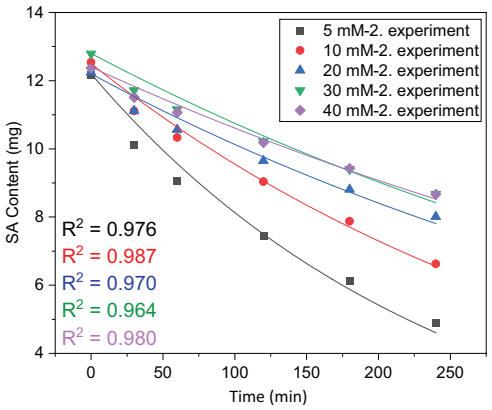

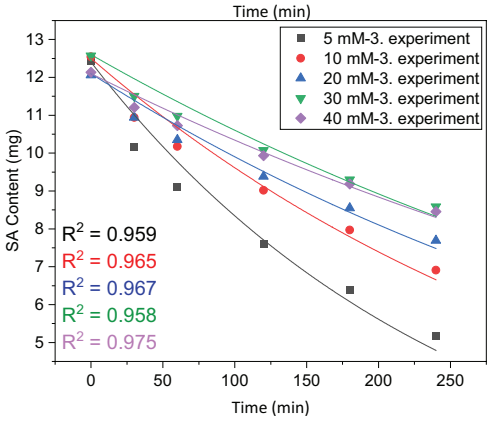

Concentration (mM)	ue (µm/min)	µe (µmcm/Vs)
5	−1.716	−0.249
5	−2.029	−0.305
5	−1.981	−0.314
10	−1.406	−0.204
10	−1.345	−0.222
10	−1.313	−0.212
20	−1.082	−0.231
20	−0.93	−0.191
20	−1.002	−0.214
30	−0.841	−0.195
30	−0.873	−0.199
30	−0.862	−0.197
40	−0.775	−0.187
40	−0.78	−0.188
40	−0.785	−0.19

Figure A.5.7: Sinapic acid (SA) retentate content during the process. Dots are the experimental data and the solid lines are fitted model equation lines ($C_{outlet} = C_{inlet} \cdot exp\ (-u_e \cdot t / W)$).

Table A.5.2: Changes in pH during the processing

Buffer Concentration (mM) / Sample	5	10	20	30	40
			pH		
Retentate (0 min)	8.03 ± 0.02	8.01 ± 0.01	8.01± 0.01	8.02 ± 0.01	8.02 ± 0.01
Permeate (0 min)	8.03 ± 0.00	8.02 ± 0.02	8.01 ± 0.00	8.00 ± 0.00	8.02 ± 0.02
Retentate (30 min)	8.00 ± 0.00	8.02 ± 0.02	8.06 ± 0.02	8.04 ± 0.04	8.04 ± 0.01
Permeate (30 min)	8.00 ± 0.00	8.00 ± 0.02	8.05 ± 0.02	8.04 ± 0.02	8.04 ± 0.04
Retentate (60 min)	7.99 ± 0.03	8.00 ± 0.06	8.05 ± 0.02	8.04 ± 0.02	8.02 ± 0.01
Permeate (60 min)	8.01 ± 0.01	8.01 ± 0.06	8.07 ± 0.01	8.04 ± 0.03	8.06 ± 0.01
Retentate (120 min)	8.01 ± 0.01	7.99 ± 0.03	8.02 ± 0.03	8.00 ± 0.02	8.02 ± 0.02
Permeate (120 min)	7.97 ± 0.05	8.05 ± 0.01	8.07 ± 0.01	8.05 ± 0.05	8.06 ± 0.01
Retentate (180 min)	7.90 ± 0.12	7.94 ± 0.06	8.01 ± 0.02	8.05 ± 0.03	8.01 ± 0.03
Permeate (180 min)	7.95 ± 0.08	8.04 ± 0.08	8.09 ± 0.02	8.07 ± 0.04	8.05 ± 0.01
Retentate (240 min)	7.91 ± 0.10	7.89 ± 0.09	8.00 ± 0.03	7.96 ± 0.02	7.97 ± 0.04
Permeate (240 min)	7.91 ± 0.08	8.04 ± 0.07	8.06 ± 0.04	8.05 ± 0.04	8.05 ± 0.02

Table A.5.3: Changes in conductivity during the processing.

Buffer Concentration (mM) / Sample	5	10	20	30	40
			Conductivity (µS/cm)		
Retentate (0 min)	1086.3 ± 7.5	2031.7 ± 78.2	3914.7 ± 18.8	5281.3 ± 28.0	7370.0 ± 29.5
Permeate (0 min)	1089.3 ± 5.8	2051.3 ± 81.7	3971.7 ± 18.5	5324.7 ± 52.2	7459.3 ± 16.3
Retentate (30 min)	984.0 ± 13.9	1846.7 ± 102.0	3644.0 ± 53.0	4924.0 ± 19.7	6938.7 ± 80.0
Permeate (30 min)	1121.7 ± 28.3	2065.3 ± 119.8	4015.7 ± 25.7	5315.3 ± 31.4	7463.7 ± 50.4
Retentate (60 min)	904.3 ± 27.1	1681.3 ± 122.7	3442.3 ± 94.9	4643.0 ± 51.4	6571.3 ± 77.0
Permeate (60 min)	1155.0 ± 32.9	2122.0 ± 149.3	4146.3 ± 59.3	5363.3 ± 49.3	7551.3 ± 37.6
Retentate (120 min)	750.3 ± 34.1	1401.0 ± 126.2	3027.7 ±146.0	4090.7 ± 25.7	5846.7 ± 50.9
Permeate (120 min)	1253.7 ± 40.4	2266.3 ± 185.7	4380.0 ± 101.3	5488.7 ± 89.6	7761.0 ± 46.8
Retentate (180 min)	601.3 ± 27.1	1155.3 ± 117.4	2625.7 ± 142.7	3605.7 ± 7.5	5177.7 ± 39.4
Permeate (180 min)	1357.0 ± 24.2	2427.0 ± 188.9	4618.0 ± 141.2	5660.3 ± 81.7	8027.3 ± 44.5
Retentate (240 min)	450.3 ± 27.1	888.7 ± 81.2	2222.7 ± 130.5	3148.0 ± 30.2	4543.0 ± 52.8
Permeate (240 min)	1471.3 ± 6.4	2602.3 ± 181.9	4865.3 ± 173.3	5873.3 ± 87.4	8276.7 ± 34.2

Table A.5.4: Changes in temperature during the processing

Buffer Concentration (mM)	5	10	20	30	40
Sample	Temperature (°C)				
Retentate (0 min)	21.6 ± 1.0	22.7 ± 1.4	21.8 ± 1.0	23.5 ± 1.2	21.8 ± 2.1
Permeate (0 min)	21.7 ± 1.3	22.3 ± 0.9	21.8 ± 1.0	23.5 ± 1.4	21.8 ± 2.3
Retentate (240 min)	24.4 ± 0.6	24.4 ± 0.8	25.0 ± 1.4	24.3 ± 0.6	24.0 ± 0.1
Permeate (240 min)	24.2 ± 0.5	24.6 ± 0.8	24.9 ± 1.6	24.4 ± 1.1	24.1 ± 0.2
Joule Heating Effect (°C)	0.1 ± 0.0	0.3 ± 0.0	0.5 ± 0.1	0.5 ± 0.0	0.8 ± 0.0

Table A.5.5: Changes in pH during the processing rapeseed protein extract

Sample	pH	Conductivity	Temperature	
			Experimental	Joule Heating Effect (°C)
Retentate (0 min)	8.02 ± 0.01	2920.3 ± 32.5	23.6 ± 3.0	
Permeate (0 min)	8.02 ± 0.01	2038.7 ± 50.0	23.1 ± 2.2	
Retentate (30 min)	8.03 ± 0.02	2918.0 ± 26.9		
Permeate (30 min)	8.02 ± 0.01	2021.0 ± 63.7		
Retentate (60 min)	8.02 ± 0.00	2897.7 ± 38.7		
Permeate (60 min)	8.07 ± 0.03	2019.3 ± 79.9		
Retentate (120 min)	8.04 ± 0.04	2862.0 ± 36.5		
Permeate (120 min)	8.08 ± 0.03	2020.3 ± 92.4		
Retentate (180 min)	8.03 ± 0.02	2828.0 ± 34.6		
Permeate (180 min)	8.07 ± 0.06	2041.0 ± 97.3		
Retentate (240 min)	8.01 ± 0.02	2801.7 ± 29.2	27.0 ± 2.5	
Permeate (240 min)	8.04 ± 0.01	2078.3 ± 83.8	27.0 ± 2.5	0.1 ± 0.0

CHAPTER 6

General discussion

6.1. INTRODUCTION

The use of oilseeds to produce functional and nutritional food ingredients is crucial for sustainable food processing and feeding a rapidly growing population. Nevertheless, the current practices focusing on oil extraction are not environmentally friendly and often compromise the functionality of the oleosomes and proteins due to the use of organic solvents/chemicals, and elevated temperatures (Nehmeh et al., 2022). This underscores the need for gentler and novel processes.

This thesis investigates the electric field-based separation of oilseed components following their aqueous extraction to develop a more sustainable separation process. The thesis aimed to develop a complete, gentle and efficient fractionation process to obtain oleosomes and phenolic-free proteins from oilseeds using electrophoretic separation. The migration rate in an electric field is proportional to the electrophoretic mobility, influenced by the charge and size of the compounds. Given the distinct size of oleosomes, proteins and phenolics, it is hypothesized that they exhibit different electrophoretic mobilities, enabling their electro-separation. Utilizing the differences in their electro-migration, components can be separated either by combining their electro-migration with an oppositely oriented hydrodynamic flow or by inserting a membrane allowing the electrophoresis of only smaller compounds. This method achieves separation based on particle migration; thus, it can eliminate the need for organic solvents and dispersion – precipitation steps.

Rapeseed was used as a model oilseed to demonstrate the devised electrophoretic separation process. Two mechanisms, charge-based and size-based separation, were studied. The charge based mechanism was demonstrated using a microfluidic device to separate rapeseed oleosomes and proteins under a balanced electrophoresis rate and counteracting hydrodynamic flow rate. Subsequently, a possible approach for upscaling the separation of oleosomes and proteins was discussed using lab-scale electrophoretic system. For separation of proteins and phenolics, electrodialysis was employed. Here, the major phenolic compound in rapeseed, sinapic acid, migrated through a porous membrane while proteins were retained due to their larger size.

This chapter reflects on the main findings and limitations throughout the conducted research, places it in a broader scientific context, and discusses future opportunities in the electrophoretic oilseed fractionation process.

6.2. ELECTROPHORETIC SEPARATION OF RAPESEED COMPONENTS: MAIN FINDINGS

Oleosomes and proteins are the two most valuable ingredients to be extracted from rapeseeds. To obtain these compounds, multiple separation steps are needed. First, oleosomes and proteins must be separated from each other. Subsequently, proteins must be purified, removing anti-nutrients like phenolics. **Chapters 2** and **3** focused on oleosome – protein separation, while **Chapters 3** and **4** concentrated on dephenolization of rapeseed proteins.

Chapter 2 introduced an electro-separation mechanism for rapeseed oleosomes and proteins, both theoretically and practically. Their separation relies on differences in electrophoretic mobility, allowing separation by combining electrophoresis and hydrodynamic flow in the opposite direction. The ultimate migration direction of oleosomes and proteins was determined according to their net velocity, which is the sum of the negative electrophoretic velocity and the positive convective flow velocity (in itself a combination of pressure driven and electroosmotic flow). The concentration of a compound in either permeate or retentate depends on the ratio of the convective flow velocity and the electromigration velocity. Full retention occurs when the electrophoresis rate exceeds the convective flow velocity. Microfluidic experiments demonstrated the principle, and that both the migration direction and the net velocity could be changed by modifying the electric field strength and/or the convective flow velocity (pressure).

The experiments showed that next to pressure-driven flow, also electroosmotic flow has to be taken into account. The latter increases with an increasing electric field strength, its direction aligns with that of the pressure-driven flow in the case of negatively charged channel walls, and it is quite significant compared to the other contributions. Thus, it is important to quantify the electroosmotic mobility to adjust the magnitude of solvent flow.

In **Chapter 3**, the electrophoretic separation was brought to lab scale by increasing the number of channels using a porous frit. As the electro-separation solely relied on balancing the electrophoresis rate with a counter-current convective flow rate, the approach proved successful. The placement of the electrodes on both sides of the porous medium ensured that the separation took place in the membrane rather than in the bulk solution. The flux of the components through the membrane clearly indicated the effect of the increasing electric field, with higher electrophoresis rates reducing the flux and improving the retention.

The average electrophoretic mobility of oleosomes (-3.1 µmcm/Vs) and proteins (-2.1 µmcm/Vs) at pH 8.0 and the convective flow velocity (113.2 µm/s) suggested that an electric field between 36.1 and 53.6 V/cm should be sufficient for their separation. The best separation, with the highest average selectivity of 9.84, was indeed achieved at 50 V/cm. Unlike the theoretical infinite selectivity value in **Chapter 2** assuming identical

electrophoretic mobility for all oleosomes, the lab-scale system suffered from inequalities in the electrophoretic mobility, causing some oleosomes to permeate with the proteins. This suggests that the separation selectivity can be increased by decreasing the overlap in the electrophoretic mobility distribution of the compounds, potentially by altering ionic strength or buffer type.

For this research, sodium and potassium phosphate buffers were tested, and potassium phosphate buffer resulted in a higher electrophoretic mobility difference (1.023 µmcm/Vs) than with a sodium phosphate buffer (0.628 µmcm/Vs). While the aim of this study was to demonstrate the system's scalability, a more detailed assessment of the effects of the ionic strength and type of solution must be performed to further improve the mobility differences.

Chapter 4 explores electrodialysis (ED) based dephenolization of rapeseed proteins. This effectively removes sinapic acid (SA) through adsorption in a membrane and subsequent transmembrane permeation driven by both electrophoresis and diffusion. ED typically selectively removes anions and cations through counter-charged membranes under an external electric field. This chapter combines the use of an electrophoretic force with the use of the size differences between the negatively charged sinapic acid (MW: 0.22 kDa) from the proteins (MW: 17 – 300 kDa). For the size exclusion by the membrane, pore size and surface charge are critical factors, and therefore, both negatively charged ultrafiltration (UFM, 3 kDa pore size) and positively charged anion exchange membranes (AEM) were tested. The ED system was operated both below and above the limiting current density (LCD).

Below the LCD, the use of an AEM gave superior SA removal, facilitated by enhanced SA adsorption via electrostatic attraction between the membrane matrix and SA. Conversely, a UFM gave nearly 50% less SA permeation, attributed to electrostatic repulsion forces and poor SA adsorption. At over-limiting conditions, a UFM showed higher SA permeation, as the electrostatic repulsion forces were dominated by the enhanced electrophoretic forces. In this case, the AEM maintained a comparable level of SA removal but provided 34% lower SA permeation. That means that the combination of electrophoretic and electrostatic forces was efficient to remove SA from the feed solution, but the permeation through the membrane was restricted. Exceeding the LCD accelerates the salt transport through an AEM, partially displacing SA and therefore potentially reducing SA transport number. On the other hand, a UFM, lacking specific selectivity towards SA or salt ions, permeates all compounds smaller than the membrane pore size, and permeation increases with the increasing electrophoretic driving force.

Despite differences in the various membrane and potential difference combinations, the total SA removal was similar (~30 wt %) with potential differences of 1.5 V and 3.0 V using an AEM and 3.0 V using a UFM. Other factors such as stability against changes in pH and loss of proteins were evaluated as well. Significant protein loss occurred due to electrostatic interactions with an AEM under 3.0 V application, which was not the case with a UFM.

Application of 3.0 V, irrespective of the type of membrane used, altered the pH dramatically because of water splitting reactions caused by the excess current passing through retentate and permeate solutions. Thus, ED based SA removal was achieved optimally with 1.5 V and the use of an AEM. **Chapter 4** demonstrated the upscaling of the ED based SA separation process to improve the total SA removal by enlarging the membrane surface area. Use of five AEMs resulted in 90.3 wt% SA removal on average. Initially the removal is primarily due to fast adsorption into the AEM, after which transfer into the permeate becomes important.

Considering the dilute nature of the sample with 0.1 wt% solid content in 1.0 mM buffer in **Chapter 4**, **Chapter 5** elaborated the electrophoretic SA removal as a function of ionic strength. Industrially relevant applications often feature higher ionic strengths. SA electro-migration decreased with increasing ionic strength due to the reduction in the electrophoretic mobility and average electric field strength. This effect of the increasing ionic strength was not linear, and reached a plateau at 10 mM. Above 10 mM, SA removal decreased due to the reduced electric field strength with increasing conductivity.

As **Chapter 4** indicated, SA was initially adsorbed in the membrane matrix. Permeation started later, due to the lower diffusional and electrophoretic mobility in the membrane matrix, attributed to the constricting structure of the membranes. The estimated electrophoretic mobilities inside the membrane were more than 60 times lower than in the bulk solution in **Chapter 5**. Besides, the predicted transport numbers showed selectivity of the AEM towards the anionic buffer components ($H_2PO_4^-$ and HPO_4^{-2}) due to higher valence of HPO_4^{-2} and their lower molecular weight resulting in higher mobilities. On average, buffer components made up 98.1 – 99.7% of the total charge permeation through the membrane. This actually can create a synergistic effect as the feed solution is concurrently desalinated (usually done in a separate process step), which then increases the electrophoretic mobility and the removal of SA by time.

Chapter 5 demonstrated the applicability of ED for electrophoretic dephenolization of whole rapeseed protein extract containing around 8.0 wt% of solid. Despite using a larger membrane surface area, a lower SA removal (30.3 ± 4.1 wt%) was obtained compared to SA-only solution (46.3 ± 1.2 wt%). This result together with 10-fold lower desalination indicates that the presence of co-extracted compounds affected the adsorption of SA and salt ions. Besides, the lower LCD resulted in a reduced electric field (2.1 ± 0.1 V/m) when compared to single layer AEM (10.6 ± 0.8 V/m). Overall, this treatment achieved 14.9 ± 2.8 wt% total phenolic removal, indicating that ED system can indeed be used for dephenolization, but may require some redesign.

The findings from **Chapters 2** to **5** collectively show the feasibility and scalability of electrophoretic separation of rapeseed components. The results highlight the importance of electrophoretic mobility differences to achieve a sufficient oleosome – protein separation, and ED based dephenolization process needs further optimization to handle complex mixtures efficiently.

6.3. MAIN CHALLENGES AND FURTHER IMPROVEMENT

This thesis explored two electrophoretic approaches to fractionate rapeseed components. Several challenges need to be addressed through further research and technical advancements.

6.3.1. Electrophoretic mobility differences

The separation of oleosomes and proteins was based on electrophoretic mobility differences. Their overlapping electrophoretic mobility distributions caused lower separation selectivity (9.84) in the upscaled system compared to theoretical infinite selectivity obtained in **Chapter 2**.

In the present case, the overlapping mobility could be attributed to their overlapping particle size, as the protein was aggregated into particles of similar sizes. For the experiments, both oleosomes and proteins were extracted and purified; additionally, the proteins were freeze-dried. The purified oleosomes and proteins were redispersed in a buffer solution to create the model system. This was done to remove other compounds that could interfere with their electrophoretic mobility measurements and the separation; however, it also caused aggregation.

The electrophoretic separation method did separate oleosomes from protein particles; however, native proteins probably exhibit different electrophoretic mobility, and may give much better separation from the oleosomes. Typically, native rapeseed proteins dissolved in an alkaline solution are a few nm in size, while native rapeseed oleosomes are around 0.5 µm. To asses the feasibility of their electrophoretic separation in their native state, it is crucial to limit aggregation during both the electrophoretic mobility measurement and the separation process. In practical applications, the electrophoretic separation will be performed directly following their aqueous extraction, thus eliminating aggregation by purification and drying. Besides, salts in the aqueous phase impact their mobility as well as their solubility. Therefore, further investigation should focus on performing the electrophoretic separation of rapeseed aqueous extraction obtained using varying salt ion species.

6.3.2. The effect of electrical potential on water splitting and pH

When an electric potential difference above a certain value is used in contact with an aqueous environment, electrolysis reactions, generating H^+ and OH^- ions at the anode and cathode electrodes, occur. In **Chapters 2** and **3**, the simplest design of the electrophoretic separation with positioning the electrodes inside the separation channel caused accumulation of the electrolysis products which created a pH gradient. From **Chapter 2**, it is evident that the

electrophoretic mobility of oleosomes and proteins is pH dependent, and a decreasing pH (near the anode electrode and sample solution) reduced all electrophoretic mobilities, also reducing the differences in mobility. The application of 75 V/cm electric field in the upscaled separation is a clear example of the effect of pH changes on the flux values, as it did not cause further retention of oleosomes and proteins, which would be theoretically possible. Therefore limiting the pH changes is necessary for a complete electrophoretic separation process.

This can be achieved by separating the electrodes from the sample and buffer solutions using cation exchange membranes (CEM) and electrode rinse chambers, as demonstrated in the ED system. However, this only eliminates the electrolysis products formed at the electrodes. When the electric current passes through the liquid, it causes water molecules to split when the LCD is exceeded. **Chapter 4** showed that the retentate solution was neutralized when an AEM is used due to the transfer of the formed H^+ and OH^- ions through the CEM and AEM. This does affect the system's stability as it leads to a significant pH increase in the permeate solution and inside the AEM matrix. Increasing the pH inside the membrane may enhance electrostatic interactions between SA (phenolics) and the membrane as a result of enhanced charge under the strong alkaline conditions (pH 9.0 – 10.0), impairing its permeation. On the other hand, the use of a UFM allowed an increasing pH in both retentate and permeate solution. This may be utilized to increase the electrophoretic mobility of SA; however, strongly alkaline conditions must be prevented as proteins and phenolics may form covalent bonds, making their separation impossible (Yang et al., 2021). This effect can be mitigated by using an ED system operating below the LCD.

6.3.3. Membrane properties and fouling

Electrophoretic separation in **Chapters 3**, **4** and **5** was performed employing membranes, which created some challenges.

In **Chapter 3**, the main issue with using a glass frit membrane was its fouling due to the presence of larger oleosomes aggregates, retention of the oleosomes near the anode electrode positioned on the membrane, and a lower pressure drop to push the samples through the membrane. Besides, the local pH drop near the anode electrode is expected to induce aggregation as soon as it approaches the isoelectric point. These factors limited the process duration to max 20 min, and would hinder full electro-separation of oleosomes and proteins. This challenge must be overcome for a comprehensive understanding of the applicability of electrophoretic oleosome and protein separation. A straightforward solution is to use a membrane with larger pore size to limit the fouling. However, this would not be enough to eliminate issues sourced from electrode positioning. Therefore, separating the electrodes from the separation channel is required.

Chapter 4 discussed the impact of the type of the membranes and surface charge on the electro-separation process. The separated compounds are all negatively charged; thus, their separation was achieved based on their distinct size. The challenge is that the larger proteins migrating in the same direction as SA may deposit on the membrane surface and cause membrane fouling especially when a positively charged AEM was used. To remove the adsorbed proteins, the electrode polarity can be periodically inverted as proposed for reverse electrodialysis systems (Strathmann, 2010). To clearly observe the effect of the electrode polarity switch, the system was operated at 50.0 V and then the polarity was inverted. Figure 6.1A showed protein loss due to adsorption in 180 min; however, 84.5 ± 1.0 wt% of the adsorbed proteins were desorbed in 30 min as a result of the altered electrode polarity. Figure 6.1B shows that the deposited fraction mainly consists of cruciferins, which have a higher electrophoretic mobility (**Chapter 2**), while napins do not deposit on the membrane but stay in the feed solution. This gives us an opportunity to integrate one more separation in the system, and separate albumins from globulins, which have very different properties and have different uses. During normal operation, the phenolics are removed from the proteins. Before polarity reversal, the feed solution can be replaced by another solution, allowing the cruciferins to be separated from the napins, which stay in the feed solution. One should note that there was much less protein adsorption and membrane fouling when operated at 1.5 and 3.0 V for 240 min, but the effect can be more pronounced at longer process times.

The use of a negatively charged UFM can eliminate protein loss and blockage of the membrane as a result of the electrostatic repulsion forces, however, it also causes rejection of SA below the LCD. It is expected that assessing the effects of different charge densities to find the optimal membrane will help improve the efficiency and effectivity of the process.

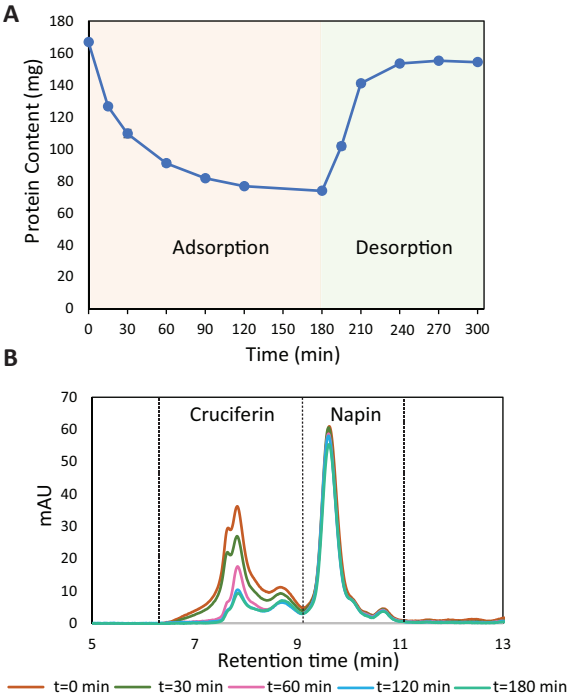

Figure 6.1: A) Amount of adsorbed and desorbed protein content in 300 min operation (180 min for adsorption and 120 min for desorption) and B) HPSEC chromatogram of the adsorbed cruciferins and napin fractions.*Total protein content was estimated using BCA Assay.

Chapter 5 highlighted the membrane selectivity and affinity. By design, AEMs have selectivity to anions, and their dense structure allows faster passage of smaller ions than relatively larger phenolic compounds. The transport numbers revealed that the largest portion of the AEM is indeed used mostly for salt transfer and only for a minor part allows SA permeation. This has a dual effect. The advantage is that desalination and dephenolization can be done simultaneously, while the reducing ionic strength over time allows greater adsorption and faster migration of SA. However, this also means compromising the SA removal at the early stages of the process.

To balance desalination and dephenolization, a further study investigating the membrane affinities towards a variety of ions and rapeseed phenolics is needed. The membrane affinity depends on the membrane charge density, its material, the fixed charge-bearing groups and the matrix's hydrophobicity (Luo et al., 2018). Membranes can be modified by incorporation of phenolic selective groups as well. For example, polyether block amide (PEBA) membranes are used for phenolics removal due to its affinity to aromatic groups (Xue et al., 2022). This membrane, on the other hand, must restrict phenolic – membrane interaction to some extent to enable their permeation with diffusive and electrophoretic forces, and should have very low affinity to proteins.

6.3.4. Electrophoretic separation of other rapeseed components

This thesis investigated the electrophoretic separation of oleosomes and proteins, and of proteins and phenolics. The actual rapeseed protein extract is much more complex, containing diverse carbohydrates and other antinutrients (free, esterified, bound phenolic acids, tannins, phytic acid, and glucosinolates). To remove all these impurities, adaptation of the electrophoretic separation is necessary.

Defatted rapeseed contains 35% total carbohydrates which are around 15% soluble and 20% insoluble. The soluble carbohydrates generally comprise monosaccharides and sucrose, while the insoluble carbohydrate contains cell wall components and starch (Rommi et al., 2014). Some carbohydrates remain in the solid residue as larger insoluble fibers after the aqueous extraction of rapeseed, and are separated by the twin-screw press. The remaining sugars and starch in the slurry can be separated from the oleosomes and proteins, since they are chargeless, for example using electrophoresis and counter-current hydrodynamic flow (Ji et al., 2020). It has to be noted that removing carbohydrates is not always necessary, depending on the impact of the carbohydrates on the protein's functionality (Fetzer et al., 2020).

Antinutrients such as phenolics, tannins, phytic acid and glucosinolates, have to be at least partially removed to be able to use rapeseed proteins as functional food ingredients (Tian et al., 2023). To represent the free phenolic acids, SA was used and its removal and permeation through an AEM and UFM were demonstrated; however, other esterified and bound phenolic compounds may behave differently. In their free form, p-Coumaric acid (0.164 kDa, pKa: 4.65), syringic acid (0.198 kDa, pKa: 3.93), gallic acid (0.170 kDa, pKa: 4.40), caffeic acid (0.180 kDa, pKa: 4.62) and ferulic acid (0.194 kDa, pKa: 4.61) were reported in the literature as being present (Le et al., 2021; Zhang et al., 2019). Given their low molecular weight and pKa values, they can be removed electrophoretically at pH 8.0 like SA removed. The esterified phenolics, mostly sinapine (0.310 kDa, pKa: 9.26), accounting for the largest portion of the total phenolics, cannot be removed by permeation through an AEM. Instead, it has to be removed by permeation through a CEM towards the cathode electrode due to the positive charge of its choline moiety (Boulghobra et al., 2020). Alternatively, it can be eliminated during the previously proposed carbohydrate separation step. Unlike the free and esterified phenolics, the bound phenolics are part of a complex structure. They constitute a small portion of the total phenolics; therefore, their presence is not expected to have a great effect on the structure and/or solubility of the protein.

Tannins, generally present in rapeseed hulls, are higher molecular weight (0.5 – 3 kDa) polyphenols, which makes their electrophoretic removal through an ion exchange membrane challenging (Naczk et al., 2000). Considering the average pKa (9.9) value of tannins, they carry positive charge at pH 8.0 and can thus again be separated from negatively charged

oleosomes and proteins using the counter-current electrophoresis system (Oh & Hoff, 1987). Nevertheless, the electrostatic interaction between tannins and proteins may trigger their complexation at pH 8.0. To prevent this, the tannin content can already be reduced before aqueous extraction, by dehulling the rapeseeds.

Phytic acid (0.66 kDa) must also be removed to limit its interaction with proteins. Phytic acid contains phosphorus groups with varying charge. It does have a net negative charge at pH 8.0 and can be removed together with the phenolic compounds (Humer et al., 2015; Lai et al., 2013). Rapeseed glucosinolates with molecular weight of 0.36 – 0.48 kDa are also negatively charged, and must be removed to enhance the protein digestibility and solubility (Blažević et al., 2020; Miklavčič Višnjevec et al., 2021). Here, the only challenge might be slow permeation of phytic acid through an AEM due its relatively higher molecular weight. To investigate this, experimental studies with the use of different types of AEMs and UFMs will be useful.

With a practical seed extract, the effect of its concentrations must also be evaluated as many interactions are different at higher concentrations (Ho et al., 2000; Huisman et al., 1999). **Chapter 5** showed that an increasing ionic strength reduced the mobility of SA. In a complex medium like an aqueous rapeseed extract, there are many components that may interact and associate such as protein–phenolics, protein–carbohydrates and oleosomes–proteins. These interactions and associations can impair their electro-separation. Besides, the increasing feed concentration can aggravate membrane fouling, which will impact the system efficiency. An optimal concentration of the feed solution must therefore be determined to ensure separation efficiency. The content of rapeseeds is strongly dependent on the seed's variety, the cultivated season and their maturity (Long et al., 2022; Zhang et al., 2019). Therefore, the dependence of the process operation on the exact composition of the extract should be investigated.

6.4. ELECTROPHORETIC SEPARATION OF RAPESEED COMPONENTS IN A BROADER CONTEXT AND OUTLOOK

Obtaining valuable compounds such as oleosomes and proteins from rapeseed is of significant importance. Given the drawbacks of the conventional methods, the development of novel resource-efficient techniques is desirable, and various methods have been proposed to improve the rapeseed fractionation.

Centrifugation is the only method currently used to separate co-extracted oleosomes and proteins. The protein fraction contains 11.9 ± 0.5 wt% oil, and oleosomes contained 7.8 ± 0.2 wt% proteins on dry basis after a single centrifugation cycle (Ntone et al., 2020). Therefore, repeated washing cycles with sodium bicarbonate and water are needed to obtain purer oleosomes, leading to much higher water consumption and production of dilute effluents, containing proteins. This results in an inefficient process with a large waste stream, and suboptimal use of the raw material. In the electrophoretic separation proposed in this thesis, however, the composition of the retentate and permeate can be controlled by adjusting the electric field strength under a constant solvent flow velocity as basically demonstrated in **Chapter 3**. As the electric field induces migration of the dispersed components and not of the solvent itself, extra water consumption is not needed for further purification but a more precise adjustment of the electric field strength and counter-current solvent flow rate is required. However, the extent of the separation was limited by the electrophoretic mobility differences and membrane fouling. Thus, the oleosome – protein electro-separation needs further investigation and improvement to compete with the well-developed centrifugal systems. To make their electro-separation more robust, a microfiltration membrane can be integrated in an ED cell, which was restricted by the flow channels design in the ED cell used for the experiments. However technical improvements can render this process feasible.

In contrast to oleosome-protein separation, purification of rapeseed proteins have been achieved through several techniques. Ultrafiltration is widely applied to purify rapeseed proteins retaining their native structure and functionality while removing antinutrients. To retain the rapeseed proteins (12 – 300 kDa), 3 – 10 kDa membranes are used, which allow removal of smaller impurities such as phenolics, phytates, glucosinolates, and monosaccharides (Dong et al., 2011; Jia et al., 2021; Ntone et al., 2020; Tan et al., 2011). Using ultrafiltration in concentration mode reduces the energy requirement for subsequent drying, but this is also possible by combining counter-current convective flow and electric field. However, the degree of concentration must be controlled in both systems as a high feed concentration may enhance membrane fouling and reduce separation efficiency. The incorporation of the electric field can provide, however, continuous release of adsorbed material from the membrane surface by changing electrode polarity as demonstrated in Section 6.3.3. This is not easily done in ultrafiltration, and the membranes are generally cleaned after the operation.

Ultrafiltration is usually followed by diafiltration or dialysis for desalination. Both steps require large amounts of water. As shown in **Chapters 4** and **5**, ED can desalt the feed solution simultaneously which reduces water consumption for desalination. Here, the important limitation is the conductivity of the feed solution and LCD. To prevent unnecessary energy use and water splitting due to operating the ED system under over-potential conditions, desalination must be conducted in a controlled way. The fact that ED is already used industrially for whey protein demineralization indicates its potential to be used for rapeseed protein extract (Greiter et al., 2002).

ED systems can be equipped with UFMs in an ED-UF process, taking advantage of larger pore sizes and an extra driving force for particle and salt ion migration; however, **Chapter 4** indicates that the negative surface charge of the used UFM caused rejection of SA below the LCD, and a stronger electric field was needed to observe SA permeation. This was also reported for tobacco polyphenols (Bazinet et al., 2005). ED-UF can be improved with regard to SA or phenolic compounds permeation by introducing a pressure difference between the retentate and permeate cells causing solvent flow. This has been shown to have a strong effect on the net velocity and the migration direction (**Chapters 2** and **3**). In this case, a solvent flow parallel to electrophoresis can overcome the electrostatic repulsion force and enhance permeation of small compounds.

Cyclic adsorption – desorption utilizing ion exchange columns (IEC) are considered selective processes to purify rapeseed proteins. However, ethanol-water mixtures and salt solutions are needed for efficient desorption of phenolics (sinapic acid) and proteins from the IEC, respectively (Moreno Gonzalez, 2021). In ED, desorption of the captured SA or other small molecules was achieved as a result of their electrophoretic migration and diffusion. Electrochemical adsorption – desorption process also utilizes charge and electrical properties to adsorb (electrostatic interaction) and desorb (electric potential) proteins from electrode surface. Thus, using of an electric field can eliminate the need for auxiliary solvents for the desorption step (Fritz, 2019). The desalination in electrical processes was mentioned also by Fritz (2019). Simultaneous desalination can integrate the currently sequential purification and desalination processes into a single-step process. Table 6.1 summarizes the main advantages and disadvantages of different applications.

The electrophoretic separation process has significant potential for rapeseed fractionation, enabling the production of oleosome-rich and protein-rich fractions. The advantages of the electrophoretic separation include: (i) the elimination of multi-stage washing cycles to remove impurities, (ii) simultaneous desalting without the use of excess water, (iii) adaptability for the separation of different compounds based on their charge and size, (iv) the elimination of the need for auxiliary organic solvents and (v) scalable. These benefits collectively contribute to reducing water, chemical and energy consumption, thus, promoting more sustainable downstream processing. Additionally, the adaptability of the electrophoretic separation process allows for its use in the fractionation of other types of biomass.

CONCLUDING REMARKS

This thesis demonstrated the feasibility and potential of different forms of electrophoretic separation for rapeseed fractionation. The findings highlight that electrophoretic separation can be accomplished through charge differences (counter-current electrophoresis) and through size differences (electrodialysis). It may strongly reduce water consumption through simultaneous desalting and need for organic solvents for phenolic removal. Despite its potential, the developed process principles still need further improvement to enhance the separation selectivity and efficiency.

Table 6.1: Summary of the comparison of the electrophoretic separation system with other processes.

Method	Application	Advantages	Disadvantages
Centrifugation	Oleosome – protein separation	• Easy operation • Well – developed system • Mild process conditions	• Requires extra washing steps for purification (increases water consumption) • Higher energy consumption to separate smaller particles
Ultrafiltration	Protein purification	• Energy efficient process • Effectively removes small impurities • Eliminates the need for organic solvents for dephenolization • Concentrate the feed solution • Mild process conditions • Scalable (increasing membrane surface area) • Can be combined with electrical separation systems	• Requires water - intensive process for desalination (diafiltration or dialysis) • Membrane fouling • Membranes are cleaned after the operation • Not tested for oleosome – protein separation • Selectivity is based on only size differences
Ion exchange chromatography	Protein purification	• Effectively purifies proteins • Scalable (increasing column diameter)	• Requires ethanol– water mixture (phenolics) and salt solutions (proteins) for efficient desorption • Additional desalting process is required
Electrochemical separation	Protein purification	• Selective protein isolation • Simultaneous desalination • Electrically driven adsorption – desorption eliminates the need for chemicals • Mild process conditions • Scalable (increasing electrode surface area)	• Currently not suitable for complex mixtures, and needs further improvement • Electrode fouling
Electrophoretic separation	Oleosome – protein separation and protein purification	• Can separate compounds based on both size and charge (electrophoretic mobility) • Simultaneous desalination • Eliminates the need for organic solvents for dephenolization • Electrically driven adsorption – desorption can provide membranes cleaning during the operation • Concentration of feed solution (counter-current electrophoresis) • Scalable (increasing membrane surface area)	• Membrane fouling • Separation selectivity is limited by electrophoretic mobility differences •Requires monitoring of pH and conductivity during the operation

References

Agostino, F. J., Cherney, L. T., Kanoatov, M., & Krylov, S. N. (2014). Reducing pH gradients in free-flow electrophoresis. *Analytical Chemistry*, 86(12), 5656–5660. https://doi.org/10.1021/ac501081b

Akbari, A., & Wu, J. (2015). An integrated method of isolating napin and cruciferin from defatted canola meal. *LWT - Food Science and Technology*, 64(1), 308–315. https://doi.org/10.1016/j.lwt.2015.05.046

Alara, O. R., Abdurahman, N. H., & Ukaegbu, C. I. (2021). Extraction of phenolic compounds: A review. *Current Research in Food Science*, 4, 200–214. https://doi.org/10.1016/j.crfs.2021.03.011

Alu'datt, M. H., Rababah, T., Ereifej, K., Brewer, S., & Alli, I. (2013). Phenolic-protein interactions in oilseed protein isolates. *Food Research International*, 52(1), 178–184. https://doi.org/10.1016/j.foodres.2013.03.010

Arrutia, F., Binner, E., Williams, P., & Waldron, K. W. (2020). Oilseeds beyond oil: Press cakes and meals supplying global protein requirements. *Trends in Food Science and Technology*, 100, 88–102. https://doi.org/10.1016/j.tifs.2020.03.044

Ayan, K., Ganar, K., Deshpande, S., Boom, R. M., & Nikiforidis, C. V. (2023). Continuous counter-current electrophoretic separation of oleosomes and proteins from oilseeds. *Food Hydrocolloids*, 144(118), 109053. https://doi.org/10.1016/j.foodhyd.2023.109053

Bahga, S. S., Bercovici, M., & Santiago, J. G. (2010). Ionic strength effects on electrophoretic focusing and separations. *Electrophoresis*, 31(5), 910–919. https://doi.org/10.1002/elps.200900560

Balandrán-Quintana, R. R., Mendoza-Wilson, A. M., Ramos-Clamont Montfort, G., & Huerta-Ocampo, J. Á. (2019). Plant-Based Proteins. *Proteins: Sustainable Source, Processing and Applications,* 97 – 130 . https://doi.org/10.1016/B978-0-12-816695-6.00004-0

Banach, J. L., Berg, J. P. Van Der, Kleter, G., Veen, H. V. B. De, Pouvreau, L., & Asselt, E. D. Van. (2023). Alternative proteins for meat and dairy replacers: Food safety and future trends. *Critical Reviews in Food Science and Nutrition*, 63(32), 11063–11080. https://doi.org/10.1080/10408398.2022.2089625

Bazinet, L., DeGrandpré, Y., & Porter, A. (2005). Electromigration of tobacco polyphenols. *Separation and Purification Technology*, 41(1), 101–107. https://doi.org/10.1016/j.seppur.2004.05.003

Bazinet, L., DeGrandpré, Y., & Porter, A. (2005). Enhanced tobacco polyphenol electromigration and impact on membrane integrity. *Journal of Membrane Science*, 254(1–2), 111–118. https://doi.org/10.1016/j.memsci.2004.11.029

Berghout, J. A. M., Boom, R. M., & Van Der Goot, A. J. (2014). The potential of aqueous fractionation of lupin seeds for high-protein foods. *Food Chemistry*, 159, 64–70. https://doi.org/10.1016/j.foodchem.2014.02.166

Berghout, J. A. M., Pelgrom, P. J. M., Schutyser, M. A. I., Boom, R. M., & Goot, A. J. Van Der. (2015). Sustainability assessment of oilseed fractionation processes: A case study on lupin seeds. *Journal of Food Engineering*, 150, 117–124. https://doi.org/10.1016/j.jfoodeng.2014.11.005

Blažević, I., Montaut, S., Burčul, F., Olsen, C. E., Burow, M., Rollin, P., & Agerbirk, N. (2020). Glucosinolate structural diversity, identification, chemical synthesis and metabolism in plants. *Phytochemistry*, 169. https://doi.org/10.1016/j.phytochem.2019.112100

Boulghobra, D., Grillet, P. E., Laguerre, M., Tenon, M., Fauconnier, J., Fança-Berthon, P., Reboul, C., & Cazorla, O. (2020). Sinapine, but not sinapic acid, counteracts mitochondrial oxidative stress in cardiomyocytes. *Redox Biology*, 34. https://doi.org/10.1016/j.redox.2020.101554

Boussetta, N., Vorobiev, E., Deloison, V., Pochez, F., Falcimaigne-Cordin, A., & Lanoisellé, J. L. (2011). Valorisation of grape pomace by the extraction of phenolic antioxidants: Application of high voltage electrical discharges. *Food Chemistry*, 128(2), 364–370. https://doi.org/10.1016/j.foodchem.2011.03.035

Buszewski, B., Dziubakiewicz, E., & Szumski, M. (2013). Electromigration Techniques Theory and Practice. *Springer Series in Chemical Physics*, 105. https://doi.org/10.1007/978-3-642-35043-6

Callahan, D. J., Stanley, B., & Li, Y. (2014). Control of Protein Particle Formation During Ultrafiltration / Diafiltration Through Interfacial Protection. *Journal of Pharmaceutical Sciences*, 103(3), 862–869. https://doi.org/10.1002/jps.23861

Chao, Y. M., & Liang, T. M. (2008). A feasibility study of industrial wastewater recovery using electrodialysis reversal. *Desalination*, 221(1–3), 433–439. https://doi.org/10.1016/j.desal.2007.04.065

Chemat, F., Abert Vian, M., Fabiano-Tixier, A. S., Nutrizio, M., Režek Jambrak, A., Munekata, P. E. S., Lorenzo, J. M., Barba, F. J., Binello, A., & Cravotto, G. (2020). A review of sustainable and intensified techniques for extraction of food and natural products. *Green Chemistry*, 22(8), 2325–2353. https://doi.org/10.1039/c9gc03878g

De Chirico, S., di Bari, V., Foster, T., & Gray, D. (2018). Enhancing the recovery of oilseed rape seed oil bodies (oleosomes) using bicarbonate-based soaking and grinding media. *Food Chemistry*, 241, 419–426. https://doi.org/10.1016/j.foodchem.2017.09.008

Dong, X., Guo, L., Wei, F., Li, J., & Jiang, M. (2011). Some characteristics and functional properties of rapeseed protein prepared by ultrasonication , ultrafiltration and isoelectric*. Journal of the Science of Food and Agriculture*, 91(8), 1488-1498.. https://doi.org/10.1002/jsfa.4339

Doyen, A., Roblet, C., Beaulieu, L., Saucier, L., Pouliot, Y., & Bazinet, L. (2013). Impact of water splitting phenomenon during electrodialysis with ultrafiltration membranes on peptide selectivity and migration. *Journal of Membrane Science,* 428, 349–356. https://doi.org/10.1016/j.memsci.2012.10.036

Everette, J. D., Bryant, Q. M., Green, A. M., Abbey, Y. A., Wangila, G. W., & Walker, R. B. (2010). Thorough study of reactivity of various compound classes toward the Folin-Ciocalteu reagent. *Journal of Agricultural and Food Chemistry*, 58(14), 8139–8144. https://doi.org/10.1021/jf1005935

Fetzer, A., Müller, K., Schmid, M., & Eisner, P. (2020). Rapeseed proteins for technical applications: Processing, isolation, modification and functional properties – A review. *Industrial Crops and Products*, 158, 1–18. https://doi.org/10.1016/j.indcrop.2020.112986

Franck, N., Vera Candioti, L., Gerlero, G. S., Urteaga, R., & Kler, P. A. (2024). A simple method for the assessment of electrophoretic mobility in porous media. *Electrophoresis,* 45, 7-8. https://doi.org/10.1002/elps.202300180

Fritz, P. A. (2019). Electrochemical Separation: From Ions to Proteins (PhD Dissertation, Wageningen University). https://doi.org/https://doi.org/10.18174/500781

Fukasawa, T., Ono, K., Ishigami, T., & Fukui, K. (2020). Electrophoretic classification based on differences in electrophoretic mobility caused by change in the applied electric field. *Powder Technology*, 362, 586–590. https://doi.org/10.1016/j.powtec.2019.12.027

Gagour, J., Ahmed, M. N., Bouzid, H. A., Oubannin, S., Bijla, L., Ibourki, M., Hajib, A., Koubachi, J., Harhar, H., & Gharby, S. (2022). Proximate Composition, Physicochemical, and Lipids Profiling and Elemental Profiling of Rapeseed (Brassica napus L.) and Sunflower (Helianthus annuus L.) Grown in Morocco. *Evidence-Based Complementary and Alternative Medicine*, 2022(1), 3505943. https://doi.org/10.1155/2022/3505943

Galli, M., Sáringer, S., Szilágyi, I., & Trefalt, G. (2020). A simple method to determine critical coagulation concentration from electrophoretic mobility. *Colloids and Interfaces*, 4(2). https://doi.org/10.3390/colloids4020020

Gharby, S. (2022). Refining Vegetable Oils: Chemical and Physical Refining. *Scientific World Journal*, 2022(1), 6627013. https://doi.org/10.1155/2022/6627013

Gironi, F., & Piemonte, V. (2011). Temperature and solvent effects on polyphenol extraction process from chestnut tree wood. *Chemical Engineering Research and Design*, 89(7), 857–862. https://doi.org/10.1016/j.cherd.2010.11.003

Gopmandal, P. P., & Duval, J. F. L. (2022). Electrostatics and electrophoresis of engineered nanoparticles and particulate environmental contaminants: Beyond zeta potential-based formulation. *Current Opinion in Colloid and Interface Science*, 60, 101605. https://doi.org/10.1016/j.cocis.2022.101605

Greiter, M., Novalin, S., Wendland, M., Kulbe, K.-D., & Fischer, J. (2002). Desalination of whey by electrodialysis and ion exchange resins: analysis of both processes with regard to sustainability by calculating their cumulative energy demand. *Journal of Membrane Science*, 210(1), 91-102. https://doi.org/10.1016/S0376-7388(02)00378-2

Guillén, M. D., & Ruiz, A. (2003). 1H nuclear magnetic resonance as a fast tool for determining the composition of acyl chains in acylglycerol mixtures. *European Journal of Lipid Science and Technology*, 105(9), 502–507. https://doi.org/10.1002/ejlt.200300799

Guzman, J. R. (2020). Designing a sustainable oleosome aqueous extraction. (PhD Dissertation, Wageningen University). ISBN: 9789463952651

Hadidi, M., Aghababaei, F., & McClements, D. J. (2024). Sunflower meal/cake as a sustainable protein source for global food demand: Towards a zero-hunger world. *Food Hydrocolloids*, 109329. https://doi.org/10.1016/j.foodhyd.2023.109329

Herrero, M., Sánchez-Camargo, A. del P., Cifuentes, A., & Ibáñez, E. (2015). Plants, seaweeds, microalgae and food by-products as natural sources of functional ingredients obtained using pressurized liquid extraction and supercritical fluid extraction. *Trends in Analytical Chemistry*, 71, 26–38. https://doi.org/10.1016/j.trac.2015.01.018

Ho, A. K., Perera, J. M., & Stevens, G. W. (2000). The effect of protein concentration on electrophoretic mobility. *Journal of Colloid and Interface Science*, 224(1), 140–147. https://doi.org/10.1006/jcis.1999.6658

Honarparvar, S., & Reible, D. (2020). Modeling multicomponent ion transport to investigate selective ion removal in electrodialysis. *Environmental Science and Ecotechnology*, 1, 100007. https://doi.org/10.1016/j.ese.2019.100007

Huisman, I. H., Trägårdh, G., & Trägårdh, C. (1999). Particle transport in crossflow microfiltration–II. Effects of particle–particle interactions. *Chemical Engineering Science*, 54(2), 281-289. https://doi.org/10.1016/S0009-2509(98)00223-1

Humer, E., Schwarz, C., & Schedle, K. (2015). Phytate in pig and poultry nutrition. *Journal of Animal Physiology and Animal Nutrition*, 99(4), 605–625. https://doi.org/10.1111/jpn.12258

Isaacson, M. S., & Sonin, A. A. (1976). Sherwood Number and Friction Factor Correlations for Electrodialysis Systems, with Application to Process Optimization. *Industrial & Engineering Chemistry Process Design and Development* , 15(2), 313–321. https://doi.org/10.1021/i260058a017

Ji, Y., Lin, X., & Yu, J. (2020). Preparation and characterization of oxidized starch-chitosan complexes for adsorption of procyanidins. *LWT*, 117. https://doi.org/10.1016/j.lwt.2019.108610

Jia, W., Rodriguez-Alonso, E., Bianeis, M., Keppler, J. K., & van der Goot, A. J. (2021). Assessing functional properties of rapeseed protein concentrate versus isolate for food applications. *Innovative Food Science and Emerging Technologies*, 68. https://doi.org/10.1016/j.ifset.2021.102636

Kenyon, S. M., Weiss, N. G., & Hayes, M. A. (2012). Using electrophoretic exclusion to manipulate small molecules and particles on a microdevice. *Electrophoresis*, 33(8), 1227–1235. https://doi.org/10.1002/elps.201100622

Khosravanipour Mostafazadeh, A., Zolfaghari, M., & Drogui, P. (2016). Electrofiltration technique for water and wastewater treatment and bio-products management: A review. *Journal of Water Process Engineering,* 14, 28–40. https://doi.org/10.1016/j.jwpe.2016.10.003

Kim, Y., Walker, W. S., & Lawler, D. F. (2012). Competitive separation of di- vs. mono-valent cations in electrodialysis: Effects of the boundary layer properties. *Water Research*, 46(7), 2042–2056. https://doi.org/10.1016/j.watres.2012.01.004

Knežević, K., Reif, D., Harasek, M., Krampe, J., & Kreuzinger, N. (2022). Assessment of Graphical Methods for Determination of the Limiting Current Density in Complex Electrodialysis-Feed Solutions. *Membranes*, 12(2). https://doi.org/10.3390/membranes12020241

Kniaginicheva, E., Pismenskaya, N., Melnikov, S., Belashova, E., Sistat, P., Cretin, M., & Nikonenko, V. (2015). Water splitting at an anion-exchange membrane as studied by impedance spectroscopy. *Journal of Membrane Science*, 496, 78–83. https://doi.org/10.1016/j.memsci.2015.07.050

Knorr, D., Augustin, M. A., & Tiwari, B. (2020). Advancing the Role of Food Processing for Improved Integration in Sustainable Food Chains. *Frontiers in Nutrition*, 7(34), 1–8. https://doi.org/10.3389/fnut.2020.00034

Koval, D., Kašička, V., & Zusková, I. (2005). Investigation of the effect of ionic strength of Tris-acetate background electrolyte on electrophoretic mobilities of mono-, di-, and trivalent organic anions by capillary electrophoresis. *Electrophoresis*, 26(17), 3221–3231. https://doi.org/10.1002/elps.200500260

Lai, Y. P., Mondor, M., Moresoli, C., Drolet, H., Gros-Louis, M., Ippersiel, D., Lamarche, F., & Arcand, Y. (2013). Production of soy protein isolates with low phytic acid content by membrane technologies: Impact of the extraction and ultrafiltration/diafiltration conditions. *Journal of Food Engineering*, 114(2), 221–227. https://doi.org/10.1016/j.jfoodeng.2012.08.012

Lamberg-Allardt, C., Bärebring, L., Arnesen, E. K., Nwaru, B. I., Thorisdottir, B., Ramel, A., Söderlund, F., Dierkes, J., & Åkesson, A. (2023). Animal versus plant-based protein and risk of cardiovascular disease and type 2 diabetes: a systematic review of randomized controlled trials and prospective cohort studies. *Food and Nutrition Reseach*, 67, 9003. https://doi.org/http://dx.doi.org/10.29219/fnr.v67.9003

Le, T. T., Framboisier, X., Aymes, A., Ropars, A., Frippiat, J. P., & Kapel, R. (2021). Identification and capture of phenolic compounds from a rapeseed meal protein isolate production process by-product by macroporous resin and valorization their antioxidant properties. *Molecules*, 26(19). https://doi.org/10.3390/molecules26195853

Li, Y., Cheng, Y., Zhang, Z., Wang, Y., Mintah, B. K., Dabbour, M., Jiang, H., He, R., & Ma, H. (2020). Modification of rapeseed protein by ultrasound-assisted pH shift treatment: Ultrasonic mode and frequency screening, changes in protein solubility and structural characteristics. *Ultrasonics Sonochemistry*, 69, 1–10. https://doi.org/10.1016/j.ultsonch.2020.105240

Li, Y., Miao, S., Tan, J., Zhang, Q., & Chen, D. D. Y. (2023). Capillary Electrophoresis: A Three-Year Literature Review. *Analytical Chemistry*, 96(20). https://doi.org/10.1021/acs.analchem.4c00857

Liang, X., Zhang, J., Huang, Z., & Guo, Y. (2023). Sustainable recovery and recycling of natural deep eutectic solvent for biomass fractionation via industrial membrane-based technique. *Industrial Crops and Products*, 194, 116351. https://doi.org/10.1016/j.indcrop.2023.116351

Lie-Piang, A., Braconi, N., Boom, R. M., & van der Padt, A. (2021). Less refined ingredients have lower environmental impact – A life cycle assessment of protein-rich ingredients from oil- and starch-bearing crops. *Journal of Cleaner Production*, 292. https://doi.org/10.1016/j.jclepro.2021.126046

Lie-Piang, A., Yang, J., Schutyser, M. A. I., Nikiforidis, C. V., & Boom, R. M. (2023). Mild Fractionation for More Sustainable Food Ingredients. *Annual Review of Food Science and Technology*, 14, 473–493. https://doi.org/10.1146/annurev-food-060721-024052

Lim, A. E., & Lam, Y. C. (2021). Electroosmotic flow hysteresis for fluids with dissimilar ph and ionic species. *Micromachines*, 12(9). https://doi.org/10.3390/mi12091031

Liu, H., & She, Q. (2022). Influence of membrane structure-dependent water transport on conductivity-permselectivity trade-off and salt/water selectivity in electrodialysis: Implications for osmotic electrodialysis using porous ion exchange membranes. *Journal of Membrane Science*, 650, 120398. https://doi.org/10.1016/j.memsci.2022.120398

Liu, L., Li, K., Zhao, S., Wang, J., Lan, H., & Wang, J. (2021). The effects of electrophoresis, bubbles and electroosmosis for conductive membrane performance in the electro-filtration process. *Journal of Membrane Science*, 620. https://doi.org/10.1016/j.memsci.2020.118955

Long, C., Qi, X.-L., & Venema, K. (2022). Chemical and nutritional characteristics, and microbial degradation of rapeseed meal recalcitrant carbohydrates: A review. *Frontiers in Nutrition*, 9, 948302. https://doi.org/10.3389/fnut.2022.948302

Lv, M., & Wu, W. (2019). An advanced aqueous method of extracting rapeseed oil with high quality. *Journal of Food Process Engineering*, 42(2), 1–9. https://doi.org/10.1111/jfpe.12957

Ma, K. K., Greis, M., Lu, J., Nolden, A. A., McClements, D. J., & Kinchla, A. J. (2022). Functional Performance of Plant Proteins. *Foods*, 11(4), 594. https://doi.org/10.3390/foods11040594

Mahler, H. C., Friess, W., Grauschopf, U., & Kiese, S. (2009). Protein aggregation: Pathways, induction factors and analysis. *Journal of Pharmaceutical Sciences*, 98(9), 2909–2934. https://doi.org/10.1002/jps.21566

Manouchehri, H. R., Rao, K. H., & Forssberg, K. S. E. (2000). Review of electrical separation methods - Part 1: Fundamental aspects. *Minerals and Metallurgical Processing*, 17(1), 23–36. https://doi.org/10.1007/BF03402825

Marina, M. L., Ríos, A., & Valcárcel, M. (Eds.). (2005). *Analysis and detection by capillary electrophoresis*. Elsevier.

Meighan, M. M., Keebaugh, M. W., Quihuis, A. M., Kenyon, S. M., & Hayes, M. A. (2009). Electrophoretic exclusion for the selective transport of small molecules. *Electrophoresis*, 30(21), 3786–3792. https://doi.org/10.1002/elps.200900340

Miklavčič Višnjevec, A., Tamayo Tenorio, A., Steenkjær Hastrup, A. C., Hansen, N. M. L., Peeters, K., & Schwarzkopf, M. (2021). Glucosinolates and isothiocyantes in processed rapeseed determined by HPLC-DAD-qTOF. *Plants*, 10(11). https://doi.org/10.3390/plants10112548

Moreno Gonzalez. (2021). From waste to products Valorizing food side streams to recover natural products (PhD Dissertation, TU Delft University). https://doi.org/10.4233/uuid

Moshtarikhah, S., Oppers, N. A. W., de Groot, M. T., Keurentjes, J. T. F., Schouten, J. C., & van der Schaaf, J. (2017). Nernst–Planck modeling of multicomponent ion transport in a Nafion membrane at high current density. *Journal of Applied Electrochemistry*, 47(1), 51–62. https://doi.org/10.1007/s10800-016-1017-2

Moura Bernardes, A., Rodrigues, M. A., & Ferreira, J. Z. (2013). General aspects of electrodialysis. In *Electrodialysis and Water Reuse: Novel Approaches* (pp. 11-23). Berlin, Heidelberg: Springer Berlin Heidelberg.

Mubita, T. M., Porada, S., Biesheuvel, P. M., van der Wal, A., & Dykstra, J. E. (2022). Strategies to increase ion selectivity in electrodialysis. *Separation and Purification Technology*, 292, 120944. https://doi.org/10.1016/j.seppur.2022.120944

Munialo, C. D. (2023). A review of alternative plant protein sources, their extraction, functional characterisation, application, nutritional value and pinch points to being the solution to sustainable food production. *International Journal of Food Science and Technology*, 1–11. https://doi.org/10.1111/ijfs.16467

Naczk, M., Amarowicz, R., Pink, D., & Shahidi, F. (2000). Insoluble condensed tannins of canola/rapeseed. *Journal of Agricultural and Food Chemistry*, 48(5), 1758–1762. https://doi.org/10.1021/jf9908401

Najjar, Y. S. H., & Abu-Shamleh, A. (2020). Harvesting of microalgae by centrifugation for biodiesel production: A review. *Algal Research*, 51. https://doi.org/10.1016/j.algal.2020.102046

Nandasiri, R., Michael Eskin, N. A., Eck, P., & Thiyam-Höllander, U. (2020). Application of green technology on extraction of phenolic compounds in oilseeds (Canola). *Cold Pressed Oils: Green Technology, Bioactive Compounds, Functionality, and Applications,* 81–96. https://doi.org/10.1016/B978-0-12-818188-1.00008-6

Nde, D. B., & Foncha, A. C. (2020). Optimization methods for the extraction of vegetable oils: A review. *Processes*, 8(2). https://doi.org/10.3390/pr8020209

Nehmeh, M., Rodriguez-donis, I., Cavaco-soares, A., Evon, P., Gerbaud, V., & Thiebaud-roux, S. (2022). Bio-Refinery of Oilseeds : Oil Extraction , Secondary Metabolites Separation towards Protein Meal Valorisation — A Review. *Processes*, 10(5), 841. https://doi.org/10.3390/pr10050841

Nićiforović, N., & Abramovič, H. (2014). Sinapic acid and its derivatives: Natural sources and bioactivity. *Comprehensive Reviews in Food Science and Food Safety*, 13(1), 34–51. https://doi.org/10.1111/1541-4337.12041

Nikiforidis, C. V. (2019). Structure and functions of oleosomes (oil bodies). *Advances in Colloid and Interface Science*, 274, 102039. https://doi.org/10.1016/j.cis.2019.102039

Nikiforidis, C. V., & Kiosseoglou, V. (2009). Aqueous extraction of oil bodies from maize germ (Zea mays) and characterization of the resulting natural oil-in-water emulsion. *Journal of Agricultural and Food Chemistry*, 57(12), 5591–5596. https://doi.org/10.1021/jf900771v

Nikonenko, V. V., Kovalenko, A. V., Urtenov, M. K., Pismenskaya, N. D., Han, J., Sistat, P., & Pourcelly, G. (2014). Desalination at overlimiting currents: State-of-the-art and perspectives. *Desalination*, 342, 85–106. https://doi.org/10.1016/j.desal.2014.01.008

Ntone, E., Bitter, J. H., & Nikiforidis, C. V. (2020). Not sequentially but simultaneously: Facile extraction of proteins and oleosomes from oilseeds. *Food Hydrocolloids*, 105598. https://doi.org/10.1016/j.foodhyd.2019.105598

Ntone, E., Wesel, T. Van, Sagis, L. M. C., Meinders, M., Bitter, J. H., & Nikiforidis, C. V. (2021). Adsorption of rapeseed proteins at oil / water interface. Janus-like napins dominate the interface. *Journal of Colloid And Interface Science*, 583, 459–469. https://doi.org/10.1016/j.jcis.2020.09.039

Obata, K., van de Krol, R., Schwarze, M., Schomäcker, R., & Abdi, F. F. (2020). In situ observation of pH change during water splitting in neutral pH conditions: impact of natural convection driven by buoyancy effects. *Energy and Environmental Science*, 13, 5104–5116. https://doi.org/10.1039/d0ee01760d

Oh, H. -I, & Hoff, J. E. (1987). pH Dependence of Complex Formation Between Condensed Tannins and Proteins. *Journal of Food Science*, 52(5), 1267–1269. https://doi.org/10.1111/j.1365-2621.1987.tb14059.x

Östbring, K., Nilsson, K., Ahlström, C., Fridolfsson, A., & Rayner, M. (2020). Emulsifying and Anti-Oxidative Properties of Proteins Extracted from Industrially Cold-Pressed Rapeseed Press-Cake. *Foods*, 9(678). https://doi.org/doi:10.3390/foods9050678

Peng, L. P., Xu, Y. T., Li, X. T., & Tang, C. H. (2020). Improving the emulsification of soy β-conglycinin by alcohol-induced aggregation. *Food Hydrocolloids*, 98. https://doi.org/10.1016/j.foodhyd.2019.105307

Peng, Y., Kersten, N., Kyriakopoulou, K., & van der Goot, A. J. (2020). Functional properties of mildly fractionated soy protein as influenced by the processing pH. *Journal of Food Engineering*, 275, 109875. https://doi.org/10.1016/j.jfoodeng.2019.109875

Pereira, R. N., Rodrigues, R., Avelar, Z., Leite, A. C., Leal, R., Pereira, R. S., & Vicente, A. (2024). Electrical Fields in the Processing of Protein-Based Foods. *Foods*, 13(4). https://doi.org/10.3390/foods13040577

Pouliot, Y., Conway, V., & Leclerc, P. L. (2014). Separation and Concentration Technologies in Food Processing. *Food Processing: Principles and Applications: Second Edition*, 33–60. https://doi.org/10.1002/9781118846315.ch3

Precupas, A., & Popa, V. T. (2024). Impact of Sinapic Acid on Bovine Serum Albumin Thermal Stability. *International Journal of Molecular Sciences*, 25(2). https://doi.org/10.3390/ijms25020936

Ptasinski, K. J., & Kerkhof, P. J. A. M. (1992). Electric Field Driven Separations: Phenomena and Applications. *Separation Science and Technology*, 27(8–9), 995–1021. https://doi.org/10.1080/01496399208019021

Rajha, H. N., Boussetta, N., Louka, N., Maroun, R. G., & Vorobiev, E. (2014). A comparative study of physical pretreatments for the extraction of polyphenols and proteins from vine shoots. *Food Research International*, 65, 462–468. https://doi.org/10.1016/j.foodres.2014.04.024

Rodrigues, M., Sleutels, T., Kuntke, P., Buisman, C. J. N., & Hamelers, H. V. M. (2022). Effects of Current on the Membrane and Boundary Layer Selectivity in Electrochemical Systems Designed for Nutrient Recovery. *ACS Sustainable Chemistry and Engineering*, 10(29), 9411–9418. https://doi.org/10.1021/acssuschemeng.2c01764

Romero-Guzmán, M. J., Jung, L., Kyriakopoulou, K., Boom, R. M., & Nikiforidis, C. V. (2020). Efficient single-step rapeseed oleosome extraction using twin-screw press. *Journal of Food Engineering*, 276. https://doi.org/10.1016/j.jfoodeng.2019.109890

Romero-Guzmán, M. J., Köllmann, N., Zhang, L., Boom, R. M., & Nikiforidis, C. V. (2020). Controlled oleosome extraction to produce a plant-based mayonnaise-like emulsion using solely rapeseed seeds. *LWT - Food Science and Technology*, 123. https://doi.org/10.1016/j.lwt.2020.109120

Romero-Guzmán, M. J., Petris, V., De Chirico, S., di Bari, V., Gray, D., Boom, R. M., & Nikiforidis, C. V. (2020). The effect of monovalent (Na+, K+) and divalent (Ca2+, Mg2+) cations on rapeseed oleosome (oil body) extraction and stability at pH 7. *Food Chemistry*, 306. https://doi.org/10.1016/j.foodchem.2019.125578

Romero-Guzmán, M. J., Vardaka, E., Boom, R. M., & Nikiforidis, C. V. (2020). Influence of soaking time on the mechanical properties of rapeseed and their effect on oleosome extraction. *Food and Bioproducts Processing*, 121, 230–237. https://doi.org/10.1016/j.fbp.2020.03.006

Rommi, K., Hakala, T. K., Holopainen, U., Nordlund, E., Poutanen, K., & Lantto, R. (2014). Effect of enzyme-aided cell wall disintegration on protein extractability from intact and dehulled rapeseed (Brassica rapa L. and Brassica napus L.) press cakes. *Journal of Agricultural and Food Chemistry*, 62(32), 7989–7997. https://doi.org/10.1021/jf501802e

Roselló-Soto, E., Barba, F. J., Parniakov, O., Galanakis, C. M., Lebovka, N., Grimi, N., & Vorobiev, E. (2015). High Voltage Electrical Discharges, Pulsed Electric Field, and Ultrasound Assisted Extraction of Protein and Phenolic Compounds from Olive Kernel. *Food and Bioprocess Technology*, 8(4), 885–894. https://doi.org/10.1007/s11947-014-1456-x

Rosenthal, A., Pyle, D. L., & Niranjan, K. (1996). Aqueous and enzymatic processes for edible oil extraction. *Enzyme and Microbial Technology*, 19(6), 402–420. https://doi.org/10.1016/S0141-0229(96)80004-F

Rosset, M., Acquaro, V. R., & Beléia, A. D. P. (2014). Protein extraction from defatted soybean flour with Viscozyme L pretreatment. *Journal of Food Processing and Preservation*, 38(3), 784–790. https://doi.org/10.1111/jfpp.12030

Roy, I., & Gupta, M. N. (2004). Freeze-drying of proteins: some emerging concerns. *Biotechnology and Applied Biochemistry*, 39(2), 165–177. https://doi.org/10.1042/ba20030133

Rudge, S. R., & Monnig, C. A. (2000). Electrophoresis techniques. *Separation and Purification Methods*, 29(1), 129–148. https://doi.org/10.1081/SPM-100100006

Sadek, S. H., Pimenta, F., Pinho, F. T., & Alves, M. A. (2017). Measurement of electroosmotic and electrophoretic velocities using pulsed and sinusoidal electric fields. *Electrophoresis*, 38(7), 1022–1037. https://doi.org/10.1002/elps.201600368

Salazar-Villanea, S., Bruininx, E. M. A. M., Gruppen, H., Hendriks, W. H., Carré, P., Quinsac, A., & van der Poel, A. F. B. (2016). Physical and chemical changes of rapeseed meal proteins during toasting and their effects on in vitro digestibility. *Journal of Animal Science and Biotechnology*, 7(1), 1–11. https://doi.org/10.1186/s40104-016-0120-x

Santos-Buelga, C., Gonzalez-Manzano, S., Dueñas, M., & Gonzalez-Paramas, A. M. (2012). Extraction and isolation of phenolic compounds. *Methods in Molecular Biology*, 864, 427–464. https://doi.org/10.1007/978-1-61779-624-1_17

Saucedo-espinosa, M. A., & Lapizco-encinas, B. H. (2016). Refinement of current monitoring methodology for electroosmotic flow assessment under low ionic strength conditions. *Biomicrofluidics*, 10, 1–15. https://doi.org/10.1063/1.4953183

Schneider, C. A., Rasband, W. S., & Eliceiri, K. W. (2012). HISTORICAL commentary NIH Image to ImageJ : 25 years of image analysis. *Nature Methods*, 9(7), 671–675. https://doi.org/10.1038/nmeth.2089

Semenov, I., Papadopoulos, P., Stober, G., & Kremer, F. (2010). Ionic concentration- and pH-dependent electrophoretic mobility as studied by single colloid electrophoresis. *Journal of Physics: Condensed Matter*, 22, 1–5. https://doi.org/10.1088/0953-8984/22/49/494109

Shao, Q., Fan, Y., Yang, L., & Qin Gao, Y. (2012). From protein denaturant to protectant: Comparative molecular dynamics study of alcoholprotein interactions. *Journal of Chemical Physics*, 136(11). https://doi.org/10.1063/1.3692801

Sharma, K. R., & Giri, G. (2022). Quantification of Phenolic and Flavonoid Content, Antioxidant Activity, and Proximate Composition of Some Legume Seeds Grown in Nepal. *International Journal of Food Science*, 2022(1). https://doi.org/10.1155/2022/4629290

Sharma, S., Lindquist, J. C., & Hwang, D. C. (2023). Canola/rapeseed as a potential source of alternative protein. *Food Reviews International*, 1-15. https://doi.org/10.1080/87559129.2023.2272950

Shi, L., Zhao, W., Yang, Z., Subbiah, V., & Suleria, H. A. R. (2022). Extraction and characterization of phenolic compounds and their potential antioxidant activities. *Environmental Science and Pollution Research*, 29(54), 81112–81129. https://doi.org/10.1007/s11356-022-23337-6

Srinivas, P.R. (2012). Introduction to Protein Electrophoresis. In *Protein Electrophoresis. Methods in Molecular Biology*, 869. Humana Press, Totowa, NJ. https://doi.org/10.1007/978-1-61779-821-4_2

Stastna, M. (2020). Continuous flow electrophoretic separation — Recent developments and applications to biological sample analysis. *Electrophoresis*, 41(1–2), 36–55. https://doi.org/10.1002/elps.201900288

Stellwagen, E., & Stellwagen, N. C. (2020). Electrophoretic Mobility of DNA in Solutions of High Ionic Strength. *Biophysical Journal*, 118(11), 2783–2789. https://doi.org/10.1016/j.bpj.2020.02.034

Strathmann, H. (2004). Operating Principle of Electrodialysis and Related Processes. *Ion-Exchange Membrane Separation Processes*, 9, 147–225. Elsevier.

Strathmann, H. (2010). Electrodialysis, a mature technology with a multitude of new applications. *Desalination*, 264(3), 268–288. https://doi.org/10.1016/j.desal.2010.04.069

Sun, L., Chen, Q., Lu, H., Wang, J., Zhao, J., & Li, P. (2020). Electrodialysis with porous membrane for bioproduct separation: Technology, features, and progress. *Food Research International*, 137(38), 109343. https://doi.org/10.1016/j.foodres.2020.109343

Szepessy, S., & Thorwid, P. (2018). Low Energy Consumption of High-Speed Centrifuges. *Chemical Engineering & Technology*, 41(12), 2375-2384. https://doi.org/10.1002/ceat.201800292

Szydlowska-Czerniak, A., Trokowski, K., Karlovits, G., & Szlyk, E. (2010). Determination of antioxidant capacity, phenolic acids, and fatty acid composition of rapeseed varieties. *Journal of Agricultural and Food Chemistry*, 58(13), 7502–7509. https://doi.org/10.1021/jf100852x

Tamborrino, A., Perone, C., Catalano, F., Squeo, G., Caponio, F., & Bianchi, B. (2019). Modelling Energy Consumption and Energy-Saving Numerical Study and Experimental Validation. *Energies*, 12(2592), 1–20. https://doi.org/10.3390/en12132592

Tan, S. H., Mailer, R. J., Blanchard, C. L., & Agboola, S. O. (2011). Canola Proteins for Human Consumption: Extraction, Profile, and Functional Properties. *Journal of Food Science*, 76(1). https://doi.org/10.1111/j.1750-3841.2010.01930.x

Tekinalp, Ö., Zimmermann, P., Holdcroft, S., Burheim, O. S., & Deng, L. (2023). Cation Exchange Membranes and Process Optimizations in Electrodialysis for Selective Metal Separation: A Review. *Membranes*, 13(6). https://doi.org/10.3390/membranes13060566

Tian, Y., Zhou, Y., Kriisa, M., Anderson, M., Laaksonen, O., Kütt, M. L., Föste, M., Korzeniowska, M., & Yang, B. (2023). Effects of fermentation and enzymatic treatment on phenolic compounds and soluble proteins in oil press cakes of canola (Brassica napus). *Food Chemistry*, 409. https://doi.org/10.1016/j.foodchem.2022.135339

Torres-Acosta, M. A., Mayolo-Deloisa, K., González-Valdez, J., & Rito-Palomares, M. (2019). Aqueous Two-Phase Systems at Large Scale: Challenges and Opportunities. *Biotechnology Journal*, 14(1). https://doi.org/10.1002/biot.201800117

USDA. (2022). Oilseeds : World Markets and Trade. July 2021, 1–38. https://downloads.usda.library.cornell.edu/usda-esmis/files/tx31qh68h/r781xd48h/4f16d011j/oilseeds.pdf

Van der Bruggen, B. (2018). Ion-exchange membrane systems-Electrodialysis and other electromembrane processes. In *Fundamental Modeling of Membrane Systems: Membrane and Process Performance*, 251 - 300. Elsevier. https://doi.org/10.1016/B978-0-12-813483-2.00007-1

van Oss, C. J. (1975). The influence of the size and shape of molecules and particles on their electrophoretic mobility. *Separation & Purification Reviews*, 4(1). https://doi.org/10.1080/03602547508066038

Wagner, J., Andreadis, M., Nikolaidis, A., Biliaderis, C. G., & Moschakis, T. (2021). Effect of ethanol on the microstructure and rheological properties of whey proteins: Acid-induced cold gelation. *LWT*, 139. https://doi.org/10.1016/j.lwt.2020.110518

Wanasundara, J. P. D. (2011). Proteins of brassicaceae oilseeds and their potential as a plant protein source. *Critical Reviews in Food Science and Nutrition*, 51(7), 635–677. https://doi.org/10.1080/10408391003749942

Wang, N., & Weatherley, L. (2023). Electric field-intensified chemical processes and reaction chemistry. *Current Opinion in Chemical Engineering*, 39. https://doi.org/10.1016/j.coche.2022.100895

Wang, R., Zhang, J., Tang, C. Y., & Lin, S. (2022). Understanding selectivity in solute–solute separation: Definitions, measurements, and comparability. *Environmental Science & Technology*, 56(4), 2605-2616. https://doi.org/10.1021/acs.est.1c06176

Wang, Y., Jiang, C., Bazinet, L., & Xu, T. (2018). Electrodialysis-based separation technologies in the food industry. In *Separation of Functional Molecules in Food by Membrane Technology* (pp. 349–381). Academic Press. https://doi.org/10.1016/B978-0-12-815056-6.00010-3

Weiss, J., & Zhang, H. (2020). Recent advances in the composition , extraction and food applications of plant-derived oleosomes. *Trends in Food Science & Technology*, 106, 322–332. https://doi.org/10.1016/j.tifs.2020.10.029

Yang, J., Lamochi Roozalipour, S. P., Berton-Carabin, C. C., Nikiforidis, C. V., van der Linden, E., & Sagis, L. M. C. (2021). Air-water interfacial and foaming properties of whey protein - sinapic acid mixtures. *Food Hydrocolloids*, 106467. https://doi.org/10.1016/j.foodhyd.2020.106467

Yılmaz, H., & Gultekin Subasi, B. (2023). Distinctive Processing Effects on Recovered Protein Isolates from Laurel (Bay) and Olive Leaves: A Comparative Study. *ACS Omega*, 8(39), 36179–36187. https://doi.org/10.1021/acsomega.3c04482

Zhang, M., Zheng, C., Yang, M., Zhou, Q., Li, W., Liu, C., & Huang, F. (2019). Primary Metabolites and Polyphenols in Rapeseed (Brassica napus L.) Cultivars in China. *Journal of the American Oil Chemists' Society*, 96(3), 303–317. https://doi.org/10.1002/aocs.12179

Zhou, Y., Zhao, W., Lai, Y., Zhang, B., & Zhang, D. (2020). Edible Plant Oil : Global Status , Health Issues , and Perspectives. *Frontiers in Plant Science*, 11, 1315. https://doi.org/10.3389/fpls.2020.01315

Zimmermann, P., Tekinalp, Ö., Solberg, S. B. B., Wilhelmsen, Ø., Deng, L., & Burheim, O. S. (2023). Limiting current density as a selectivity factor in electrodialysis of multi-ionic mixtures. *Desalination*, 558. https://doi.org/10.1016/j.desal.2023.116613

Summary

Oilseeds, valuable crops with substantial annual production and rich oil and protein content, play a crucial role in the food industry. To efficiently utilize these crops, it is essential to recover both oils and proteins. Current industrial practices, while successful in increasing oil extraction yield, are not fully sustainable due to the need for elevated temperatures and organic solvents. This not only denatures the remaining proteins but also makes their extraction challenging. Therefore, there is a pressing need for gentler methods to extract both oils and proteins from oilseeds.

This thesis delves into the exploration of electrophoretic techniques, a novel approach, to develop a complete, gentle and efficient fractionation process. The goal is to deliver natural oil-storing organelles (oleosomes) and phenolic-free proteins from rapeseed, a model oilseed. The hypothesis is that distinct sizes of oleosomes, proteins, and phenolics exhibit different electrophoretic mobilities, enabling their electrophoretic separation.

The initial investigation focused on the electro-separation of oleosomes and proteins. In **Chapter 2**, the electrophoretic mobility differences between oleosomes and rapeseed proteins (cruciferins and napins) at various pH values were analyzed to identify the optimal pH value for their separation. Separation was achieved by combining electrophoresis and counter–current hydrodynamic flow. This retained the oleosomes (higher electrophoretic mobility) under an electric field but permeated the proteins (lower electrophoretic mobility) together with the solvent flow at pH 8.0. The process was quantified using the Nernst – Planck equation and demonstrated using a microfluidic channel under a microscope.

The proposed electrophoretic separation process principle was scaled up in **Chapter 3** by increasing the number of the separation channels, using a porous frit. The effect of an increasing electric field under a constant anti-parallel solvent flow rate on oleosomes and protein permeation flux and separation selectivity was investigated. The increasing electric field reduced the permeation flux of oleosomes and proteins based on their electrophoretic mobilities until 50 V/cm, where a separation selectivity of up to 9.84 was achieved. However, complete separation of oleosomes from proteins was hindered by the overlap in their electrophoretic mobility distributions, by membrane fouling and by pH gradient formation in the separation channel (porous medium) due to Faradaic reactions. To improve the electrophoretic oleosome and protein separation selectivity, the following strategies were recommended: (i) increasing their electrophoretic mobility differences by preventing protein aggregation, changing buffer type and ionic strength, (ii) separating the electrodes from the separation channel and (iii) preventing pH change.

Next to the electrophoretic separation of oleosomes and proteins, **Chapters 4** and **5** investigated the electrophoretic removal of phenolic compounds, such as sinapic acid (SA), employing an electrodialysis system. Here, SA was removed from the proteins using a membrane that permits only SA electro-migration but retains the proteins due to their larger size. In **Chapter 4**, the effects of pore size and surface charge of membranes on SA removal

were tested using both below and above limiting current densities (LCD) using positively charged anion exchange (AEM) and negatively charged ultrafiltration (UFM) membranes.

Below the LCD, an AEM provided higher SA removal due to the synergistic effect of co-current electrophoretic and electrostatic attraction forces. SA removal was limited by electrostatic repulsion forces when a UFM was used. Above the LCD, the use of AEM and UFM showed similar SA removal; however, SA permeation was much higher when the UFM was used due to the suppressed electrostatic repulsion force by the enhanced electrophoretic force. The lower permeation in the AEM is related to the accelerated salt transport through the membrane when employing an over-potential, decreasing the SA transport number, and/or the enhanced electrostatic interaction between SA and the fixed charge groups of the membrane. The different surface charges of the membranes and operating conditions also affected the protein loss. The combined effect of electrophoresis and electrostatic attraction forces led to significant protein loss when the AEM membrane was used above the LCD. Operation with the AEM below the LCD was optimal for SA removal, maintaining stable pH and protein content in the feed solution. However, the SA removal was just around 30 wt%. Five-fold enlargement of the membrane surface area then yielded 90.3 wt% SA removal.

The separation in **Chapter 4** was conducted in a dilute environment, which does not match the concentrations of natural oilseed protein extracts. To assess the effects of ionic strength on SA removal, **Chapter 5** investigated the use of different buffer concentrations from 5 to 40 mM. The SA removal decreased with increasing ionic concentration due to the reduced electrophoretic mobility caused by SA charge screening and the average electric field strength. A natural rapeseed extract was then used to demonstrate the practical feasibility of electrodialysis-based phenolic removal. Here, 30.3 ± 4.1 wt% of SA and 14.9 ± 2.8 wt% of other phenolic compounds were removed when using five AEMs.

Within this thesis, two different electrophoretic separation processes have been explored, presenting innovative alternatives for oilseed fractionation. **Chapter 6** not only reflects on the main findings but also contextualizes the electrophoretic fractionation process by comparing it with other non-conventional approaches. The electrophoretic fractionation process, being scalable and adaptable to separate various compounds based on their charge and/or size, holds great potential for the fractionation of other biomass. To pave the way for this, **Chapter 6** finalizes by outlining the future research directions to overcome the existing limitations and enhance separation selectivity and efficiency. Thus, this work sets the stage for future advancements in the development of gentler and efficient fractionation processes.

Appendices

Acknowledgement

About the author

Publications

Overview of completed training activities

ACKNOWLEDGEMENT

As I come to the end of my PhD journey, I would like to acknowledge all the people who have contributed to this achievement in various ways.

First of all, I would like to thank my promotors, Costas and Remko, for giving me the opportunity to work in their groups during my PhD. Costas, you have always supported me whenever I needed help, and your open-minded perspective allowed me to grow as an independent researcher. Remko, thank you for generously sharing your knowledge and supporting me in learning new skills. Your wisdom helped me overcome many challenges.

When my project started from scratch, many people helped me move forward. Pina, thank you for sharing your experience with electrical separation processes. Saskia, thank you for guiding me in the FPE labs in my first times. Conducting my initial separation experiments was possible with the collaboration of Siddharth and Ketan. Thank you both for allowing me to use your lab at PCC, assisting me, and for our discussions. I also want to thank the technicians and other colleagues at PCC who helped me tackle the problems I encountered. Finally, Kieke, thank you for explaining the microfluidics manufacturing process to me.

Doing all the experiments would not have been possible without the help of the FPE technicians. Maurice, Jos and Wouter, thank you for all the instructions you provided, your assistance with the analysis, arranging the orders I made, and, most importantly, for keeping an eye on the labs and ensuring a safe work environment. Martin, thank you for your help with the financial arrangements. Although we did not work together, Jarno, Lyneth and Kasia, I valued your kindness and enjoyed our chats.

I owe an acknowledgement to those who helped me with the confocal microscope. Arjen Bader and Jan Willem Borst, thank for assisting with my experiments and for sharing your expertise. I would also like to acknowledge Helene Mocking from FBR for her invaluable help with protein purification.

When I think about all the assistance from technicians, I must acknowledge the workshop technicians, Eric Karruppannan, Hans Meijer and Hans de Rooij, who made it possible to design the custom experimental setups. I valued your willingness to help.

For coordinating the administrative processes, I would like to thank all the secretaries: Marjan, Danielle (BCT), Evelyn, Ilona and Ilone.

My PhD journey was filled with discussions, questions and attempts to find answers. At this point, I cannot overlook the contributions of my colleagues from BCT and FPE. I would like to thank Eleni for assisting me in BCT labs and sharing her experience with the analysis; Laura for checking my samples in TEM and for our discussions about the results; Lorenz for his help with NMR analysis; Roel for inspiring me regarding the use of electrochemical cells;

Regina for her assistance with the Soxhlet extraction and Dumas; Herehau for sharing her knowledge on the microfluidics; Eric, Luc and Wanqing for our filtration setup discussions; Marcel for his interest in my project and his valuable feedback on the calculations. Besides, I would like to thank Harry Bitter for providing useful comments on the flash reports and for all his suggestions for the analysis.

Apart from the technical assistance, I would like to thank my colleagues – Anouk, Ana, Dan, Eric, Fathinah, Herehau, Hilda, Iris, Jiarui, Lingfeng, Luc, Mahsa, Murat, Solange, Ting and Yafei – for making the stressful PhD period much more bearable with laughter, tasty food, shared complaints, and mutual support. I also thank my office mates for our office dinners and for creating the most aesthetic office in FPE (or maybe at WUR? :)). Laurens and Martijn, thank you for your creative LinkedIn posts highlighting the latest publications! Anna and Anouk thank you for being very short-term housemates. I also want to thank my colleagues in FPE for the Christmas market excursions, lab-uitje and our PhD trip to Singapore. Additionally, I would like to extend my gratitude to all members of the BioSoM team for being helpful colleagues, for our discussions and for the nice trip to Strasbourg. A very special thanks to my paranymphs, Dan and Lingfeng, for being my biggest supporters on the stage! :)

Ayrıca, doktora çalışmam için gerekli her türlü desteği sağlayan Türkiye Cumhuriyeti Millî Eğitim Bakanlığı'na ve çalışanlarına çok teşekkür ederim. Hollanda'da geçirdiğim süre boyunca yardımlarını hiç bir zaman esirgemeyen Lahey Eğitim Müşavirliği çalışanlarına ve Miyase Koyuncu Kaya'ya da içtenlikle teşekkür ederim.

Bu teşekkür metnini aileme yer vermeden bitirmem olanaksızdı. Çok değerli ailem, size her ne kadar teşekkür etsem de yeterli olmayacağının farkındayım. Yine de aramızdaki mesafeden bağımsız olarak beni her zaman ve her koşulda desteklediğiniz için çok teşekkür ediyorum. Size sahip olduğum için çok şanslıyım, iyi ki varsınız.

While finishing the acknowledgement and reflecting on my PhD experience, I would also like to thank the 2020, 2021, 2022, 2023 and 2024 versions of myself, each of whom played a role in this achievement! :)

ABOUT THE AUTHOR

Kübra Ayan was born in Istanbul, Türkiye, on September 26, 1993. In 2011, she started her Bachelor´s degree at Food Engineering Department at Hacettepe University. After completing the first two years of her studies in Ankara, she continued the food engineering education at Istanbul Technical University. She worked on the extraction and functional properties of *Nigella sativa* seed proteins for her BSc thesis.

Upon graduating in 2016, she began Food Engineering Master´s program at Istanbul Technical University to deepen her knowledge on food production. During this program, she specialized on the design and production of functional foods. For her MSc thesis, she researched the encapsulation of beetroot antioxidants to enhance their stability in a food matrix. She obtained her MSc degree in 2018 and was subsequently awarded a government scholarship (YLSY) in 2019 to conduct PhD research on novel food processing techniques.

In 2020, she started working as a PhD candidate at Food Process Engineering and Biobased Chemistry & Technology groups at Wageningen University. Her research focused on electrical fractionation processes of oilseed components, culminating in her PhD thesis titled `*Electrophoretic Separation Strategies for Gentle Fractionation of Rapeseed*´.

PUBLICATIONS

This Thesis

Ayan, K., Ganar, K., Deshpande, S., Boom, R. M., & Nikiforidis, C. V. (2023).Continuous counter-current electrophoretic separation of oleosomes and proteins from oilseeds. *Food Hydrocolloids*, 144, 109053.

Ayan, K., Boom, R. M., & Nikiforidis, C. V. (2024). Scaling the electrophoretic separation of rapeseed proteins and oleosomes. *Journal of Food Engineering*, 381, 112188.

Ayan, K., Boom, R. M., & Nikiforidis, C. V. (2024). Electrophoretic removal of sinapic acid from rapeseed protein extract. *Submitted - Under Review*

OVERVIEW OF COMPLETED TRAINING ACTIVITIES

Discipline Specific Activities		
Conference: Science and Technology for Meat Analogues	WUR	2021
Lipid droplets & Oleosomes Young Scientists Online Event	VLAG	2021
Lipid droplets & Oleosomes Conference[a]	WUR & ibmp	2021
Advanced Food Analysis[a]	VLAG	2022
Microscopy and Spectroscopy in Food and Plant Sciences	VLAG - EPS	2022
International Congress on Separation and Purification Technology	Elsevier	2022
International Congress on Engineering and Food (ICEF'14)[b]	IAEF	2023
3rd International Lipid Droplets and Oleosomes Conferences[b]	WUR	2023
Food proteins[a]	VLAG	2024
Bi-annual Food Sciences Symposium[b]	FCH-WUR	2024
IUFoST 2024[b]	AITA	2024
General Courses		
VLAG PhD week	VLAG	2021
The Essentials of Scientific Writing and Presenting	WGS	2020
Pitching your research	WGS	2021
Mindful productivity for PhD Candidates	WGS	2021
Introduction to R & R studio	PE&RC/WIMEK	2021
RmarkDown	WGS	2021
Scientific Artwork & Data Visualization	WGS	2022
Effective behaviour in your professional surroundings	WGS	2022
Adobe InDesign - from Dissertation Layout to Poster Design	WGS	2024
Assisting in teaching and supervision activities		
Advanced Biorefinery	BCT	2022-2023
Supervision of thesis students	FPE & BCT	2022-2023
Other Activities		
Preparation of research proposal	FPE	2021
FPE Weekly Group Meetings	FPE	2020-2024
BCT Weekly Group Meetings	BCT	2020-2024
PhD Study Tour to Singapore[a,b]	FPE	2022

a: Oral Presentation b: Poster Presentation

This research was financially supported by the Republic of Türkiye Ministry of National Education under the YLSY scholarship program.

Financial support from Wageningen University for printing this thesis is gratefully acknowledged.

Cover design by Kübra Ayan
Printed by ProefschriftMaken | proefschriftmaken.nl